

Systematic analysis of genes expressed in the retinal pigment epithelium (RPE) and identification of candidates for genetic susceptibility to age-related macular degeneration (AMD)

Dissertation zur Erlangung des
naturwissenschaftlichen Doktorgrades
der Bayerischen Julius-Maximilians-Universität Würzburg

vorgelegt von
Faisal Mirghani Abdel Rahman
aus dem Sudan

Würzburg 2003

Eingereicht am:

Mitglieder der Promotionskommission:

Vorsitzender: Prof. Dr. Rainer Hedrich

Gutachter: Prof. Dr. Bernhard Weber

Gutachter: Prof. Dr. Recardo Benavente

Tag des Promotionskolloquiums:.....

Doktorurkunde ausgehändigt am:.....

Erklärung

Hiermit erkläre ich, dass ich die vorliegende Dissertation selbständig verfasst und keine anderen als die angegebenen Quellen und Hilfsmittel verwendet habe.

Diese Dissertation wurde weder in gleicher noch in ähnlicher Form zu einem anderen Prüfungsverfahren vorgelegt.

Es wurde zuvor kein anderer akademischer Grad erworben.

Würzburg, den.....

ACKNOWLEDGEMENTS

The work in this thesis has been performed during 2000-2003 at the Institute of Human Genetics, Wuerzburg University, Germany. I would like to express my sincere gratitude to the following:

Prof. Dr. Bernhard Weber, my supervisor, for welcoming me to his lab and allowing me to share his expertise in human genetics and for his guidance throughout this work.

Prof. Dr. Recardo Benavente, my cosupervisor, for his support, encouragement and expressing interest in my work.

Prof. Dr.med. Holger Höhn, director of the institute of human genetics, for his help, support, advice and encouragement.

Prof. Dr.med Awad Omer, father in law, for his support and encouragement.

Faisal Mola, for his contribution in the database construction and computational analyses.

Andrea Gehrig, for her contribution in the library construction and help with the expression analysis.

Andrea Rivera, for her help with the SNPs.

Claudia Berger and Nicole Mohr for their help with sequencing.

I would like also to thank all my colleagues in the lab and all members of the institute of human genetics.

I wish to express my gratitude to my family, mother, sisters and brothers and my extended family and special thanks to my wife Rasha, and my daughters Lena and Razan for their support and patience.

TABLE OF CONTENTS

ABBREVIATIONS.....	iv
ZUSAMMENFASSUNG.....	vi
SUMMARY.....	viii
1. INTRODUCTION.....	1
1.1 Retina and retinal pigment epithelium.....	1
1.2 Single gene retinopathies	3
1.2.1 Peripheral retinal dystrophies.....	5
1.2.1.1 Retinitis pigmentosa.....	5
1.2.2 Central retinal dystrophies.....	5
1.2.2.1 Vitelliform macular dystrophy (Best's disease).....	5
1.3 Phenotype oriented molecular genetic approach.....	6
1.3.1 Genetic linkage analysis.....	6
1.3.2 Positional cloning.....	6
1.3.3 Positional candidate gene approach.....	7
1.4 Gene oriented molecular genetic approach	7
1.5 Age related macular degeneration.....	7
1.5.1 Disease phenotype.....	8
1.5.2 Pathogenesis	8
1.5.2.1 Drusen.....	8
1.5.2.2 Geographic atrophy.....	9
1.5.2.3 Choroidal neovascularization (CNV).....	10
1.5.3 Suspected pathological pathways	11
1.5.3.1 Oxidative stress.....	11
1.5.3.2 Lysosomal enzymes dysfunction.....	12
1.5.3.3 Immune complex and inflammation pathogenesis.....	13
1.5.4 Risk factors.....	14
1.5.4.1 Age.....	14
1.5.4.2 Genetic predisposition.....	15
1.5.4.3 Cigarette smoking.....	16
1.5.4.4 Other suspected risk factors.....	17
2. AIMS OF THE PRESENT STUDY.....	18
3. MATERIALS AND METHODS.....	19
3.1 Bovine RPE subtracted cDNA library construction.....	19
3.1.1 Isolation of poly (A) ⁺ RNA and cDNA synthesis.....	19
3.1.2 Suppression subtraction hybridization (SSH).....	19
3.2 Heat shock transformation.....	19
3.3 Colony picking and mini-culture preparation.....	20
3.4 Replica plating.....	20
3.5 Generation of expressed sequence tags (ESTs).....	20
3.5.1 Direct isolation of PCR insert from pCRII vector.....	20
3.5.2 Agarose Gel electrophoresis.....	21
3.5.3 Purification of PCR products	21
3.5.3.1 Exonuclease 1/Shrimp alkaline phosphatase (SAP) treatment ..	21
3.5.4 Cycle sequencing reaction.....	21
3.5.5 Ethanol (EtOH) DNA precipitation	22

3.6 Bioinformatics.....	22
3.7 Expression analysis of ESTs.....	22
3.7.1 Reverse Northern blot analysis	22
3.7.1.1 Nylon membrane transfer of cDNA.....	23
3.7.1.2 Probe synthesis and radioactive labelling.....	23
3.7.1.3 Prehybridization and hybridization.....	23
3.7.1.4 Washing and exposure of filters on phosphor imaging screens.....	24
3.7.2 Northern blot hybridizations	24
3.7.2.1 RNA size fractionation in formaldehyde-agarose gel.....	24
3.7.2.2 Capillary transfer of RNA onto nylon membrane.....	25
3.7.2.3 Vacuum transfer of RNA onto nylon membrane.....	25
3.7.2.4 Probe labelling with random priming.....	26
3.7.2.5 Membrane prehybridization preparation.....	26
3.7.2.6 Probe preparation.....	26
3.7.2.7 Hybridization.....	27
3.7.2.8 Membrane washings, film exposure and development.....	27
3.7.3 Reverse Transcriptase (RT)-PCR analysis.....	27
3.7.3.1 RNA purification.....	27
3.7.3.2 First strand cDNA syntheses.....	27
3.7.3.3 cDNA quality check and normalization.....	28
3.8 Cloning and characterization of AMD candidate genes.....	28
3.8.1 Bioinformatics.....	28
3.8.2 Cloning of the MGC2477 predicted gene and 2 novel isoforms of the TRPM3 gene	29
3.8.2.1 Preparation of competent cells	29
3.8.2.2 Ligation.....	29
3.8.2.3 Electroporation transformation.....	30
3.8.3 Standard polymerase chain reaction (PCR) amplification.....	30
3.8.4 Nested PCR.....	30
3.8.5 Touch down PCR	31
3.8.6 PCR library screening.....	31
3.8.7. DNA extraction from agarose gel.....	32
3.9 Identification of single nucleotide polymorphism	32
3.9.1 Bioinformatics.....	32
3.9.2 Identification of high frequency SNPs and determination of allele frequency.....	32
3.9.3 Ready to use gel electrophoreses.....	33
3.9.4. Denaturing high performance liquid chromatography (dHPLC).....	33
3.9.5. DNA sequencing.....	33
4. RESULTS.....	35
4.1 Generation of ESTs derived from the bovine RPE cDNA library.....	35
4.2 Bioinformatics.....	35
4.3 Expression analysis.....	36
4.3.1 Reverse Northern blot analysis.....	36
4.3.2 Northern blot hybridizations.....	41
4.4 AMD candidate clones.....	48
4.4.1 Analysis of 2 novel isoforms of the transient receptor potential cation channel, subfamily M, member 3 (TRPM3).....	49
4.4.1.1 Cloning of the 2 novel isoforms of TRPM3.....	49
4.4.1.2 Genomic structure	49

4.4.1.3 Protein analysis.....	51
4.4.1.4 Expression analysis (RT-PCR).....	52
4.4.2 Analysis of MGC2477 gene.....	53
4.4.2.1 Isolation and characterization of the MGC2477 gene.....	53
4.4.2.2 Genomic structure.....	55
4.4.2.3 Protein analysis.....	56
4.4.2.4 Expression analysis.....	56
4.4.3 SNP identification in the MT-protocadherin gene.....	57
4.4.4 SNP identification in the TRPM3 gene.....	59
4.4.5 SNP identification in the MGC2477 gene.....	61
5. DISCUSSION.....	64
6. CONCLUSION AND FUTURE PERSPECTIVES.....	79
7. REFERENCES.....	80
8. APPENDIX.....	95
Table 1: Oligonucleotides primers and conditions (MT-Protocadherin gene).....	95
Table 2: Oligonucleotide primers and conditions (TRPM3 gene).....	96
Table 3: Oligonucleotide primers and conditions (MGC2477 gene).....	98
Table 4: Group II of the reverse Northern blot analyses.....	98
Table 5: Genes from pathways suspected to be involved in AMD Pathogenesis.....	103
Table 6: cDNA libraries used in the isolation of MGC2477 gene.....	103
Table 7: Sequence of the Lambda Triple Ex vector specific primers.....	103
Publication and presentations.....	104
Curriculum vitae.....	105

ABBREVIATIONS

aa	amino acids
ABCA4	ATP-binding cassette, sub-family A (ABC1), member 4
AD	autosomal dominant
AIPL1	aryl hydrocarbon receptor interacting protein-like 1 23746
AMD	age related macular degeneration
Amp	ampicillin
AR	autosomal recessive
ARM	age related maculopathy
ASB	arylsulfatase B
BD	Bothnia dystrophy
CACNA1F	calcium channel, voltage-dependent, alpha 1F subunit
CAP3	contig assembly program
CatD	cathepsin D
cDNA	complementary DNA
CHM	choroideremia (Rab escort protein 1)
cM	centimorgan
CNGA1	cyclic nucleotide gated channel alpha 1
CNGA3	cyclic nucleotide gated channel alpha 3
CNGB1	cyclic nucleotide gated channel beta 1
CNGB3	cyclic nucleotide gated channel beta 3
CNV	choroidal neovascularization
COCRD	cone or cone-rod Dystrophy
CRAOD	chorioretinal atrophy or degeneration
CRB1	crumbs homolog 1 (Drosophila)
CRX	cone-rod homeobox
CSNB	congenital stationary night blindness
dbEST	expressed sequence tag databases
ECM	extracellular membrane
EFEMP1	EGF-containing fibulin-like extracellular matrix protein 1
ELOVL4	elongation of very long chain fatty acids-like 4
EST	expressed sequence tag
EtOH	Ethanol
FSCN2	fascin homolog 2, actin-bundling protein, retinal
GA	geographic atrophy
GNAT1	guanine nucleotide binding protein (G protein), alpha transducing activity polypeptide 1
GNAT2	guanine nucleotide binding protein (G protein), alpha transducing activity polypeptide 2
GUCA1A	guanylate cyclase activator 1A (retina)
GUCY2D	guanylate cyclase 2D, membrane
GUSB	β -glucuronidase
HPRP3P	U4/U6-associated RNA splicing factor
htgs	high throughput genomic sequences
IMPDH1	IMP (inosine monophosphate) dehydrogenase 1
LCA	Leber congenital amaurosis
LOD	logarithm of the odds ratio
LRAT	lecithin retinol acyltransferase
MD	macular degeneration
MERTK	c-mer proto-oncogene tyrosine kinase
MGC	mammalian gene collection
min	minutes
NEI	National Eye Institute
nr	non redundant
NR2E3	nuclear receptor subfamily 2, group E, member 3
NRL	neural retina leucine zipper
NYX	nyctalopin
OAT	ornithine aminotransferase
OCA	oculo-cutaneous albinism
OPN1LW	opsin 1 (cone pigments), long-wave-sensitive
OPN1MW	opsin 1 (cone pigments), medium-wave-sensitive

OPN1SW	opsin 1 (cone pigments), short-wave-sensitive
PCR	Polymerase chain reaction
PDE6A	phosphodiesterase 6A, cGMP-specific, rod, alpha
PDE6B	phosphodiesterase 6B, cGMP-specific, rod, beta
PDT	Photodynamic therapy
PROM1	prominin 1
PRPF31	PRP31 pre-mRNA processing factor 31 homolog (yeast)
PRPF8	PRP8 pre-mRNA processing factor 8
PUFAs	polyunsaturated fatty acids
RDA	representational difference analysis
RDH5	retinol dehydrogenase 5
RDS	retinal degeneration, slow
RFLP	restriction fragment length polymorphisms
RGR	retinal G protein coupled receptor
RHO	rhodopsin (opsin 2, rod pigment)
RHOK	rhodopsin kinase
RIMS1	regulating synaptic membrane exocytosis
RLBP1	retinaldehyde binding protein
ROM1	retinal outer segment membrane protein 1
ROS	reactive oxygen species
RP	retinitis pigmentosa
RP1	retinitis pigmentosa 1 (autosomal dominant)
RP2	retinitis pigmentosa 2
RP9	retinitis pigmentosa 9
RPA	retinitis punctata albescens
RPE	retinal pigment epithelium
RPE65	retinal pigment epithelium-specific protein
RPGR	retinitis pigmentosa GTPase regulator
RPGRIP1	retinitis pigmentosa GTPase regulator interacting protein 1
RS1	retinoschisis (X-linked, juvenile)
RT	room temperature
SAG	S-antigen; retina and pineal gland (arrestin)
SAP	Shrimp alkaline phosphatase
SNP	Single nucleotide polymorphism
SSCPs	single strand conformation polymorphisms
TIMP3	tissue inhibitor of metalloproteinase 3
TULP1	tubby like protein 1
UNC119	unc-119 homolog (C. elegans)
UV	ultraviolet
VMD2	vitelliform macular dystrophy
XL	Xlink
α -Mann	α -mannosidase

In addition, abbreviations for retina layers are presented in Figure 1 and abbreviations for genes from pathways suspected to be involved in AMD pathogenesis are presented in Appendix Table 5.

ZUSAMMENFASSUNG

Die altersabhängige Makuladegeneration (AMD) ist die häufigste Ursache von gravierenden Einschränkungen des Sehvermögens im fortgeschrittenen Lebensalter. In den Industriestaaten ist die AMD zudem die Hauptursache für Altersblindheit. Die molekularen Mechanismen, die zur Entstehung der AMD führen, sind bisher nur unzureichend bekannt. In den letzten Jahren hat es sich jedoch herausgestellt, dass das retinale Pigmentepithel (RPE) eine primäre Rolle in der Pathogenese der AMD spielt.

Ziel dieser Arbeit war die systematische Analyse von Genen, welche im RPE differentiell exprimiert werden. Entsprechende Kandidatengene sollten auf deren mögliche Beteiligung an der Entstehung von Erkrankungen der Retina, insbesondere der AMD, untersucht werden.

Zunächst wurden 2379 ESTs aus einer innerhalb der Arbeitsgruppe generierten RPE cDNA Bibliothek definiert. Die dazu verwendete cDNA Bibliothek wurde durch die Suppressions-Subtraktions Hybridisierungs-Technik (SSH) konstruiert. Diese Technik gestattet eine Normalisierung gegenüber redundanten Sequenzen und begünstigt gleichzeitig die Anreicherung von seltenen Transkripten. In einer ersten Phase wurden 1002 ESTs sequenziert und einer umfassenden bioinformatischen Analyse mit Hilfe der verfügbaren DNA- und Protein Datenbanken unterzogen. Der Vergleich der 1002 ESTs mit der Draft Sequenz des menschlichen Genoms ergab den Hinweis auf 168 bereits bekannte Gene, 51 mögliche Gene, 15 völlig unbekannte Transkripte und 41 nicht weiter zuordenbare cDNA Klone. 318 EST Cluster wurden einer reversen Northern-Blot Analyse unterzogen um hochexprimierte Gene zu identifizieren und damit Prioritäten für die weiteren Analysen zu setzen.

Im Rahmen der Northern-Analyse wurden repräsentative Klone von 107 EST-Klustern mit cDNA Sonden der ursprünglichen cDNA-Bibliothek hybridisiert. Als Ergebnis dieser Analyse fanden sich 7 RPE-spezifische, 3 Retina-spezifische, 7 sowohl RPE- als auch Retina-spezifische sowie 7 auf einzelne Gewebe limitierte Transkripte. 29 EST Cluster erwiesen sich als ubiquitär exprimiert, und 54 Kluster konnten nicht näher zugeordnet werden. Von den 24 Transkripten mit spezifischer oder zumindest begrenzter Expression wurden 16 Klone zur weiteren Charakterisierung ausgewählt.

Aus diesen Material wurden im Rahmen dieser Arbeit das Kandidatengen MGC2477 sowie 2 neue Isoformen des menschlichen TRPM3-Gens kloniert und näher charakterisiert. Weiterhin wurden polymorphe Varianten dieser beiden Isoformen und des menschlichen MT-Protocadherin-Gens definiert. Im Gen MGC2477 wurden 15 SNPs identifiziert, wovon die Allelhäufigkeit des selteneren Allels bei 13 der SNPs über 20% lag. Für 10 der insgesamt 15

SNPs dieses Gens fanden sich bisher keine Einträge in den entsprechenden Datenbanken. Die SNP-Suche wurde auch für das TRPM3-Gen durchgeführt und ergab 35 SNPs, wovon 30 (85,7%) als hochfrequent eingestuft werden konnten. 14 dieser 35 SNPs waren bisher nicht in den Datenbanken verzeichnet. Beim MT-Protocadherin-Gen fanden sich ebenfalls 35 SNPs, wobei 80% eine hohe Frequenz des selteneren Allels aufwiesen. In diesem Fall handelte es sich bei 23 der insgesamt 35 SNPs um bisher unbekannte Allele. Diese SNPs bilden den Ausgangspunkt zur Konstruktion der häufigsten Haplotypen der genannten Gene.

Mit der Charakterisierung der Einzel-Nukleotid Polymorphismen der Kandidatengene wurde die Grundlage zur Durchführung von Fall/Kontrollstudien gelegt, in deren Rahmen die Bedeutung der jeweiligen Kandidatengene in der Pathogenese der AMD untersucht werden kann.

SUMMARY

Age related macular degeneration (AMD) is the leading cause of visual impairment in the elderly and the major cause of blindness in the developed world. To date, the molecular mechanisms underlying the disease are not well understood although in recent years a primary involvement of the retinal pigment epithelium (RPE) has become evident.

The aim of the present study is to systematically analyse genes which are differentially expressed in the RPE, and to assess their possible association with mechanisms and pathways likely to be related to retinal disease, in particular AMD.

Towards this goal, 2379 expressed sequence tags (ESTs) were established from an in-house generated RPE cDNA library. This library was constructed by using the suppression subtraction hybridization (SSH) technique which normalises redundant sequences and ensures enrichment of rare transcripts. In a first phase, 1002 ESTs were sequenced and subjected to comprehensive alignment with public nucleotide and protein databases. A search of the 1002 ESTs against the human genome draft sequence yielded 168 known genes, 51 predicted genes, 15 unknown transcripts and 41 clones with no significant similarity.

Reverse Northern blot hybridization was performed for 318 EST clusters to identify abundantly expressed genes in the RPE and to prioritize subsequent analyses. Representative clones were spotted onto a nylon membrane and hybridized with cDNA probes of driver (heart and liver) and tester (RPE) used in the cDNA library construction.

Subsequently, 107 EST clusters were subjected to Northern blot hybridizations. These analyses identified 7 RPE-specific, 3 retina-specific, 7 RPE/retina-specific, and 7 tissue restricted transcripts, while 29 EST clusters were ubiquitously expressed, and evaluation was not possible for another 54 EST clusters. Of the 24 transcripts with specific or restricted expression, 16 clones were selected for further characterization.

The predicted gene MGC2477 and 2 novel isoforms of the human transient receptor potential cation channel, subfamily M, member 3 (TRPM3) were cloned and further described in detail. In addition, polymorphic variations for these 2 genes as well as for the human MT-Protocadherin gene were determined. For MGC2477, 15 single nucleotide polymorphisms (SNPs) were identified, with 13 having a frequency of the

minor allele greater than 20%. 10 of the 15 SNPs have not been reported in so far in public SNP repertoires. Partial assessment of the TRPM3 gene yielded 35 SNPs. Of these, 30 (85.7%) were highly frequent (0.17-0.5%), and 14 (40%) were novel. The MT-Protocadherin gene revealed 35 SNPs, including 28 (80%) with high frequency of the minor allele. 23 (65.7%) were novel SNPs.

These SNPs will be used to construct the most common haplotypes. These will be used in case/control association studies in 400 AMD patients and 200 ethnically and aged matched controls to assess a possible contribution of these genes in the etiology of AMD.

1. INTRODUCTION

1.1 Retina and retinal pigment epithelium

The retina is the inner layer of the eye and contains several cell types. The retina can be divided into two main parts. The neural retina or the inner part, and the retinal pigment epithelium or the outer layer (Figure 1). The neural retina is composed of 9 layers: i) cone and rod photoreceptor cells, including the inner segment where metabolic processes take place and the outer segment which is filled with flattened membrane sacs called discs. Rods represent 95% of human photoreceptor cells and mediate dim light. Cones represent only 5 % of human photoreceptor cells (Rattner et al., 1999) and they are of three types, short-wave or blue, middle-wave or green and long-wave or red. Cones mediate bright light and colour vision, they are concentrated in the macula (Figure 1) which is the central portion of the retina, enabling the most distinct vision. The fovea centralis is the very centre of the macula and contains only cone photoreceptors, ii) external (outer) limiting membrane, iii) outer nuclear layer contains the cell bodies and nuclei of photoreceptors, iv) outer plexiform layer includes the cone and rod axons, bipolar cell dendrites and the horizontal cell dendrites, v) inner nuclear layer is the area where nuclei of the horizontal cells, amacrine cells, bipolar cells and Müller cells reside, vi) inner plexiform layer contains the axons of amacrine cells and bipolar cells, and dendrites of ganglion cells, vii) ganglion cell layer includes the nuclei of ganglion cells and displaced amacrine cells, viii) nerve fibre layer contains the axons of the ganglion cells which exit the eye at the optic disc forming the optic nerve which convey the photoreceptor signal response to the brain, ix) internal limiting membrane which separate the retina from the vitreous.

The outer layer or the retinal pigment epithelium is a single hexagonal cell layer located between the photoreceptor cells of the neural retina and the choroidal capillaries (Zinn and Marmor, 1979). The apical surface of the cells is loosely associated with the photoreceptor outer segment through microvilli processes, whereas the basement membrane is firmly attached to form part of Bruch's membrane. Laterally, RPE cells are attached to each other by tight junctions, which form a network of strands encircling cells and play part in the blood–retinal barrier. The retinal pigment epithelium is an important component of the retina

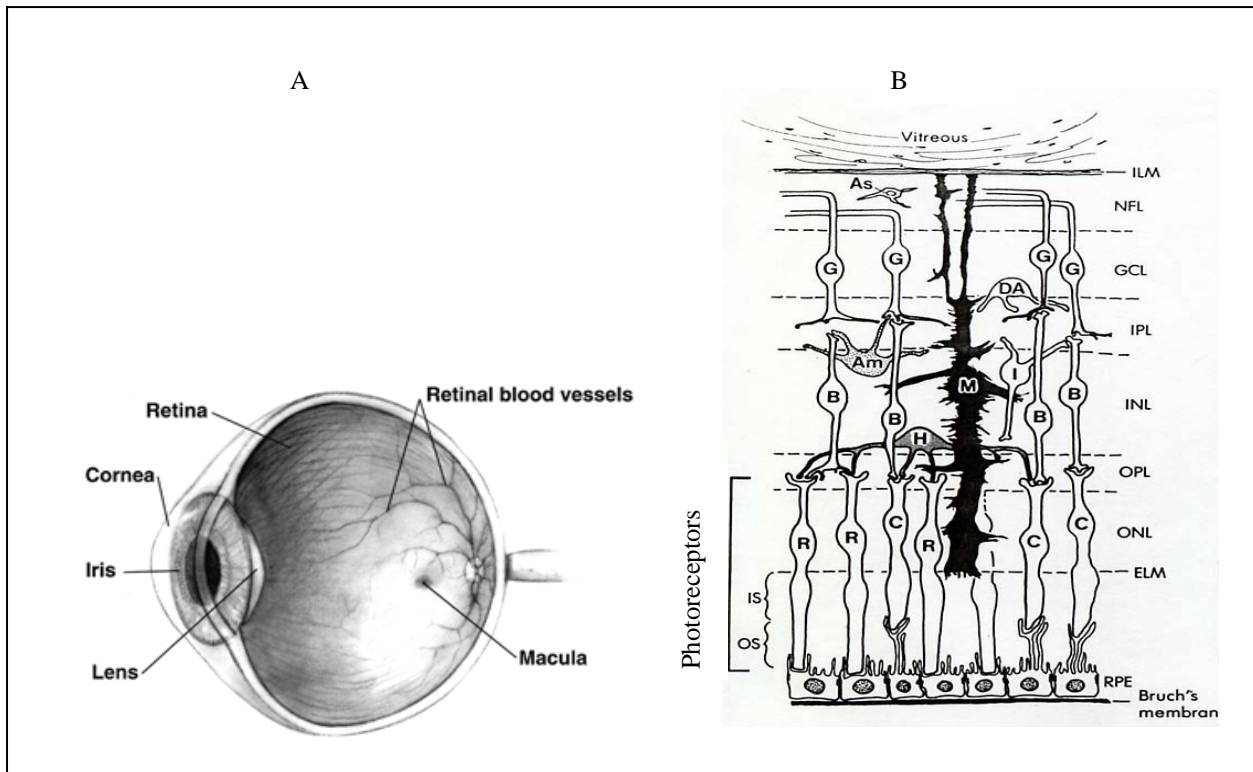


Figure 1: Schematic diagram of the Human eye showing the macula, and major cell types and layers in the retina A/. The macula is a light-sensitive area in the centre of the retina, at the back of the eye. The macula subserves high resolution central and colour vision. The centre of the macula is the foveola centralis which contain only cones and is free of rods. The parafovea are is rich in rods. In age related macular degeneration (AMD) the macula area is affected and rods in the perifoveal area are the first to degenerate. Adopted from the National Eye Institute (NEI), (www.nei.nih.gov/health/maculardegen/armd%5Frisk.htm). B/ Retinal layers include; retinal pigment epithelium (RPE), cones (C), and rods (R) photoreceptors, external limiting membrane (ELM), outer nuclear layer (ONL), outer plexiform layer (OPL), inner nuclear layer (INL), Inner plexiform layer (IPL), ganglion cell layer (GCL), Nerve fibre layer (NFL) and the inner limiting membrane (ILM).Neural signals generated in the photoreceptors are conveyed to the brain via synaptic contacts with bipolar cell (B) which themselves are in contact with the ganglion cells (G). Amacrine cells (AM), and horizontal (H) cells secure the lateral connections. Muller cells subserve many functions such as stabilization of synapses, retinal architectures, and may play role in neural signalling. (Modified from Dowling and Boycott, 1966)

and has many functions. RPE cells play an important role in the transport of ions and water in an apical to basal direction preserving the neural retina in a reasonable state of dehydration and optical clarity (Bok, 1993). Also, the directional net flow of fluid maintains close apposition of the retina to the RPE (Marmor, 1990). Among other functions of the RPE are retinol storage and transport (Bok, 1993), melanin absorption which prevents light scattering within the eye and may protect against oxidative stress (Beatty et al., 1999), development and survival of photoreceptors through the secretion of cell growth factors such as pigment epithelium-derived factor (Jablonski et al., 2000) and most importantly, phagocytosis of shed distal portions of photoreceptors outer segments (Bok, 1985 and 1993).

1.2 Single gene retinopathies

Hereditary retinal dystrophies are a heterogeneous group of eye diseases involving mainly the cone-rich area of the central retina (Weber, 1998). Disorders involving the rods manifest primarily with night blindness and may cause loss of peripheral vision, whereas the presenting feature of cone disorders is loss of central visual acuity (Bessant et al., 2001). To date, more than 50 genes causing monogenic nonsyndromic retinal dystrophies have been mapped and cloned (Table 1). Previous categorization classified the disorders according to the age of onset, site of pathological features and mode of inheritance (young, 1987, Merin, 1991, Noble, 1986). However with the recent advances in molecular genetics, this classification has been questioned. First, many new disease causing genes were identified with overlapping phenotypes and some of these phenotypes may be identical (Zhang et al., 1996). Second, several mutations in the same gene can manifest the same phenotype (allelic heterogeneity) such as seen in the retinoschisis gene (XLRS1). To date, 82 different mutations were identified in 234 familial and sporadic retinoschisis cases (Retinoschisis Consortium, 1998). Third, genetic heterogeneity as seen in retinitis pigmentosa (RP), people suffering from RP could inherit the disease as dominant, X-linked or recessive (Inglehearn, 1998). Fourth, locus heterogeneity also complicates classification where mutation in different genes can cause the same disease phenotype. Mutations in rhodopsin (chromosome 3q) (Dryja et al., 1990) or the RDS peripherin gene (chromosome 6p) (Kajiwara et al., 1991) can manifest an autosomal dominant RP. Finally, mutations in the same gene can present different phenotypes, as in the Peripherin/RDS gene where a 3- base pair mutation deletion of codon 153 or 154 resulted in 3 distinct phenotypes, pattern macular dystrophy, fundus flavimaculatus and an adult RP within the same family (Weleber, et al 1993). A broad categorization is based on the clinical symptoms of patients with retinal dystrophies being central or peripheral. Peripheral vision is affected in patients with RP, who presents with narrowing of the visual field and night blindness, in contrast to another group of patients with the disease affecting the macula who lose central vision first. A third group is distinct from the central/peripheral categories, and includes phenotypes such as the chorio-retinal atrophy, or the gyrate atrophy and the oculo-cutaneous albinism (OCA) (Inglehearn, 1998).

Table 1: Monogenic nonsyndromic mapped and cloned retinal dystrophy genes. Introduction 4

Gene symbol	Disease	Function	Expression
RIMS1	AD.COCD	Transport	Ret/Brain
RS1	XL.Retinoschisis	Cell to Cell interactions	Retina specific
CNGA3	AR.Achromatopsia	Phototransduction	Retina specific
CNGB3	AR.Achromatopsia	Phototransduction	Retina specific
CNGA1	AR.RP	Phototransduction	Retina specific
CNGB1	AR.RP	Phototransduction	Retina specific
FSCN2	AD.RP	Structural	Retina specific
TULP1	AR.RP	Vision	Retina specific
RP1	AD.RP	Vision	Retina specific
RPGRIP1	AR.LCA	Unknown	Retina specific
AIPL1	AD.COCD, AR.LCA	Transport	Retina specific
OPN1LW	XL.Deuteranopia	Phototransduction	Retina specific
GUCA1A	AD.COCD	Phototransduction	Retina specific
UNC119	AD.COCD	Phototransduction	Retina specific
CACNA1F	XL.CSNB	Phototransduction	Retina specific
NR2E3	AR.RP	Transcription factor	Retina specific
CRX	AD.COCD, LCA, RP, AR.LCA,	Transcription factor	Retina specific
NRL	AD.RP	Transcription factor	Retina specific
RHO	AD.CSNB, RP, AR.RP	Phototransduction	Retina specific
RHOK	AR.CSNB	Phototransduction	Retina specific
CRB1	AR.LCA, RP	Cell to Cell interactions	Retina specific
PDE6A	AR.RP	Phototransduction	Retina specific
PDE6B	AD.CSNB, AR.RP	Phototransduction	Retina specific
SAG	AR.RP	Phototransduction	Retina specific
GUCY2D	AD.COCD, AR.LCA	Phototransduction	Retina specific
RDS	AD.MD, RP	Structural	Retina specific
ABCA4	AR.COCD, MD, RP	Vitamin A cycle	Retina specific
OPN1MW	XL.Protanopia	Phototransduction	Retina specific
OPN1SW	AD.Tritanopia	Phototransduction	Retina specific
GNAT1	AD.CSNB	Phototransduction	Retina specific
RLBP1	AR.RP, RCD, RPA, BD	Vitamin A cycle	Retina specific
GNAT2	AR.Achromatopsia	Phototransduction	Retina specific
ROM1	AD.RP	Structural	Retina specific
LRAT	AR.RP	Vitamin A cycle	RPE specific
RGR	CRAOD, AR.RP	Vitamin A cycle	RPE specific
RPE65	AR.LCA, AR.RP	Vitamin A cycle	RPE specific
RDH5	AR.COCD,CSNB	Vitamin A cycle	Ubiquitous
OAT	AR.Gyrate atrophy	Metabolism	Ubiquitous
PRPF31	AD.RP	RNA processing	Ubiquitous
NYX	XL.CSNB	Vision	Ubiquitous
HPRP3P	AD.RP	mRNA processing	Ubiquitous
CHM	XL. Choroidermai	Metabolism	Ubiquitous
EFEMP1	AD.MD	Structural	Ubiquitous
MERTK	AR.RP	phagocytosis	Ubiquitous
PROM1	AR.Retinal degeneration	Vision	Ubiquitous
IMPDH1	AD.RP	Metabolism	Ubiquitous
RP9	AD.RP	Unknown	Ubiquitous
VMD2	AD.MD	Transport	Ubiquitous
RPGR	XL.COCD, CSNB, MD, RP	Transport	Ubiquitous
TIMP3	AD.MD	Structural	Ubiquitous
RP2	XL.RP	Vision	Ubiquitous
ELOVL4	AD.MD	Metabolism	Ubiquitous
PRPF8	AD.RP	mRNA processing	Ubiquitous

Adapted from RetNet (<http://www.sph.uth.tmc.edu/Retnet/disease.htm>) and Harvard University (<http://eyegene.meei.harvard.edu/OMGI/HMG-review/html.html>). For gene symbol and disease see abbreviations

1.2.1 Peripheral retinal dystrophies

1.2.1.1 Retinitis pigmentosa

Typical retinitis pigmentosa is characterised by atrophic changes involving the retina and RPE, leading to pigmentary changes due to the release of pigment by degenerating cells (Figure 2A). The manifestation of the disease includes narrowing or loss of the visual field as well as early night blindness and a decrease in central visual acuity. Variations may be observed in cases of atypical RP. There are 19 known RP genes and at least 17 predicted to exist by genetic mapping data (Phelan and Bok, 2000). Genes causing RP fall in different functional categories such as phototransduction, transcription factors, vitamin A cycle, metabolism and RNA processing (Table 1).

1.2.2 Central retinal dystrophies

Primary involvement of the central retina is the common feature shared among this group of retinopathies which include among other phenotypes, Best vitelliform macular dystrophy, central areolar choroidal dystrophy, Stargardt's disease, cone and cone-rod dystrophy, dominant drusen, Sorby's fundus dystrophy, North Carolina macular dystrophy, and pattern dystrophy (Inglhearn, 1998).

1.2.2.1 Vitelliform macular dystrophy (Best's disease)

Best disease is an autosomal dominant disorder with onset at young age (Blodi and Stone, 1990). The disease is characterized by deposits of lipofuscin resembling an egg yolk within and under the retinal pigment epithelium (Bakall et al., 1999) (Figure 2B). Over time, the yellowish material disintegrates progressively (Marquardt et al., 1998). The disease may progress to cause loss of visual acuity due to macular atrophic changes or choroidal neovascularization (Krämer et al., 2000). The VMD2 gene localized to chromosome 11q13 and was recently shown to be mutated in Best disease patients (Marquardt et al., 1998, Petrukhin et al., 1998).

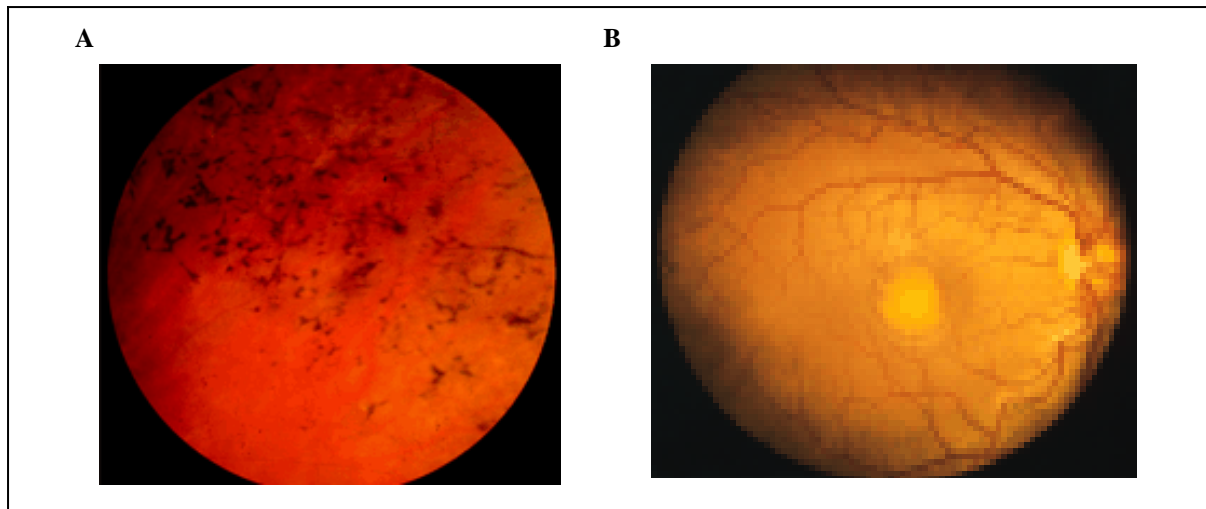


Figure 2: A/. Fundus photograph of a patient with retinitis pigmentosa. Note the pigmentary changes due to the release of pigment by degenerating RPE cells. The accumulated intraretinal pigmentary changes in peripheral retina take a morphological shape known as bone-spicule formation (Adopted from Zito et al., 2003). B/. Fundus photograph of a patient with Vitelliform macular dystrophy (Best disease). Submacular yellowish egg-yolk like material accumulates in and beneath the RPE (Adopted from Marquardt et al., 1998).

1.3 Phenotype oriented molecular genetic approach

In this approach, patients with a specific phenotype are collected and analysed using genetic linkage analyses (Dryja, 1997). Once the gene locus is identified the search can be refined using positional cloning or the candidate gene approach.

1.3.1 Genetic linkage analysis

Linkage analysis is used to identify the chromosomal location of a disease locus by demonstrating cosegregation of a disease phenotype and a DNA genetic marker. Microsatellite markers containing short tandem repeat DNA sequences are widely used in linkage analysis (Zhang et al., 1996). The likelihood that the marker allele and the disease phenotype are truly linked, compared to the likelihood that the association is only by chance is called the logarithm of the odds ratio (LOD score). LOD scores of 3 are generally regarded as significant.

1.3.2 Positional cloning

Following a locus identification of a disease causing gene by linkage analysis, fine mapping is employed to refine the chromosomal region. In most cases the narrowing is limited to about 1 centimorgan (cM) due to the limitation imposed by

the number of informative meioses. Subsequently all transcripts in the region are then analysed and confirmation of a gene as disease causing can be achieved through demonstration of a mutation (Collins, 1992).

1.3.3 Positional candidate gene approach

Known genes identified by linkage studies are analysed for cosegregation with the disease phenotype. Subsequent analysis including cloning and mutation screening are carried out for those genes which are linked to the disease phenotype (Zhang et al., 1996). Other information which can be useful for selection of a candidate gene include tissue expression, relevant function of the protein, and homology to a human gene causing similar disease.(Strachan and Read, 1999).

1.4 Gene oriented molecular genetic approach

In this approach the gene is identified first and a second step is to find out which phenotype is associated with mutation in that gene (Dryja, 1997). Gene expression can be used to narrow down the number of genes when aiming at particular phenotype known to have manifestations in a specific tissue type (Dryja, 1997). Several strategies were devised to study tissue or cell specific gene expression; these include beside others suppression subtractive hybridization (Diatchenko et al., 1996; Den Hollander et al., 1999), serial analysis of gene expression (Sharon et al., 2001) and differential display (Gorin et al., 1999).

1.5 Age related macular degeneration

Age related macular degeneration (AMD) is the most common cause of visual impairment in the elderly population and a major cause of vision loss in the western world. (Yates and Moore, 2000) The prevalence of AMD is increasing as life span is increasing. The disease is affecting the life of elderly people by decreasing the quality of life and increasing the dependency on others for care and help (Campochiaro, 1999). Several environmental factors such as smoking, hypertension, light exposure, and dietary habits have been proposed to play a role in AMD development; however, the most important risk factor appears to be the underlying genetic risks (Klaver et al., 1998).

1.5.1 Disease phenotype

Although the disease has been known for more than 100 years, classification of AMD has been difficult. This is mainly due to the partial overlapping of the clinical features between the disorders of the AMD group and secondly between the AMD and other early onset Mendelian macular dystrophies and even with other central retinopathies such as histoplasmosis (Bird et al., 1995). The classification was also complicated by the differences in the size, location, number and types of the pathological features associated with different stages of the disease (Yates and Moore, 2000). The international age – related maculopathy epidemiological study group (Bird et al., 1995) classified the disease as early age related maculopathy (ARM), if the associated lesions are either the soft drusen (whitish yellow spot), RPE atrophic changes, or there is an area of increased pigmentation. The term late ARM or AMD refer to the advanced form of the disease which is associated with visual morbidity. Presentations of the advanced form or the AMD include the geographic atrophy (GA) and choroidal neovascularization (CNV). Atrophic changes affecting the retinal pigment epithelium is the characteristic feature of the GA which is also known as dry, non–exudative, or atrophic AMD. CNV is characterized by the formation of new blood vessels which can be complicated by bleeding and scar formation ultimately leading to severe visual impairment or blindness.

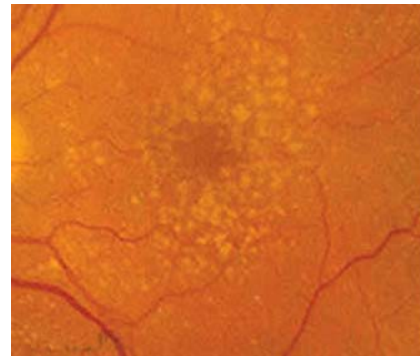
1.5.2 Pathogenesis

1.5.2.1 Drusen

Drusen are abnormal yellowish material (Figure 3), which accumulate in the extracellular matrix between the basement membrane of the RPE and the inner collagenous layer of Bruch's membrane. Several classification systems have been used with considerable variation due to the different methodology employed to describe the lesions, such as electron microscopy, fluorescein angiography, histology and histochemistry. The Wisconsin grading system (Klein et al, 1991), apply the term hard drusen to describe lesions ranging from 1-63 μ m in diameter. The term soft drusen was reserved for those lesions ranging from 63-125 μ m or larger than 125 μ m. Soft drusen can show homogenous density with clear margins or appear as graded density without clear margins (Hageman and Mullins, 1999).

Hard drusen can be found in many older people without symptoms (Leu et al., 2002), specially in the retinal periphery. The existence of multiple, or confluent soft drusen, in the macula increases the chances of developing AMD (Crabb et al., 2002). Various studies were conducted to understand the composition of drusen, but they showed discrepancies due to different drusen classification and different tissue preparation techniques (Hageman and Mullins, 1999). Nevertheless, using immunoreactivity, a partial profile of drusen composition was reported to contain immunoglobulin light chain, serum amyloid P, apolipoprotein E, complement C5A and c5b-9 complex, and factor x (Mullins et al., 2000).

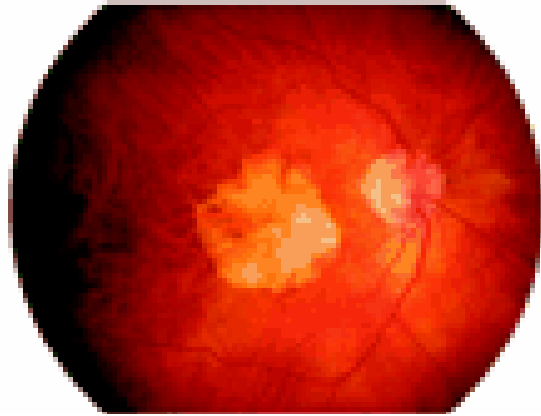
Figure 3: Drusen; abnormal yellowish material which accumulates in the extracellular matrix between the RPE basement membrane and the inner collagenous layer of Bruch's membrane. In the early stages of ARM there could be hard distinct drusen. With the advancement of the disease to the late ARM (AMD), the drusen becomes larger, confluent and indistinct with hazy margins. It contains undigested materials such as rod outer segments and cell debris (Adopted from van Leeuwen et al., 2003).



1.5.2.2 Geographic atrophy

This advanced form of AMD is characterised by atrophy of the retinal pigment epithelium (Figure 4) as well as the overlying photoreceptors (Sunness, 1999). The retinal pigment epithelium may show hypo- or hyperpigmentation (Bird, 1995). In the early stages the atrophy involves the area around the fovea (Sarks et al., 1988) and during the course of the disease, areas of atrophy increase and coalesce forming a larger area encircling the fovea. In the final stages, the fovea manifests atrophic changes. Patients with geographic atrophy suffer from central scotoma (Sunness et al., 1995) and dark adaptation abnormality progressing to gradual loss of vision (Sunness, 1999). Geographic atrophy may become apparent after flattening of RPE detachment or following fading of drusen (Schatz and McDonald, 1989). Pigmentary changes and large drusen tend to be risk factors for developing geographic atrophy as well as CNV. Geographic atrophy accounts for 20% of legal blindness caused by AMD (Ferris et al., 1984).

Figure 4: Geographic atrophy seen as an atrophic area involving the retinal pigment epithelium and the overlying photoreceptor cells in the macular area. The atrophic area is surrounded by an area of hyperpigmentation due to the displacement of the retinal pigment epithelium. Geographic atrophy can evolve as a small region of atrophy, near the fovea which enlarges gradually but sparing the fovea until late. The atrophic regions coalesce forming a large area of atrophy, and may involve centre of the fovea in the later stages. (Adopted Stone et al., 2001)



1.5.2.3 Choroidal neovascularization (CNV)

Choroidal neovascularization is the formation of new blood vessels starting from the choroid and progressively involve the Bruch's membrane and may extend into the subretinal space (Green and Enger, 1993). CNV may be followed by serious complications such as serous or haemorrhage (Figure 5) leading to RPE or retina detachment, and tears of the RPE (Green, 1999). Additionally, the formation of subretinal neovascular membrane can be complicated by haemorrhage which may lead to disciform scarring. Patients commonly complain that straight lines are no longer straight (metamorphopsia), and central acuity and vision could be lost (O'Shea, 1998). The triggering factor and the pathogenesis of CNV is poorly understood (Campochiaro, 2000), however experimental studies indicate that RPE may promote the progression of CNV in the initial stages by producing vascular endothelial growth factor (VEGF) and basic fibroblast growth factor (bFGF). Conversely, in advanced stages, RPE envelop the CNV through proliferation leading to regression (Lutty et al., 1999).

Figure 5: choroidal neovascularization complicated by haemorrhage. New blood vessels sprout in the choroid and invade the subretinal pigment epithelium spaced through the Bruch's membrane. This could result in leakage of serum or blood beneath the RPE, leading to RPE detachment or tears. CNV could also lead to disciform scarring. (Adopted from van Leeuwen et al., 2003)



1.5.3 Suspected pathological pathways

The pathogenesis of ARM/AMD is not known. Several questions remain such as what is the susceptibility factor which governs the disease and why do some patients develop GA, CNV, or RPE detachment. Sir Alan Bird suggested several sequential mechanisms through which genetic and other factors exert their effect; outer segment turnover increased, reduction of the catalytic activity of RPE degradative enzymes, toxic damage to the substrate of degradation, and Bruch's membrane abnormality leading to reduction in its capability of clearing toxic waste (quoted in Yates and Moore, 2000). Stone et al., (2001) suggested that the pathology and mechanisms of AMD may involve abnormal function of the choriocapillaris, Bruch's membrane, RPE, mitochondria, or the neurosensory retina. Other suspected mechanisms may include increased scleral rigidity, activation of the immune system, and toxic effects of light and nutritional deficiencies (Stone et al., 2001).

1.5.3.1 Oxidative stress

Oxidative stress has been suggested to be a causative factor or to participate in the pathogenesis of many diseases such as neurodegenerative diseases, heart disease and AMD (Winkler et al., 1999). Noell et al (1966) have shown that rats exposed continuously to light developed rod photoreceptor degeneration. Chronic sunlight exposures may play an important role in the development of AMD (Young, 1988). The location of the RPE in close proximity to the neurosensory retina and the choriocapillaris creates a favourable environment for chronic oxidative stress due to the high oxygen tension from the adjacent choriocapillaris (Liang and Godley, 2003). Furthermore, there is chronic sun light exposure and the photoreceptors contain high quantities of polyunsaturated fatty acids (PUFAs) mainly in the outer segments (Winkler et al., 1999). Photosensitization reactions involving these precursors may result in generation of reactive oxygen species such as singlet oxygen, hydrogen peroxide and superoxide ((Winkler et al., 1999). The generated reactive oxygen species can damage the cell components such as proteins, membrane lipids, carbohydrates and nucleic acids (Davis, 1991, Halliwell, 1991). The accumulation of lesions may act as a triggering factor for the injured RPE cell to undergo apoptosis (Cai et al., 2000).

1.5.3.2 Lysosomal enzymes dysfunction

The RPE plays an important role in phagocytosis and renewal of the photoreceptor outer segments (Bok, 1993). In rats it has been estimated that 10-15% of the rod outer segment are shed and phagocytosed daily (Young, 1976). RPE cells are equipped with a highly efficient lysosomal system, which is considered to be more effective in comparison to the liver lysosomal system (Zimmerman et al., 1983). The lipofuscin accumulation in the AMD patients is thought to result from the partially digested rod outer segments. Thus, abnormalities or malfunction of the lysosomal system in the rod outer segments may play a role in the pathogenesis of AMD (Verdugo and Ray, 1997). Several ways exist for internalization of materials into the lysosomal compartment. Large particles form autophagosomes which fuse with the lysosome (Klionsky and Emr, 2000). Minor particles can enter through a chaperone-mediated transport (Dice, 2000), or through invaginations of the lysosomal membrane (Marzella et al., 1981). The lysosomes contain a wide variety of hydrolytic degradative enzymes (Rakoczy et al., 1999), among these, α -mannosidase (α -Mann), β -glucuronidase (GUSB), arylsulfatase B (ASB) (Verdugo et al., 1996) and the cathepsin D (CatD) which is the most important among these and involved in opsin proteolysis (Hjelmeland et al., 1999). Boulton et al. (1994) reported an increase in CatD and acid phosphatase with age. Conversely, Cingle et al. (1996) reported a decrease in α -Mann activity. Comparison of many studies from different labs proved to be difficult. This could be due to differences in tissues or species analysed or different methodologies used in measuring enzyme activity (Verdugo and Ray, 1997). It was hypothesized that the age-related decrease in the lysosomal enzyme activity would lead to accumulation of lipofuscin (Ivy et al., 1989). However, Brunk and Terman, (2002) argued that the accumulation of lipofuscin may decrease the lysosomal enzyme activity. Recently it has been shown that N-retinylidene-N-retinylethanolamine (A2-E) which is an important component of the RPE lipofuscin is a strong inhibitor of the major lysosomal catabolic systems (Holz et al., 1999, Schutt et al., 2002, Bermann et al., 2001).

1.5.3.3 Immune complex and inflammation pathogenesis

Drusen are known to be associated with AMD. Several drusen constituents were identified by independent research groups (Mullins and Hageman, 1997, Klaver et al., 1998, Hageman et al., 1999, Mullins et al., 2000). Complement C5, α -antitrypsin and amyloid P are known to be members of the acute phase reactant with increased expression following inflammation, whereas apolipoprotein E, vitronectin and complement C play a role in mediated immune responses (Johnson et al., 2000).

Johnson et al., (2000), have suggested an immune complex involvement in the pathogenesis of AMD. Following genetic abnormality, oxidative stress or physical insult, new antigens expressed by RPE cells or autoantigens might be exposed to antibodies. Subsequently, immune complexes accumulate as a result of antibody-mediated complement attack on RPE cells which degenerate and contribute to drusen biogenesis.

Hageman et al., (2001) proposed an integrated hypothesis which implicates the local inflammatory and immune-mediated processes in the pathogenesis of drusen and AMD. This hypothesis speculates that injured RPE cells release cytokines or RPE debris into Bruch's membrane and may diffuse into the choroid. Neighbouring RPE cells form a seal covering the RPE debris and synthesize a new basal lamina. Molecules secreted by damaged RPE cells may act as chemoattractants for blood-born or choroidal monocytes, which migrate, and extend their terminations processes forming the drusen core into the RPE space. Molecules secreted by the RPE to antagonize dendritic cells effect, may enlarge the drusen. After maturation, the choroidal dendritic cells retract its processes and migrate, leaving behind the core drusen which may diffuse following growth and softening.

Anderson et al., (2002) suggested an involvement of local inflammation in drusen biogenesis. The entrapped cellular debris between the RPE and Bruch's membrane serve as a starting point for a myriad of inflammatory reactions and other processes including cytokine production, upregulation of acute phase proteins, complement cascade activation, dendritic cells attraction, and bystander cell lysis affecting the neighbouring RPE cells. The enlargement of drusen is

thought to occur as a result of encapsulation of the cell debris by proteins and lipids taking part in the inflammatory process.

This inflammation model is in context with spontaneous regression of drusen in some individuals and in particular those who have undergone laser photocoagulation treatment (Gass, 1972, Bressler et al., 1995), as it could act as pro-inflammatory stimuli.

1.5.4 Risk factors

1.5.4.1 Age

Several epidemiological studies were conducted to investigate the incidence and prevalence of ARM and AMD. Framingham eye study was the first major epidemiological study. In a total number of 2675 participants, the study showed an increase of prevalence with the advancement of age, for those aged 65-74 the ARM prevalence was 11% and for those aged 75-85 the prevalence was 28%. The age range of all the participants was between 52-85 years and the total ARM prevalence was 8.8% (Kahn, 1977).

Similarly other studies showed an increase in prevalence with age. The Beaver Dam study included 4962 participants with an age range between 43–86 years. Participants were categorized into 2 groups, those 75 years or older compared to those 43-54 years old. Several features were examined including large drusen which showed prevalence of 24% in the older group compared to 1.9% in the younger group, soft drusen (23% versus 2.1%), geographic atrophy (2% versus 0%), abnormalities of the RPE (26.6% versus 7.3%), and wet macular degeneration which showed 5.2% in the first group compared to 0.1% in the younger group. The authors concluded that features of ARM are common among those who are 75 years or older (Klein et al., 1992).

In another study conducted in Australia with 4345 participants, the ARM prevalence was indicated to be 15.1%. The study evaluated the presence of large drusen, soft distinct drusen, soft indistinct drusen and abnormalities of the RPE. The lesions showed prevalence rates of 6.3%, 7.5%, 4.3%, and 8.2% respectively. The study indicated that the prevalence rates of ARM and AMD increased sharply between the ages of 70 and 80 years, respectively (Mylan et al., 2000).

In an epidemiological study in Iceland, 1021 participants were evaluated for features including early ARM, geographic atrophy and exudative macular degeneration. With regard to early ARM, the prevalence of hard drusen with size below 63 μ m was found to be 85.3% for those 50-59 years old and 38.6% for those 80 years or old. When pigmentary abnormality and drusen of 63 μ m or greater were examined, the prevalence was 8.9% and 37.1% for the 2 groups respectively. Geographic atrophy was prevalent in ages of 52-87 years. Participants falling within this age range were categorized into four age groups, 50-59, 60-69, 70-79, and 80 years and older and the prevalence was 0.3%, 1.2%, 5.5%, and 25% respectively. Exudative macular degeneration was prevalent in those who are between 77-88 years and the prevalence was 2.3% for those 70 years and older and 9.8% for those 80 years and older (Jonasson et al., 2003). These studies showed strong correlation between ARM/AMD and age.

1.5.4.2 Genetic predisposition

The role of genetic factors in the pathogenesis of age related macular degeneration has been a controversial issue for many years. Several studies presented compelling arguments for the role of a genetic component in the pathogenesis of AMD. Klein et al., (1994) have reported the analysis of nine pairs of monozygotic twins with at least one member of the pair showing an advanced AMD feature. Laboratory tests were performed for Monozygosity confirmation. The ages of the twin's were in the range of 62 to 88 years, and environmental factors were similar for each twin pair. In eight twin pairs, there was concordance in the degree of visual impairment and fundus appearance. In the ninth pair, one twin showed wet AMD and blindness in one eye, while the other showed large drusen with no signs of visual impairment in both eyes. The authors concluded that a substantial genetic component may play a role in AMD pathogenesis for a large proportion of patients.

In a separate study, 36 AMD cases, 81 siblings of affected patients and 78 siblings as a control were assigned into a clinical study. Results confirmed that AMD features were present in 20 of the 81 siblings of affected patients. From the 78 control siblings only one was found to present AMD features. The result was considered to be statistically significant (Silvestri et al., 1994).

In another study, 134 twin pairs and two triplet sets were examined for signs of AMD. Results showed 100% concordance of AMD features in 25 monozygotic twins and 42% concordance in 12 dizygotic twins. The other participants did not show any features or signs of AMD. The authors concluded that the higher concordance in monozygotic compared to the relatively low concordance in dizygotic twins is statistically significant and is an indication for a strong relevance of genetic and nongenetic factors in AMD (Meyers et al., 1995).

Gottfredsdottir et al. (1999), examined 50 twin pairs and 47 spouses for signs of AMD. Zygosity was confirmed experimentally, and the environmental and other factors were similar, particularly for the twin pairs. 90% concordance of AMD features was reported in monozygotic twin pairs and 70% for the twin/spouse pairs. The result was considered statistically significant and strengthens the influence of genetic factors in AMD pathology. These analyses support the arguments that AMD might be influenced by genetic factors.

1.5.4.3 Cigarette smoking

Cigarette smoking has been well documented to be an influential factor in many types of cancer and in diseases of the cardiovascular system. Tobacco smoke contains several substances such as carbon monoxide, hydrogen cyanide, and nicotine (Evans, 2001). It has been suggested that, nicotine could increase the risk for developing AMD through two mechanisms. Firstly, it may reduce the antioxidant plasma levels, increasing the detrimental effects of oxidative stress. Secondly it could increase the choriocapillaris pressure through direct effect (Evans, 2001).

Also, cigarette smoking has been linked to reduction in macular pigment density (Hammond et al., 1996). Macular pigment is thought to protect the retina and enhance vision through the absorption of the short wavelength light (Wooten and Hammond, 2002), and through its antioxidant properties (Beatty et al., 1999).

Delcourt et al. (1998) conducted a population based study to assess smoking effect on AMD morbidity. Examining 2196 participants, the authors concluded that both smokers and former smokers are at high risk for developing signs of late age related macular degeneration. Early signs of AMD were found not to be associated with smoking in this study.

Several other studies presented strong evidence of association between smoking and the increased risk of developing AMD (Vinding et al., 1992, Smith et al., 1996, Christen et al., 1996, Seddon et al., 1996, Klein et al., 1998, Tamakoshi et al., 1998, Hyman et al., 1983).

1.5.4.4 Other suspected risk factors

Other risk factors such as social class, alcohol, and oestrogen were suspected to play a role in AMD development. However, evidence is inconclusive and conflicting (Evans, 2001, Gibson et al., 1986).

2. AIMS OF THE PRESENT STUDY

A long term RPE project was initiated to systematically analyse genes which are expressed in the RPE, and to assess their possible association with age related macular degeneration. Towards this goal a systematic approach was designed and the present study has four aims.

First, to establish a catalogue of differentially expressed ESTs from a bovine RPE cDNA library constructed in house using the suppression subtractive hybridization technique.

Second, to conduct extensive expression analyses for the bovine ESTs through the use of reverse Northern blot analyses and Northern blot hybridizations.

Third, to clone and characterize full length cDNA for 1-2 transcripts exclusively or preferentially expressed in the RPE and to determine their genomic structure and organization (human orthologous genes).

Finally, to identify highly frequent SNPs in the coding and non-coding genomic sequences of candidate genes for genetic susceptibility to age related macular degeneration (MGC2477, MT-Protocadherin and TRPM3 genes).

With the availability of appropriate SNPs and the respective haplotype frequencies, association studies can be undertaken in large cohorts of AMD patients and ethnically and age matched controls.

3. MATERIALS AND METHODS

3.1 Bovine RPE subtracted cDNA library construction

3.1.1 Isolation of poly (A)⁺ RNA and cDNA synthesis

A subtracted bovine RPE cDNA library was constructed in house by A. Gehrig. Briefly, RPE poly (A)⁺ RNA (50 ng) was isolated (oligotex mRNA kit, Qiagen) from total RNA and used for tester cDNA synthesis. Heart and liver poly (A)⁺ RNA (150 ng each) was isolated from total RNA and used to synthesize the driver cDNA. cDNA synthesis was performed following a modified SMART cDNA synthesis kit (Clontech, California). The first strand synthesis was primed with a modified random SMART CDS primer II (5'-AGCAGTGGTAACAACGCAGAGTACNNNNNTGTGG-3'). As the reverse-transcriptase has a tendency to add extra deoxycytidine nucleotides at the 5', a second primer, SMART II (5'-AAGCAGTGGTATCAACGCAGAGTACGCGGG-3'), rich in oligo (G) sequences was added to anneal to the deoxycytidine (C) nucleotides to create an extended template with universal priming site. A full length double stranded cDNA was obtained by long distance PCR using a 5' PCR primer II A (5'-AAGCAGTGGTATCAACGCAGAGT-3'), anchoring to the universal priming site.

3.1.2 Suppression subtraction hybridization (SSH)

According to the PCR-Select cDNA Subtraction kit (Clontech, California.), driver and tester cDNAs were digested with RsaI. The tester was separated into two portions; one sample was ligated to adaptor 1 (5'-CTAATACGACTCACTATAGGGCTCGAGCGGCCGCCCCGGGCAGGT-3') and the other was ligated to adaptor 2R (5'-CTAATACGACTCACTATAGGGCAGCGTGGTCGCGGCCGAGGT-3'), both samples were then hybridized separately with excess driver cDNA followed by a second round of hybridization where all samples were mixed together in excess of the driver. Two rounds of PCR reactions were performed and PCR products were inserted into a T/A cloning vector pCRII (Invitrogen, California).

3.2 Heat shock transformation

Agar-LB medium culture plates were prepared (30-50 ml medium each including 100 µg/ml ampicillin) and left to solidify. Culture plates were incubated at 37°C for 1 hour. Under sterile conditions, 100 µl X-Gal (20 mg/ml in Dimethylformamid) and 10

μl IPTG (200 mg/ml) were spread on each plate for colour selection of recombinant colonies. Plates were left under the hood for 30 minutes. Ligation reactions and competent cells TOP10F (Invitrogen, Karlsruhe) were thawed on ice and 2 μl of ligation reaction were mixed gently with competent cells. The vial was incubated on ice for 30 minutes. DNA uptake was induced by heat shock for exactly 30 seconds in 42°C water bath and the vial was again placed on ice. SOC medium (250 μl) was added and the vial was placed on a shaking incubator at 37°C for 20 minutes. Under sterile conditions, 70 μl from the transformation reaction were spread on an agar-LB medium culture plate, and plates were labelled and incubated at 37°C overnight.

SOC medium (100ml)

2g	Bacto®-Tryptone
0.5g	Bacto®-Yeast Extract
1ml	NaCl
0.25ml	1M KCl
1ml	2M Mg ²⁺ stock, filter sterilized
1ml	2M glucose, filter sterilized

Agar-LB medium (per liter)

10g	Bacto®-Tryptone
5g	Bacto®-Yeast Extract
5g	NaCl
15g	Bacto-agar

3.3 Colony picking and mini-culture preparation

Sterile 96 well Nuclon miniculture plates (Nunc, Wiesbaden, Germany) were prepared. Each well was filled with a 100 μl LB medium mixed with ampicillin (100 $\mu\text{g}/\text{ml}$) and inoculated with a single recombinant (white colour) colony from the transformation plates. Miniculture plates were then incubated at 37°C overnight.

LB medium (per liter)

10g	Bacto®-Tryptone
5g	Bacto®-Yeast Extract
5g	NaCl
The pH was adjusted to 7.0 with NaOH	

3.4 Replica plating

Nuclon 96-well replica plates were prepared with each well containing a 100 μl LB medium mixed with ampicillin (100 $\mu\text{g}/\text{ml}$). Corresponding wells were inoculated with 5 μl from the previous miniculture and plates were incubated at 37°C overnight. 45 μl of glycerol (15%) were then mixed with the content of each well and plates were stored at -80.

3.5 Generation of expressed sequence tags (ESTs)

3.5.1 Direct isolation of PCR inserts from pCRII vector

Plasmid DNA from the miniculture plates served as template for PCR amplification with M13 sense primer (5'-CGCCAGGGTTTTCCCAGTCACGAC-3') and M13

antisense primer (5'-AGCGGATAACAATTTTCACACAGGA-3'). PCR reactions were carried out in 25 µl volume containing 2 µl plasmid DNA (10-100 ng), 1.25 mM dNTPs, 10 pmol each M13 sense and antisense primer, 1X PCR buffer, 1.0 mM MgCl₂, and 1 unit Taq DNA polymerase. Thermal cycling was as follows: initial denaturation incubation at 94°C/5 min, followed by 29 cycles of 94°C/30 sec, 65°C/30 sec, 72°C/1 min. and a final extension cycle at 72°C/5 min.

3.5.2 Agarose gel electrophoresis

PCR fragments were separated by electrophoresis on a 1% agarose gel cast (1 g agarose in 100 ml 1x TBE buffer). After the agarose was completely dissolved, 1µl of ethidium bromide (200 ng / ml) was added. Wells were loaded with a mixture of 5 µl of the DNA sample and 3 µl of the loading buffer. The gel cast was run at 100 - 120 V in an electrophoresis chamber containing 1X TBE buffer. The bands were visualized on a transilluminator emitting ultraviolet (UV) light with wavelength range 250-400nm.

10x TBE buffer

89mM	Tris base
89mM	boric acid
20mM	Na ₂ EDTA, pH 8.3

3.5.3 Purification of PCR products

3.5.3.1 Exonuclease 1/Shrimp alkaline phosphatase (SAP) treatment

The advantages of this method are cost effectiveness, easy use and high sample throughput. At 37°C, both enzymes are active and residuals of PCR primers and nucleotides will be removed by the Exonuclease 1 and SAP treatment. At 80°C the enzymes are then inactivated and the PCR product used for subsequent reactions. Purification reactions were carried out in 10 µl volume containing, 2 µl of PCR product, 0.2 µl of exonuclease 1 (1 U/µl), 0.5 µl of SAP (1 U/µl), and 7.3 µl HPLC water. Reactions were incubated in a thermal cycling machine at 37°C for 15 minutes followed by 15 minutes at 80°C.

3.5.4 Cycle sequencing reaction

The pCRII vector nested primers were used for sequencing, either pCRII sense (5'-CTCGGATCCACTAGTAACGG-3') or pCRII antisense primer (5'GCCGCCAGTG

TGATGGATAT-3') and the sequencing reactions were performed following the ABI Prism Ready Reaction Sequencing Kit. Typically a 10 µl reaction volume contains 5 µl of the purified PCR product, 10 pmol of either forward or reverse primer, 2 µl HPLC water, and 2 µl of the Big dye master mix. Reactions were run in a thermal cycling machine as follows: initial denaturation incubation at 96°C/10 sec, followed by 24 cycles at 96°C/10 sec, 60°C/5 sec and 60°C for 4 minutes.

3.5.5 Ethanol (EtOH) DNA precipitation

The DNA resulting from the cycle sequencing reaction was precipitated according to the following protocol: 0.1 vol. 3M sodium acetate (Na OAc), 0.8 vol. HPLC water and 2.5 vol. of EtOH (95%) were added to 10 µl of DNA from the sequencing reaction. Thereafter the tubes were centrifuged for 15 minutes at full speed (14000 rpm). The DNA was precipitated and the pellet was then washed with 3 vol. EtOH (75%) before they were air dried (15-30 minutes). The pellets were then resuspended in 20-30 µl HPLC water and were analysed on an ABI 310 automated sequencer (Perkin-Elmer, Norwalk, USA).

3.6 Bioinformatics

Sequence search was performed using BlastN against databases, non redundant (nr), high throughput genomic sequences (htgs), and expressed sequence tag databases (dbEST) at the (http://searchlauncher.bcm.tmc.edu/seq-search/nucleic_acid-search.html) and against the human genome draft sequence (<http://www.ncbi.nlm.nih.gov/BLAST/>). The sequences were clustered into contigs, using the contig assembly program CAP 3 (<http://genome.cs.mtu.edu/sas.html>). Reverse Northern blot analyses was performed using Aida (Raytest GmbH) and GeneSpring (Silicon Genetics) softwares.

3.7 Expression analysis of ESTs

3.7.1 Reverse Northern blot analysis

Reverse Northern blot is a high throughput technique where many clones can be analysed simultaneously. Representative clones from the established EST clusters, were spotted onto a nylon membrane and hybridized with probes from cDNA of tester (RPE) and driver (heart and liver).

3.7.1.1 Nylon membrane transfer of cDNA

cDNA transfer analysis was carried out following Nucleic Acid Dot/Blot standard protocol (Schleicher & Schuell) with some minor modifications. Briefly, 3 μ l (300-500 ng) of target cDNA was suspended in 50 μ l TE buffer (pH 8.0) and denatured at 100 °C for 5 minutes and put on ice. Membrane was washed with deionised water then soaked in 6X SSC prior to use. 2 sheets of 3MM Whatman paper, prewet in 6X SSC were placed on the filter support of the Minifold II slot-blot apparatus (Schleicher&Schuell). Then, the membrane was placed on top of the filter paper and the apparatus was clamped. The diluted cDNA target was loaded on each well and the volume was adjusted to 400 μ l per well by topping with 6X SSC. Low vacuum was applied (\sim 1 ml/min). Then membrane was removed, labelled and target cDNA was immobilized by UV cross linking.

TE buffer, pH 8.0

10mM Tris-Cl, pH 8.0
1mM EDTA, pH8.0

20 X SSC 100 ml, pH7.0

17.53 g NaCl
8.82 g sodium citrate

3.7.1.2 Probes synthesis and radioactive labelling

First strand cDNA was synthesized from RPE, heart and liver and labelled radioactively. ThermoscriptTM RT increases the yield of cDNA product by allowing the use of high reaction temperatures which help prevent RNA secondary structures. Similarly, RNase inhibitor increases cDNA availability by degrading the RNA strand in RNA:DNA hybrids. For the RPE probe, 10 μ l of total RNA were mixed with 2 μ l of oligo-(dt) adaptor primer (1 μ g / μ l) and 2 μ l DEPC treated H₂O, and for the heart and liver probe, 3 μ l of total liver RNA (8 μ g / μ l) were mixed with 6 μ l of total heart RNA (4 μ g / μ l) and from this mixture, 1.5 μ l total RNA was adjusted to 14 μ l volume, adding 2 μ l oligo-(dt) adaptor primer (1 μ g / μ l) and 10.5 DEPC treated H₂O. Both probes were incubated at 72°C for 2 minutes and were put on ice before adding the following reagents for each reaction: 6 μ l first strand buffer, 1 μ l DTT (0.1 M), 1.5 μ l dNTP (20 mM dATP, dGTP, dTTP), 1 μ l RNase inhibitor, 5 μ l P³³-dCTP and 1.5 μ l ThermoscriptTM RT. Reactions were incubated at 55°C for 90 min.

3.7.1.3 Prehybridization and hybridization

Filters were prehybridized in MicrohybTM buffer (Research Genetics) for 2 hours at 42°C. Prior to hybridization, probes were purified by centrifugation through a

Sephadex (G-25) column and denatured at 95°C for 3 min, and then filters were hybridized with probes at 42°C overnight.

Sephadex G-25

12 g	sephadex
180 ml	TE buffer

3.7.1.4 Washing and exposure of filters on phosphor imaging screens

Filters were washed in 2X SSC/1% SDS/50°C/15 min, 1X SSC/1% SDS/50°C/15 min followed by 0.5X SSC/1% SDS/50°C/15 min, before exposure on phosphor imaging screens (Pharmacology labs) overnight.

10% SDS

10 g	SDS
ddH ₂ O to 100 ml	

3.7.2 Northern blot hybridizations

Northern blot hybridization reactions depend on the specificity of the probe, that it can only bind to targets with complementary sequence, and this in turn require the RNA to be physically separated by molecular weight on agarose gel, and transferred to a solid support such as nylon or nitrocellulose membranes. The RNA molecules must then be immobilized on the membrane to ensure that they can withstand the procedures of probing and washing. After the non-specifically bound probe is washed away, the probe–target complex can be identified, presumably the probe was already radioactively labelled or other tagging procedure was used. The complex location will help provide information about the target molecule.

3.7.2.1 RNA size fractionation in formaldehyde-agarose gels

Despite the fact that RNA is single–stranded, secondary structures can be formed in small regions of the RNA molecule. To prevent this, formaldehyde is included to the RNA loading buffer and the agarose gel cast.

Formaldehyde agarose gel includes 1.2 g agarose, 87 ml DEPC treated water, 10 ml of 10 X MOPS, and 3 ml formaldehyde (added after cooling below 60°C). Mini-Northern blot hybridizations were performed with RNA from 6 bovine tissues including, heart, liver, brain, retina, RPE, kidney and lung. Total RNA was isolated from frozen bovine tissues (oligotex mRNA kit, Qiagen) and 7 µg from each tissue were mixed with 12 µl loading buffer, denatured for 10 minutes at 65°C before loaded onto the gel and ran at 55-75 V in 1X MOPS buffer. The gel was photographed under

the UV light with a ruler beside it and then washed thoroughly for 5 min/DEPC treated water, 15 min/0.05 NaOH, 5 min/DEPC treated water and 10 min/20X SSC before RNA transfer.

RNA loading buffer, 1 ml		10× MOPS-Puffer	
100µl	10x MOPS	0,2 M	MOPS
500µl	Formamide	50 mM	NaOAc
185µl	Formaldehyde	10 mM	Na ₂ EDTA
40mg	Ficoll400		
215µl	H ₂ O		
0.04%	Bromphenolblue		

3.7.2.2 Capillary transfer of RNA onto nylon membrane

In capillary blotting, RNA molecules are transferred in a flow of buffer from wet stack of filter paper to the dry layers of the filter paper. Membrane is placed adjacent to the gel in the middle of tissue layers. RNA molecules will bind to the membrane surface, impeded from further transfer by the small pore size of the membrane. Orientation of the transfer could be either way, upwards or downwards. A typical upward capillary blot was prepared with layers from bottom including glass support, bridge (15 cm x full length GB003 paper) (Schleicher & Schuell) immersed in 20X SSC at both sides, gel, membrane (15 x 11 cm), 3 x 3MM Whatman wet papers (15 x 12cm), 3 x GB003 dry papers (15 x 12cm), 5 folded tissues, glass support and weight. The blotting procedure was left over night. Afterwards, layers were removed and wells and date were marked followed by membrane washing in 2X SSC (5-30 min). RNA was immobilized by microwave cross linking and membrane was stored in -20.

3.7.2.3 Vacuum transfer of RNA onto nylon membrane

A vacuum transfer apparatus (VacugeneTM, Pharmacia) was used to transfer RNA onto the nylon membrane. The advantages of using the apparatus are ease of use, efficient RNA transfer, and saving of time. The sponge sheet of the apparatus was washed with DEPC water before being laid on the apparatus with the smooth side facing upwards. Membrane (14 x 11cm) was soaked in 2 x SSC and put on top of the sponge sheet. A plastic sheet was placed on top leaving only the membrane uncovered. The gel was washed in 2X SSC before being laid on top of membrane and a continuous dripping of 20X SSC on top of gel was arranged. The vacuum transfer was allowed for 3-4 hours at -60 mbar. Afterwards, lanes were marked, RNA cross linked, and membrane was stored at -20.

3.7.2.4 Probe labelling with random priming

Random primer oligolabelling is based on the method first described by Feinberg and Vogelstein (1983). PCR products of bovine ESTs were used as probes and were labelled as follows; 3 µl of the probe were added to 8 µl aqua dest. and the tube was incubated for 5 min at 100°C. The tube was centrifuged for a short time at high speed and was put immediately on ice. Afterwards, the following reagents were added, 4 µl oligolabelling buffer (OLB), 1 µl bovine serum albumin (BSA), 1 µl Klenow fragment and 3 µl [$\alpha^{32}\text{P}$]-dCTP (3.000 Ci/mmol). Finally the reaction was incubated in a lead box for 3 hour at 37°C water bath or overnight at room temperature.

5X OLB-buffer

250 Mm	Tris-HCl, pH 8,0
25 mM	MgCl ₂
50 mM	b-Mercaptoethanol
je 96 µM	dATP, dGTP, dTTP
1 M	Hepes, pH 6,6
50 U (A ₂₆₀)	pd(N) ₆

3.7.2.5 Membrane prehybridization preparation

Membrane was soaked in Church buffer (20-30 ml in a tray) after it was warmed at 55°C in water bath. Prehybridization was carried out in 50 ml falcon tubes in which membrane was spread with RNA side turned inside of the tube and 5 ml of Church buffer were added. The tube was placed in a rotating oven at 60°C for 3 hours.

Church-Puffer

0,5M	Na ₃ PO ₄ , pH 7.2
1 mM	Na ₂ EDTA, pH 8.0
7%	SDS

3.7.2.6 Probe preparation

For probe purification a Sephadex G-25 column was prepared. Typically, a small amount of glass wool was placed at the bottom of a 1 ml syringe. Sephadex G-25 was loaded and the mini-column was packed by spinning the 1 ml syringe in a 15 ml conical tube for 3 min at 2000 rpm. The Sephadex column was calibrated with 100 µl TE buffer and centrifuged for 3 min at 2000 rpm. The labelled probe was removed from water bath and filled up to 100 µl with TE buffer and loaded onto the Sephadex column to be centrifuged for 3 min at 2000 rpm. The radioactivity of the recovered probe was measured, and then the probe was denatured for 5min at 100°C, centrifuged for a short pulse and put on ice.

3.7.2.7 Hybridization

The prehybridization solution was replaced by fresh preheated (55°C) Church buffer. Afterwards the probe was added and the hybridization was carried out overnight at 65°C.

3.7.2.8 Membrane washings, film exposure and development

As washing stringency depends on the probe, radioactivity was monitored throughout washings and stringency conditions were decreased accordingly. Following the standard protocols, blots were washed in 2X SSC/0.1% SDS/60°C/15 min, 1X SSC/0.1% SDS/60°C/15 min, and 0.5X SSC/0.1% SDS/60°C/15 min. Afterwards, membrane was dried and covered with Saran wrap and exposed to film for 3-7 days in -80.

3.7.3 Reverse Transcriptase (RT)-PCR analysis

Total RNA was isolated from 6 frozen human tissues including brain, heart, lung, retina, RPE and placenta using the RNA Clean system (Hybaid, Heidelberg, Germany).

3.7.3.1 RNA purification

DNase 1 was used to remove DNA contamination. According to the following protocol (Ambion): 1 µl of DNase 1 (2 units) and 0.1 volume of 10X DNase 1 buffer were added to 1 µg of total RNA. The reaction was adjusted to 10 µl with DEPC treated water and incubated at 37°C / 20 min. 1 µl of inactivation reagent was added and the tube was incubated at room temperature / 2min. Then centrifuged at 10.000 g /1 min and RNA was removed and stored at -80.

3.7.3.2 First strand cDNA syntheses

Total RNA was used to generate first strand cDNAs using the Superscript™ preamplification system according to the manufacturer instructions (Life Technologies, Karlsruhe, Germany). Typically, 1 µl of oligo-(dt)₁₂₋₁₈ (0.5 µg/µl) and 1 µl dNTPs (10mM) were added to 1 µg total RNA. The reaction volume was adjusted to 13 µl with DEPC treated water and incubated at 70°C/3 min. Then the reaction was put on ice for 5 minutes. Afterwards the following reagents were added:

4 μ l of 5X first strand buffer, 2 μ l 0.1 M DTT and 1 μ l Superscript™. Finally the reaction was incubated in thermal cycling machine at 42°C/52 min followed by 70°C/15 min.

3.7.3.3 cDNA quality check and normalization

cDNA quality check was performed using the ubiquitously expressed β -*Glucuronidase* gene (*GUSB*). Primers from exon 3 and 4 were amplified to test for full length cDNA synthesis. Primers from exon 6 and 7 were used to insure cDNA integrity (Table 2). The cDNAs were normalized across tissues to contain an equal concentration of *GUSB* transcripts.

Table 2: primers of the *GUSB* gene

Position	Name	Sequence	F / R*
Ex 3	GUSB 3	ACTATCGCCATC	F
Ex 4	GUSB 5	GTGACGGTGATG	R
Ex 6	GUSB 6	GATCCACCTCTG	F
Ex 7	GUSB 7	CCTTTAGTGTTT	R

* F / R = indicate forward or reverse

3.8 Cloning and characterization of AMD candidate genes

3.8.1. Bioinformatics

To identify the human orthologous of candidate clones, BlastN search was used against the human genome draft sequence. Protein homology searches and conserved domains were analysed by Psi-Blast (<http://www.ncbi.nlm.nih.gov/BLAST/>). Functional motifs, domains and possible protein family consensuses were analysed by PROSITE (<http://www.expasy.org/prosite/>), Blocks (http://blocks.fhrc.org/blocks/blocks/_search.html), and PRINTS (<http://www.bioinf.man.ac.uk/dbbrowser/PRINTS/>). Primers were designed (Table 3 & 4) on the bases of the available sequences of MGC2477 (NM-024099).and the FLJ11726 (recently TRPM3 gene) predicted genes using oligo version 2 (NAR program) (Rychlik and Rhoads, 1989) local software and the Primer3 input web site at (http://www-genome.wi.mit.edu/cgi-bin/primer/primer3_www.cgi/), the following primers were designed:

Table 3: primers of the *MGC2477* predicted gene

Position	Name	Sequence	F / R*
Ex 1	3-E5F1	CCACTAAAAGGCTGGATTTCG	F
Ex 2	3-E5F2	AAAAGTCCCATCTGCCGTC	F
Ex 6	3-E5F3	CCAGGATGTAGAAATGAAGGAC	F
Ex 3	3-E5R2	GACAGTGGTTGGTGGCTTCC	R
3'UTR	3-E5R	AAATGACTGCTAGAGAGGCC	R

* F / R = indicate forward or reverse

Table 4: primers of the *TRPM3* gene

Position	Name	Sequence	F / R*
Ex 1	TR-F1	CTCCGGGGACTGCTTTTG	F
Ex 2	TR-F2	CATCATACCCAGCACCAAAG	F
Ex 4	TR-F4	CCAGCCAAAACCTCAAGCAAG	F
Ex 6	TR-R1	CCCGTTGTCAGCCAGAATG	R
Ex 7+	TR-R3	GATTTGAGGTCTTGTTGAGC	R
Ex8+	TR-R4	AGACAAGTGGGAGGTTAGGAC	R

* F/R = indicate forward or reverse

3.8.2 Cloning of the MGC2477 predicted gene and 2 novel isoforms of the TRPM3 gene

3.8.2.1 Preparation of competent cells

ElectroMAX DH10B strain of *E.coli* (Gibco-BRL) was used to prepare competent cells. These cells are suitable for cloning of DNA which contains methyladenine and methylcytosine and could be efficiently used to clone prokaryotic and eukaryotic DNA. Transformation of these cells can only be achieved by electroporation.

A single 2-3 mm colony was dispersed into 5 ml LB medium and incubated at 37°C for overnight. Then 400 ml autoclaved LB medium was inoculated with 5 ml from the previous culture and incubated at 37°C on a shaker until optic density of 0.75 was achieved. Afterwards the culture was centrifuged at 5300 rpm for 10 minutes and pellets were recovered and resuspended in 100 ml 10% glycerol, followed by centrifugation at 5300 rpm for 10 minutes. The last step was repeated and thereafter cells were resuspended in 50 ml 10% glycerol and centrifuged at 5300 rpm for 10 min. Finally cells were dissolved in 1-2 ml 10% glycerol and aliquots of 50 µl were frozen in a dry ice / EtOH bath and stored at -80.

3.8.2.2 Ligation

A molar ratio of 3:1 insert: vector was used in the ligation reaction. For the determination of the quantity of insert needed, the following equation was used:

$$\text{ng vector} \times \text{kb insert} / \text{kb vector} \times \text{insert} : \text{vector molar ratio} = \text{ng insert}$$

The ligation reaction was carried out in 10 µl volume including, 5µl 2X Rapid Ligation Buffer, 1µl pGEM[®]-T Easy Vector (50ng), x µl PCR product and 1 µl T4 DNA Ligase (3 Weiss units/µl). The reaction volume was adjusted with deionised water.

3.8.2.3 Electroporation transformation

Aliquot of DH10B Electrocompetent cells (50µl) were thawed and mixed with 1 µl of ligated DNA. The mixture was carefully pipetted into a cuvette and placed into the electroporation chamber of the GenePulser[®] (BioRAD) apparatus. Then an electrical shock was applied (2.5 kv) and 500 µl of SOC medium was added. Afterwards the content was placed into a 1.5 ml tube and put on ice. Prior to that 10 µl of X-gal and 100 µl IPTG were spread on LB-ampicillin plates and allowed to absorb for 30 min. Finally 100 µl of the transformation products were spread on Amp/IPTG/X-gal plates, and the plates were incubated at 37°C overnight.

3.8.3 Standard polymerase chain reaction (PCR) amplification

PCR is an *in vitro* technique to synthesize a specific DNA fragment enzymatically. The reaction requires two oligonucleotide primers which anneal to the opposite strands, flanking the area needed for amplification. The reaction is catalysed by a thermostable DNA polymerase enzyme such as *Taq*-polymerase (*Thermus aquaticus*) or *Pfu*-polymerase (*Pyrococcus furiosus*). The DNA amplification is achieved by repetitive cycles of template denaturation, annealing of the primers and extension.

In most PCR reactions the following concentrations give satisfactory results: DNA template (~ 100ng), 200 µM each dNTP, 10-15pmol each primer, 1 mM MgCl₂, and 0.2 U of *Taq*-polymerase. However, in some cases the PCR reaction needs to be optimised by varying the parameters used. Most important is the Mg⁺⁺ which stabilizes the oligo-template interaction. Higher concentrations give more PCR product but decrease the PCR specificity, whereas low concentrations produce less PCR product but increase the specificity. Satisfactory results can be achieved using concentrations of 1–2.5 mM. Similarly, varying thermal cycle conditions could alter the outcome, high GC content regions of DNA may require an increased time of denaturation, and primers rich in GC content require high annealing temperatures, whereas longer PCR products need an extended extension time. Also additives such as glycerol (5-10%), formamide (1-5%), or DMSO (2-10%) could enhance the outcome of the PCR reaction.

3.8.4 Nested PCR

Two sets of primers were used in two rounds of PCR reaction. In a first PCR reaction an outer set of primers was used to amplify the target DNA, followed by the second

round of amplification using as a template the product of the first reaction to be amplified by a nested set of primers (Figure 6). The advantage of this method is an increased sensitivity of the assay.

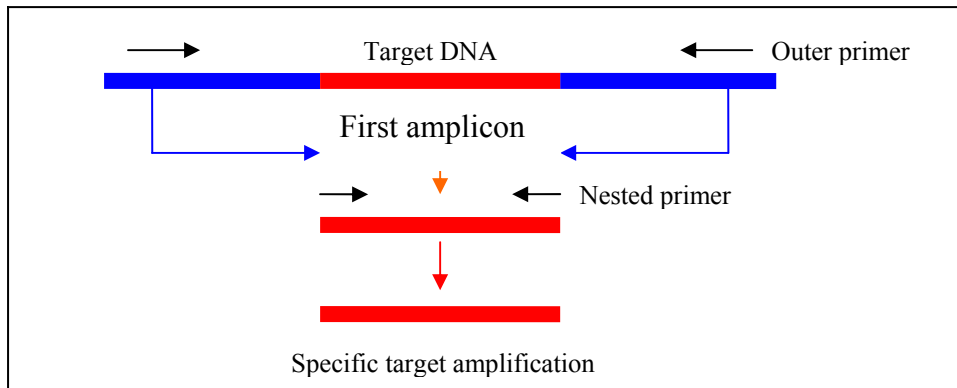


Figure 6: Nested PCR; red area= target DNA, first PCR performed with outer primers, whereas second PCR performed with nested primers.

3.8.5 Touch-down PCR

The advantage of this method is to reduce non specific PCR products. Amplification starts with cycles at higher annealing temperatures, followed by a decrease in the annealing temperature over the subsequent cycles. Temperatures frequently used are 3 cycles at 64°C as annealing temperature, followed by 3 cycles at 61°C, and finally 27 cycles at 58°C.

3.8.6 PCR library screening

This protocol was used to identify and sequence the 5' and 3' ends of inserts cloned into unidirectional libraries. The protocol requires the use of two vector primers, flanking the cloning site and four gene specific primers: As the exact position of each vector primer is not known, 4 primary PCR reactions were set, followed by secondary PCR reactions using the nested gene specific primers to increase the specificity (Figure 7).

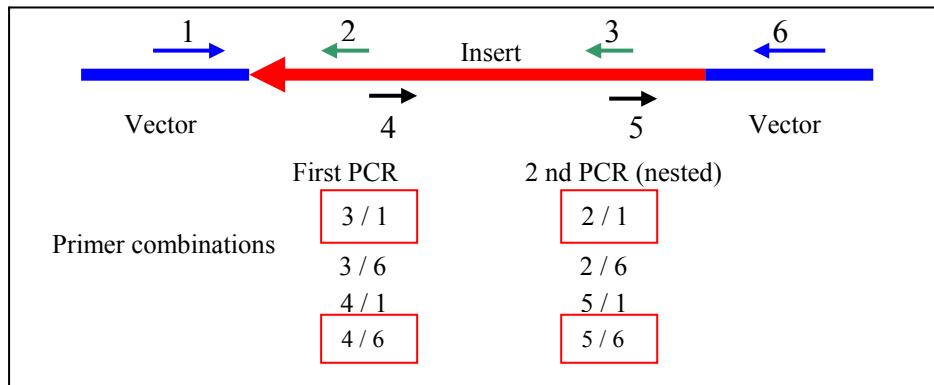


Figure 7: PCR library screening, primers 1 & 6 = vector primers, 2, 3, 4, & 5 = gene specific primers. First PCR round includes 4 reactions; 3/1, 3/6, 4/1, and 4/6. If 3/1 and 4/6 (boxed in red) were positive in first round PCR, then 2/1 and 5/6 would be positive in the second nested PCR reaction

3.8.7. DNA extraction from agarose gel

DNA was extracted from agarose gel for different purposes using the NucleoSpin[®] Extract protocol (Machery-Nagel, Düren, Germany). Typically, the gel piece containing the DNA fragment of interest was excised using a clean scalpel. 300 µl of buffer NT1 were added for each 100 mg of the gel fragment. Samples were incubated at 50°C until the gel piece was completely dissolved. Then, the samples were loaded into a NucleoSpin extract column and centrifuged at 10000 rpm/1 min. To optimise removal of inhibitors and contaminations a second washing was performed by adding 500 µl buffer NT2 and centrifuged at 14000 rpm/1 min. Afterwards 600 µl of buffer NT3 were added and samples were centrifuged at full speed/1 min, followed by a final wash with 200 µl NT3 and centrifuged at full speed/2 min to remove residual EtOH of the buffer. Finally, the column was placed into a clean 1.5 ml tube and 20-50 µl elution buffer NE were added. Then samples were left at room temperature for 1 min prior to centrifugation at full speed and recovery of DNA fragment.

3.9 Identification of single nucleotide polymorphism

3.9.1 Bioinformatics

Repeat masker (http://repeat_masker.genome.washington.edu/) was used to filter repetitive elements in the genomic sequence of genes of interest. Genes were searched against GeneCards (<http://bioinformatics.weizmann.ac.il/cards/>) and against Blat (<http://genome.ucsc.edu/cgi-bin/hgBlat?command=start>). SNPs in these databases were identified and marked. In order to verify these SNPs and to identify novel ones, all of the coding regions and 3-5 kb of up and downstream sequences of each gene were sequenced in 8 or 16 individuals (Johnson et al., 2001). In cases where these regions account for less than 30 fragments, intervening sequences were considered. Primers were designed and used in amplification of genomic DNA to yield a PCR product of approximately 500-600 bp. For primer sequences see appendix (Table 1, 2 and 3). Sequence analysis was performed using the software SeqMan[™] II (DNASTAR Inc. 1989-2002) where sequencing traces were aligned and SNPs were identified as they were marked by the sequencer program at mismatch bases.

3.9.2 Identification of high frequency SNPs and determination of allele frequency

In order to identify SNPs with frequencies of the minor allele greater than 17-20%, PCR reactions were carried out for all fragments of each gene using genomic DNA

from either 8 or 16 randomly chosen controls. Reactions were performed as a touch down PCR for 33 cycles using 1.0 or 1.5 mM MgCl₂ buffer with or without 4 % formamide. For specific conditions for each fragment see appendix (MT-Protocadherin Table 1, TRPM3 Table 2, and MGC2477 Table 3). For the MT-protocadherin gene SNP markers were genotyped in a set of 24 core Caucasian families (at least 2 members of each family, mainly father and mother) to help identify redundant SNPs.

3.9.3 Ready to use gel electrophoresis

Amplified PCR fragments were ran into ready to use agarose precast gels. The advantages of using these gels are ease of use and saving of time. 3 µl of the PCR product (from the 8 controls for MGC2477 and TRPM3 genes and 48 family controls for the MT-Protocadherin gene) were mixed with 7 µl of 1X TBE buffer into a 96 well plate. 8 µl of the mixture were loaded into the 96 well precast gel (1% agarose with ethidium bromide) using a multichannel pipette and ran in the ready to run electrophoreses system (Amersham) at 90 volts for 5min. DNA bands were visualised under UV light.

3.9.4 Denaturing high performance liquid chromatography (dHPLC)

Some fragments of the MT-protocadherin gene, including 5UTR2, 5UTR3, 5UTR4, 5UTR6, exon 2, exon 3, exon 10, exon 11, exon 13, exon 14, exon 16, 3UTR4, 3UTR5, 3UTR6 and 3UTR 11 were resolved with the WAVE DNA Fragment Analysis System (Transgenomic Inc., La Jolla, California). PCR products (5-8 µl) were eluted with a linear acetonitrile gradient including buffer A (0.1M triethylammonium acetate; TEAA, 0.1mM EDTA) and buffer B (0.1 M TEAA, 0.1 mM EDTA, 25% acetonitrile) at a flow rate of 0.9 ml/min. Optimal temperature required for the resolution of heteroduplex and homoduplex was determined by running the PCR product at increasing temperatures until a decrease in retention time was achieved.

3.9.5 DNA sequencing

The fragments of the TRPM3 and MGC2477 genes and the remaining fragments of the MT-protocadherin gene were sequenced. PCR products (25 µl) were diluted with 25 µl HPLC H₂O and 5-8 µl of the diluted product were purified by Exonuclease

1/Shrimp alkaline phosphatase. Purified PCR products were dried under the hood (~16-24 hours) and sent for commercial sequencing (MWG, Ebersberg).

4. RESULTS

4.1 Generation of ESTs derived from the bovine RPE cDNA library

A total number of 26 plates (96 wells) were randomly picked from the bovine RPE cDNA subtracted library. All plates were designated RPE as the library name and numbered from 1-26. Subsequently, 26 replica plates were generated and stored at -80°C. Clones were identified by their coordinates in the 96 well plates, so that the clone name consists of the library name, followed by the number of the plate and the clone position in the plate, i.e. RPE3-E5. 16 plates were amplified by PCR reactions using M13 forward and reverse primers (Table 5). Rest of the plates were stored at -80°C.

Table 5: Plates amplified and sequenced

Plate	Plate
RPE 1	RPE 16
RPE 2	RPE 20
RPE 3	RPE 21
RPE 6	RPE 22
RPE 7	RPE 23
RPE 8	RPE 24
RPE 10	RPE 25
RPE 12	RPE 26

Sizes of the PCR products ranged from 300-1200 bp with an average size of 600 bp. Clones with size equal or below 300 bp were not considered for further sequence analysis. In a first phase a total number of 1002 differentially expressed bovine RPE cDNA clones were sequenced as described (see materials and methods). In a second phase, a total number of 1377 bovine ESTs were generated and sequenced in collaboration with LYNKEUS BioTech, Wuerzburg.

4.2 Bioinformatics

Before the completion of the Human genome Draft, our high quality sequence data were normalised and clustered using CAP3 (<http://genome.cs.mtu.edu/sas.html>) and were searched using Blast N against the non-redundant (nr), high throughput genomic sequences (htgs) and ESTs databases (dbEST) of the GenBank. The normalised results revealed 3 groups of sequences, group 1 with identity to known genes, group 2 with matches to unknown sequences such as ESTs or unfinished genomic sequences. Group 2 was subcategorized into predicted genes, unknown transcripts, and those

with no significant similarity or homology to known sequences. Group 3 matched to mitochondrial genes (Table 6).

Table 6: Summary of first blast analysis (05 2001)

Group 1	Group 2	Group 3
Known genes	Unknown transcripts	Mitochondria genes
120	7 predicted genes 163 Unknown traces 86 No homology	3
Total 120	256	3

In this search, 1002 bovine ESTs were normalised using the contig assembly program CAP3 and searched using Blast N against nr, htgs and dbEST databases of the GenBank.

Afterwards, 376 EST clusters (correspond to 120 known genes and 256 unknown transcripts in Table 6) were blasted against the human genome draft sequence yielding 168 known human genes, 51 predicted human genes, 15 matches to unknown sequences and 41 ESTs with no homology (Table7). Bioinformatics analysis data were provided by Faisal Fadl El Mola (personal communication, 2003).

Table 7: Summary of the final blast analysis (03-2003)

Group 1	Group 2
Known human genes	Unknown transcripts
168	51 predicted genes 15 Unknown traces 41 No homology
Total 168	107

Bovines ESTs searches against the human genome draft sequence.

4.3 Expression analysis

4.3.1 Reverse Northern blot analysis

Reverse Northern blot analysis was performed to differentially screen the subtracted bovine cDNA library and to organize and prioritize subsequent work. Of the 376 EST clusters, 318 unique ESTs were spotted onto duplicate nylon membranes. Known genes such as Actin, glyceraldehyde-3-phosphate dehydrogenase GAPD and RPE-1 were spotted more than once (Table 8) to serve as controls. Five filters were generated, each filter with four copies, A, B, C, and D. Copies A and C from each filter were hybridized with bovine RPE cDNA (RPE 1, RPE 2 respectively).

	1	2	3	4	5	6	7	8	9	10	11	12
A	Empty	Actin	Actin	Actin	GAPD	GAPD	RPE-1	20-E4	10-C9	24-E4	24-F2	8-E8
B	8-H5	10-B4	20-G4	10-E7	6-H1	3-B6	20-D2	12-G3	6-C7	20-F5	23-D5	25-A6
C	23-D11	Empty	21-C7	Empty	25-D3	Empty	23-H10	21-B5	26-A11	1-A5	8-F1	16-A9
D	23-F8	12-B10	22-D3	7-G8	12-E4	25-F8	7-A12	21-D7	3-H9	21-F7	16-F1	26-G2
E	6-F8	Empty	6-F11	Empty	23-D2	Empty	25-G6	16-F8	3-D5	1-F12	26-A9	12-G5
F	10-D8	6-F6	24-C11	6-D11	23-G6	22-H5	22-E6	26-G10	16-D9	26-B3	23-E5	8-D12
G	23-C4	Empty	12-B1	Empty	3-E11	Empty	16-G10	16-H9	25-C5	6-H4	20-H6	22-E10
H	3-H11	16-E11	16-F3	24-C8	22-A2	3-F12	Actin	GAPD	GAPD	RPE-1	RPE-1	RPE-1

Table 8: Reverse Northern blot filter layout. Filter 1 of the reverse Northern blot as an example of filter layout design. The design shows a 96 well in which 74 bovine EST cDNAs were spotted randomly. The design also shows 22 controls including the water negative control (which is marked as empty) and the positive control where three known genes were spotted more than once; Actin (pink colour), glyceraldehyde-3-phosphate dehydrogenase (GAPD, red colour), and RPE1 (dull green colour).

Copies B and D were hybridized with bovine heart / liver cDNA (heart/liver 1, heart/liver 2 respectively).

Quantitative evaluation was performed using the Aida and GeneSpring software packages, three patterns of hybridization signals were identified and categorized in three groups: group I (equally strong signals on filters hybridized with RPE and heart/liver cDNA), group II (equally weak signals on filters hybridized with RPE and heart/liver cDNA) and group III (differential expression on filters hybridized with RPE) (Figure 8). In group I, 31 EST clusters were identified. Of these, 21 with identity to known genes, 3 predicted genes, 1 unknown transcript, 1 with multiple chromosome location and 5 from the no-significant similarity subcategory (Table 9). In group II (260 transcripts), 151 known genes and 109 unknown clones were included (Appendix, Table 4). Group III contains 27 clones including 14 clones with identity to known genes, 1 unknown transcript, 3 clones with no-significant similarity and 9 clones with multiple chromosomal locations (Table 10). Summary of group I, II and III of the reverse Northern blot analysis is shown in Figure 9.

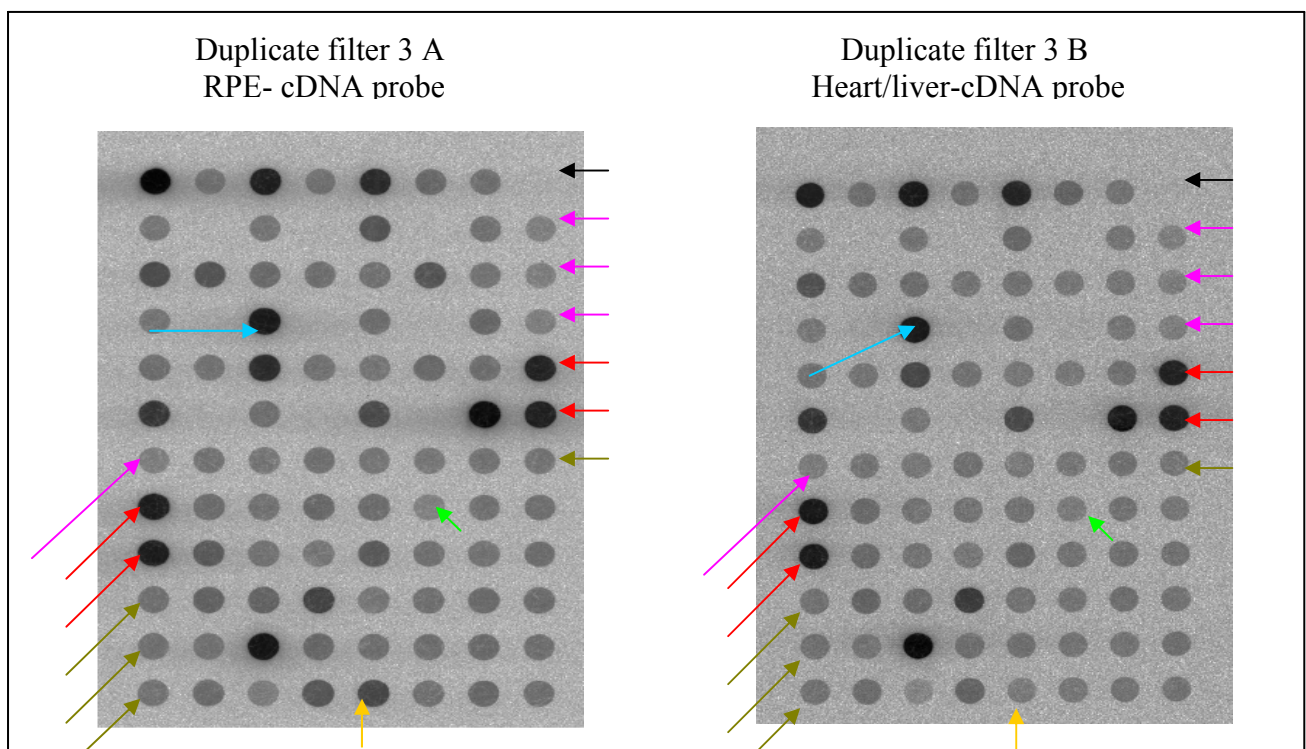


Figure 8: Reverse Northern blot quantitative evaluation of signal intensity in identical duplicate filters (3A, 3B) hybridized with different probes (RPE-cDNA probe, and Heart/liver-cDNA probe respectively). Blue arrow = group I, Green (shining) arrow = group II and Yellow arrow = group III. Controls: Black arrow = empty spot, Pink arrow = Actin, red arrow = GA₃PDH, green (Dull) = RPE1
Aida and GeneSpring software analysis was provided by Andrea Gehrig.

Table 9: Dot blot result; Group I (RPE versus Heart/Liver)

Equally strong signals on filters hybridized with RPE and heart/liver cDNA

Filter	Label	Plate	Clone	Gene Name/subcategory
1	D 08	RPE21	D07F	H. s. similar to ferritin heavy chain (ferritin H subunit) (LOC91738),
1	E 05	RPE23	D02F	M. c
1	G 03	RPE12	B01F	H. s. hydroxysteroid (17-beta) dehydrogenase 8
2	B 01	RPE01	G05R	H. s. ubiquinol cytochrome c reductase complex
2	C 10	RPE25	F04R	H. s. skip for skeletal muscle and kidney enriched inositol phosphatase
2	D 02	RPE22	H01F	H. s. retinaldehyde-binding protein 1 (RLBP1)
2	D 05	RPE24	E10F	H. s. low density lipoprotein-related protein 1B
2	D 08	RPE25	E08F	H. s. spectrin, alpha, non-erythrocytic
2	D 01	RPE21	A05F	H. s. pleckstrin homology domain containing, family B
2	E 09	RPE26	G01F	H. s. unc119 homolog
2	G 10	RPE08	H07F	No significant Similarity
2	H 01	RPE01	C01F	No significant Similarity
3	B 06	RPE08	H06F	H. s. protease, serine, 11 (IGF binding) (PRSS11), mRNA Length 2034
3	D 01	RPE07	C03F	H. s. retinaldehyde-binding protein 1 (RLBP1), mRNA, 1651 bp
3	E 10	RPE02	D12F	H. s. testis enhanced gene transcript (BAX inhibitor 1)(TEGT)
3	F 01	RPE01	F06R	Predicted gene
3	F 04	RPE24	D05F	Predicted gene
3	F 11	RPE02	A04F	No significant similarity
3	H 06	RPE20A	G08F	No significant similarity
4	C 09	RPE06	B06F	H. s. similar to ATP synthase, H ⁺ transporting, mitochondrial F1F0, subunit g (LOC63334),
4	B 04	RPE16	A04F	H. s. BCL2-like 1 (BCL2L1), mRNA, 735 bp
4	B 10	RPE20A	E10F	H. s. similar to active BCR-related gene (H. sapiens) (LOC91794), mRNA, 1234 bp
4	D 10	RPE12	A06F	H. s. ATX1 (antioxidant protein 1, yeast) homolog 1 (ATOX1), p
4	F 12	RPE20A	G05F	Human unknown (without exon-intron boundaries)
5	B 11	RPE03	F04F	H. s. retinol-binding protein 1, cellular (RBP1),
5	C 09	RPE24	B08F	H. s. component of oligomeric golgi complex 5 (COG5)
5	C 11	RPE23	C09F	H. s. defender against cell death 1 (DAD1),
5	B 01	RPE16	G03F	H. s. succinate dehydrogenase, subunit A (SDHA)
5	D 06	RPE02	E04F	H. s. siver (mouse homolog) like (SILV), mRNA
5	F 01	RPE06	B08F	No significant similarity
5	E 10	RPE21	E05F	Predicted gene

H. s. = Homo sapiens, M. c = multiple chromosomal location, label = refer to Aida and GeneSpring software labelling.

Table 10: Dot blot result; Group III (RPE versus heart/liver)

Differential expression on filters hybridized with RPE

Filter	Label	Plate	Clone	Gene Name/subcategory
1	G 09	RPE25	C05F	H. s. retinal G protein coupled receptor (RGR), mRNA 1414 bp
1	E 11	RPE26	A09F	H. s. lecithin retinol acyltransferase (phosphatd- ychohline - retinol O-acyltransferase) (LRAT).
1	G 10	RPE06	H04F	H. s. guanine nucleotide binding protein (G protein), gamma transducing activity polypeptide 1 (GNGT1), mRNA, 388 bp
1	G 11	RPE20A	H06F	H. s. guanine nucleotide binding protein (G protein), gamma transducing activity polypeptide 1 (GNGT1) mRNA, 388 bp
1	F 02	RPE06	F06F	M. c
1	B 10	RPE20A	F05F	Human unknown (without exon-intron boundaries)
1	F 11	RPE23	E05F	H. s retinal degeneration, slow (retinitis pigmentosa 7) (RDS)
1	A 10	RPE24	E04F	M. c.
2	B 12	RPE12	E01F	H .s. retinal G protein coupled receptor (RGR), mRNA,
2	F 04	RPE06	E07F	M. c.
2	F 10	RPE25	A01F	M. c.
2	E 08	RPE23	D06F	M. c.
2	E 05	RPE26	D06F	H. s. sex comb on midleg homolog 1 (SCMH1), 1937bp mRNA
3	D 12	RPE07	F04F	H. s. retinal pigment epithelium-specific protein (65kD) (RPE65)
3	C 03	RPE08	B02F	H. s. vitelliform macular dystrophy (Best disease, bestrophin) (VMD2)
3	F 05	RPE26	G04F	M. c.
3	H 01	RPE22	F08F	M. c.
3	G 03	RPE20A	B12F	No significant similarity
4	C 01	RPE22	B03F	H. s. rhodopsin (opsin 2, rod pigment) (retinitis pigmentosa 4, autosomal dominant) (RHO)
4	F 06	RPE08	A09F	No significant similarity
4	B 05	RPE03	D08F	H. s. membrane frizzled-related protein (MFRP).
4	E 07	RPE08	E10F	M. c.
4	D 02	RPE22	G01F	H. s. active BCR-related gene (ABR), mRNA
4	H 06	RPE20A	E12F	No significant similarity
5	B 08	RPE01	B02F	H. s. retinol dehydrogenase 5 (11-cis and 9-cis) (RDH5), Mrna, 1229 bp
5	B 06	RPE01	G12F	H. s. lecithin retinol acyltransferase (phosphatdy- l-chohline -retinol O-acyltransferase) (LRAT)
5	E 05	RPE23	A06F	M.c

H. s. = Homo sapiens, M. c. = multiple chromosomal location, label = refer to Aida and GeneSpring software labelling.

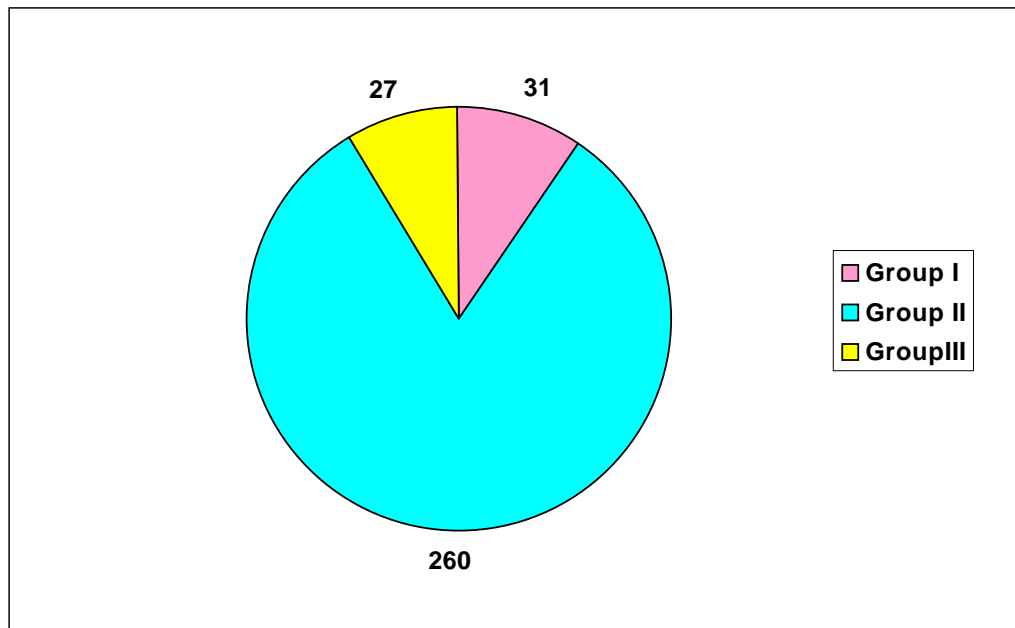


Figure 9: Summary of Reverse Northern blot results; Group I; strong signals in filters hybridized with RPE and heart/liver, group II; low signals in filters hybridized with RPE and heart/liver, group III; differential expression of RPE transcripts.

4.3.2 Northern blot hybridizations

A total number of 107 normalized predicted genes and unknown clones (Table 7) from group I, II, and III (reverse Northern blot analysis) were further analysed by Northern blot hybridization to a nylon membrane containing total RNA derived from bovine heart, liver, brain, retina, RPE, kidney, and lung.

Four expression patterns were observed including RPE-specific, retina-specific, tissue restricted (with RPE or retina, or both being included), and ubiquitous expression (Figure 10).

The Northern blot analyses of the 107 clones revealed 53 clones with detectable signals. Of these, 7 were RPE-specific, 3 retina-specific, and 14 tissue restricted transcripts, while 29 EST clusters were ubiquitously expressed (Table 11). Evaluation was not possible for 54 EST clusters due to lack of signal, unclear signals or reduced quality of the hybridization (Table 12).

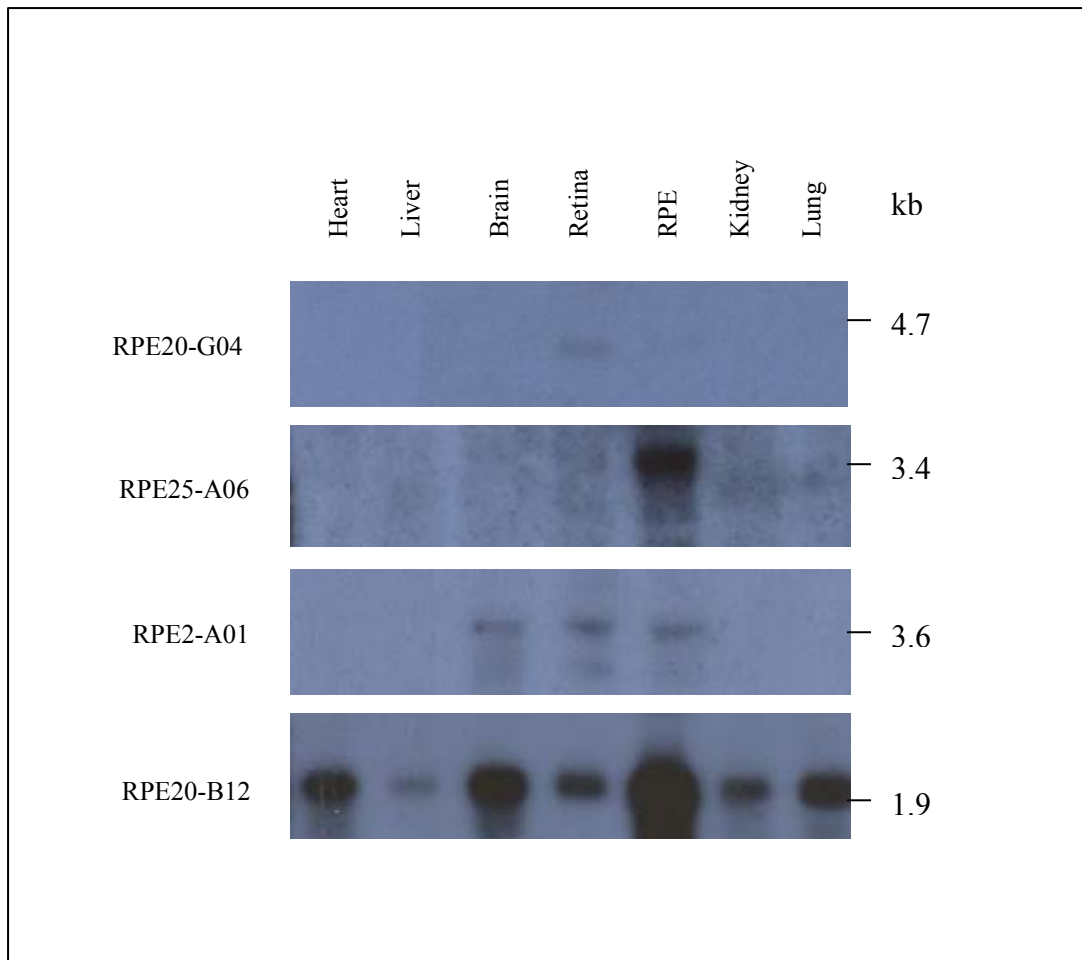


Figure 10: Expressional patterns of Northern blot analyses, RPE specific (RPE25-A06), retina specific (RPE20-G04), tissue restricted (RPE2-A01), and ubiquitous (RPE20-B12).

Table 11: Expression patterns of clones with identifiable signals in Northern blot analyses

Pattern of expression	Number of clones
RPE specific	7
Retina specific	3
Tissue restricted	
RPE / retina	7
Brain/retina/RPE	3
Brain/retina/RPE/kidney	1
Retina/RPE/kidney	1
RPE/kidney	1
RPE/liver	1
Ubiquitous	29
Total	53

Table 12: Northern blot result of 107 bovine cDNAs

Blot ID	plate ID	clone ID	Heart	Liver	Brain	Retina	RPE	Kidney	Lung	comments
090	RPE01	F06R	nep	nep	nep	nep	nep	nep	nep	Unclear signal
091	RPE01	C01F	nep	nep	nep	nep	nep	nep	nep	Unclear signal
092	RPE01	A05F	nep	nep	nep	nep	nep	nep	nep	Unclear signal
093	RPE01	D02F	-----	-----	-----	++	+	-----	-----	
094	RPE01	C07F	nep	nep	nep	nep	nep	nep	nep	Unclear signal
095	RPE01	C09F	nep	nep	nep	nep	nep	nep	nep	Reduced quality
088	RPE02	D09F	nep	nep	nep	nep	nep	nep	nep	Unclear signal
089	RPE02	D07F	nep	nep	nep	nep	nep	nep	nep	Unclear signal
107	RPE02	B07R	-----	+	-----	-----	+	-----	-----	
108	RPE02	D08R	+	+	+	+	+	+	+	
111	RPE02	A01F	-----	-----	+	+	+	-----	-----	
086	RPE03	E05F	-----	-----	-----	++	+	-----	-----	
087	RPE03	B06F	nep	nep	nep	nep	nep	nep	nep	Unclear signal
112	RPE03	D03F	+	+	+	+	++	+	+	
184	RPE03	D12R	-----	-----	-----	-----	-----	-----	-----	No signal
074	RPE06	B08F	nep	nep	nep	nep	nep	nep	nep	Unclear signal
075	RPE06	E07F	nep	nep	nep	nep	nep	nep	nep	Reduced quality
082	RPE06	F05F	nep	nep	nep	nep	nep	nep	nep	Reduced quality
083	RPE06	C08F	+	+	+	++	+	+	+	
084	RPE06	C07F	nep	nep	nep	nep	nep	nep	nep	Reduced quality
106	RPE06	F02F	nep	nep	nep	nep	nep	nep	nep	Unclear signal
115	RPE06	C10F	-----	-----	-----	+	++	-----	-----	
150	RPE06	C04F	+	+	+	+	+	+	+	
081	RPE07	F11F	-----	-----	+	++	+	-----	-----	
105	RPE07	H02F	nep	nep	nep	nep	nep	nep	nep	Reduced quality
118	RPE07	D02F	nep	nep	nep	nep	nep	nep	nep	Unclear signal
176	RPE07	G08F	-----	-----	-----	-----	-----	-----	-----	No signal
186	RPE07	B09R	-----	-----	-----	+	-----	-----	-----	
016	RPE08	F02F	nep	nep	nep	nep	nep	nep	nep	Unclear signal
032	RPE08	A09F	-----	-----	-----	+	++	-----	-----	
033	RPE08	E10F	+	+	+	+	+	+	+	
077	RPE08	F01F	nep	nep	nep	nep	nep	nep	nep	Unclear signal
078	RPE08	E04F	nep	nep	nep	nep	nep	nep	nep	Unclear signal
079	RPE08	H05F	nep	nep	nep	nep	nep	nep	nep	Unclear signal
119	RPE08	C05F	+	+	+	+	+	+	+	
120	RPE08	E05F	nep	nep	nep	nep	nep	nep	nep	Reduced quality
121	RPE08	F10R	nep	nep	nep	nep	nep	nep	nep	Reduced quality
064	RPE10	F07R	nep	nep	nep	nep	nep	nep	nep	Unclear signal
066	RPE10	B10F	-----	-----	-----	+	+	-----	-----	
068	RPE10	G09R	nep	nep	nep	nep	nep	nep	nep	Unclear signal

+ = 1 fold, +E = > 1 fold, +,- = < 1 fold, , ----- = no signal, nep = no evaluation possible.

Continue table 12: Northern blot result of 107 bovine cDNAs

Blot ID	plate ID	clone ID	Heart	Liver	Brain	Retina	RPE	Kidney	Lung	comments
069	RPE10	E07R	+	+	+	+	+	+	+	
122	RPE10	B11F	+	+	+	+	+	+	+	
124	RPE10	H01R	nep	nep	nep	nep	nep	nep	nep	Unclear signal
174	RPE10	A10F	----	-----	----	-----	+	-----	-----	
062	RPE12	H06F	+	+	+	+	+	+	+	
125	RPE12	A09F	-----	-----	----	++	+	-----	-----	
171	RPE12	B10F	-----	-----	----	-----	++	-----	-----	
172	RPE12	E04F	-----	-----	----	-----	----	-----	-----	No signal
173	RPE12	G03F	nep	nep	nep	nep	nep	nep	nep	Reduced quality
126	RPE16	G08F	-----	-----	----	-----	+	-----	-----	
127	RPE16	G12R	nep	nep	nep	nep	nep	nep	nep	Unclear signal
167	RPE16	C07F	-----	-----	-----	-----	----	-----	-----	No signal
068	RPE16	F09F	nep	nep	nep	nep	nep	nep	nep	Unclear signal
169	RPE16	D01F	+	+	+	++	+	+	+	
178	RPE16	H08F	-----	-----	-----	-----	----	-----	-----	No signal
183	RPE16	H08F	-----	-----	-----	-----	----	-----	-----	No signal
020	RPE20A	B12F	+, -	+, -	+	+, -	++	+, -	+	
042	RPE20A	E04F	+	+	+	+	+	+	+	
044	RPE20A	G04F	-----	-----	----	+	----	-----	-----	
098	RPE20A	A07R	+	+	+	++	+	+	+	
103	RPE20A	H02F	nep	nep	nep	nep	nep	nep	nep	Unclear signal
156	RPE20A	E12F	nep	nep	nep	nep	nep	nep	nep	Unclear signal
157	RPE20A	F05F	-----	-----	-----	-----	----	-----	-----	No signal
160	RPE20A	D02F	+	+	+	+ E	+	+	+	
161	RPE20A	H04F	+	+	+	+	+	+	+	
162	RPE20A	E03F	+	+	+	+	+	+	+	
163	RPE20A	D12F	-----	-----	-----	-----	----	-----	-----	No signal
182	RPE20A	E05F	-----	-----	-----	-----	----	-----	-----	No signal
101	RPE21	A09F	nep	nep	nep	nep	nep	nep	nep	Reduced quality
148	RPE21	E05F	-----	-----	-----	+	++	+	-----	
036	RPE22	F08F	+	+	+	+	+	+	+	
153	RPE22	D06F	-----	-----	-----	-----	----	-----	-----	No signal
189	RPE22	A03F	-----	-----	-----	-----	----	-----	-----	No signal
190	RPE22	D03F	-----	-----	-----	-----	----	-----	-----	No signal
052	RPE23	F08F	nep	nep	nep	nep	nep	nep	nep	Unclear signal
053	RPE23	H07F	+	+	+	+	+	+	+	
055	RPE23	D05F	+	+	+	++	+	+	+	
097	RPE23	F01F	-----	-----	-----	-----	+	-----	-----	
136	RPE23	A10R	nep	nep	nep	nep	nep	nep	nep	Reduced quality
152	RPE23	D11F	-----	-----	-----	-----	----	-----	-----	No signal

Continue table 12: Northern blot result of 107 bovine cDNAs

Blot ID	plate ID	clone ID	Heart	Liver	Brain	Retina	RPE	Kidney	Lung	comments
165	RPE23	E08F	-----	----	----	----	----	----	----	No signal
166	RPE23	D12F	+	+	+	+	++	+	+	
180	RPE23	B05F	-----	----	----	----	----	----	----	No signal
181	RPE23	G11F	-----	----	----	----	----	----	----	No signal
191	RPE23	A02F	-----	----	----	----	----	----	----	No signal
192	RPE23	F09F	-----	----	----	----	----	----	----	No signal
022	RPE24	H07F	-----	----	+	+	+	----	---	
037	RPE24	E04F	+	+	+	+	+	+	+	
071	RPE24	A09F	+	+	+	+	+	+	+	
138	RPE24	D11F	-----	----	----	----	+	----	---	
147	RPE24	D05F	+	+	+	++	+	+	+	
158	RPE24	B10F	-----	----	----	----	----	----	----	No signal
159	RPE24	F02F	-----	----	+	+	+	+	----	
024	RPE25	A06F	-----	----	----	----	+	----	----	
038	RPE25	A01F	+	+	+	+	+	+	+	
128	RPE25	E01F	nep	nep	nep	nep	nep	nep	nep	Reduced quality
140	RPE25	F11F	+	+	+	+	+	+	+	
141	RPE25	G09R	-----	----	----	----	+	++	----	
142	RPE25	H05F	-----	----	----	+	++	+	----	
164	RPE25	D03F	+	+	+	+	+	+	+	
187	RPE25	F08F	-----	----	----	+	----	----	----	
013	RPE26	C06F	+	----	+	++	+E	+	+	
039	RPE26	G04F	+	+	+	+	+	+	+	
050	RPE26	A03F	-----	----	----	----	+	----	----	
129	RPE26	A11F	nep	nep	nep	nep	nep	nep	nep	Reduced quality
144	RPE26	D03F	+	+	+	+	+	+	+	
145	RPE26	F08F	-----	----	----	+	++	----	----	
193	RPE26	C08F	-----	----	----	----	----	----	-----	No signal

+ = 1 fold, +E = > 1 fold, +,- = < 1 fold, , ----- = no signal, nep = no evaluation possible.

The 53 transcripts for which a signal was detected (Figure 11) were subcategorized into three categories; 22 human unknown transcripts, 20 human predicted genes and 11 clones with no significant similarity (Table 13). Three transcripts from the predicted gene subcategory were later isolated and characterized by other groups and one clone (RPE16-G8) became known gene by showing similarity to SLC4A5 gene (Table 13).

Table 13: Expression and subcategorization of the 53 transcripts with identifiable signal

No	Plate ID	Clone ID	Expression	Subcategory
01	RPE20A	G04F	Retina	Human unknown
02	RPE07	B09R	Retina	Human unknown
03	RPE23	F01F	RPE	Human unknown
04	RPE25	A06F	RPE	Human unknown
05	RPE25	G09R	RPE/Kidney	Human unknown
06	RPE08	A09F	RPE/Ret	Human unknown
07	RPE06	C10F	RPE/Ret	Human unknown
08	RPE24	F02F	RPE/Ret/Brain/Kidney	Human unknown
09	RPE22	F08F	Ubiquitous	Human unknown
10	RPE24	E04F	Ubiquitous	Human unknown
11	RPE25	A01F	Ubiquitous	Human unknown
12	RPE20A	E04F	Ubiquitous	Human unknown
13	RPE23	D05F	Ubiquitous	Human unknown
14	RPE12	H06F	Ubiquitous	Human unknown
15	RPE20A	A07R	Ubiquitous	Human unknown
16	RPE03	D03F	Ubiquitous	Human unknown
17	RPE08	C05F	Ubiquitous	Human unknown
18	RPE26	D03F	Ubiquitous	Human unknown
19	RPE20A	D02F	Ubiquitous	Human unknown
20	RPE23	D12F	Ubiquitous	Human unknown
21	RPE16	D01F	Ubiquitous	Human unknown
22	RPE10	E07R	Ubiquitous	Human unknown
23	RPE16	G08F	RPE	Predicted gene →kg
24	RPE24	D11F	RPE	Predicted gene
25	RPE01	D02F	RPE/Ret	Predicted gene →kg
26	RPE10	B10F	RPE/Ret	Predicted gene →kg
27	RPE03	E05F	RPE/Ret	Predicted gene
28	RPE26	F08F	RPE/Ret	Predicted gene →kg
29	RPE07	F11F	RPE/Ret/Brain	Predicted gene
30	RPE24	H07F	RPE/Ret/Brain	Predicted gene
31	RPE02	A01F	RPE/Ret/Brain	Predicted gene
32	RPE21	E05F	RPE/Ret/Kidney	Predicted gene
33	RPE24	D05F	Ubiquitous	Predicted gene
34	RPE10	B11F	Ubiquitous	Predicted gene
35	RPE25	D03F	Ubiquitous	Predicted gene
36	RPE06	C04F	Ubiquitous	Predicted gene
37	RPE26	C06F	Ubiquitous	Predicted gene
38	RPE24	A09F	Ubiquitous	Predicted gene
39	RPE20A	H04F	Ubiquitous	Predicted gene
40	RPE23	H07F	Ubiquitous	Predicted gene
41	RPE26	G04F	Ubiquitous	Predicted gene
42	RPE08	E10F	Ubiquitous	Predicted gene
43	RPE25	F08F	Retina	No significant similarity
44	RPE10	A10F	RPE	No significant similarity
45	RPE12	B10F	RPE	No significant similarity
46	RPE26	A03F	RPE	No significant similarity
47	RPE02	B07R	RPE/Liver	No significant similarity
48	RPE12	A09F	RPE/Ret	No significant similarity
49	RPE20A	E03F	Ubiquitous	No significant similarity
50	RPE25	F11F	Ubiquitous	No significant similarity
51	RPE02	D08R	Ubiquitous	No significant similarity
52	RPE06	C08F	Ubiquitous	No significant similarity
53	RPE20A	B12F	Ubiquitous	No significant similarity

Ret = retina, kg = known gene, No = correspond to the number of Northern blot analyses in Figure 11.

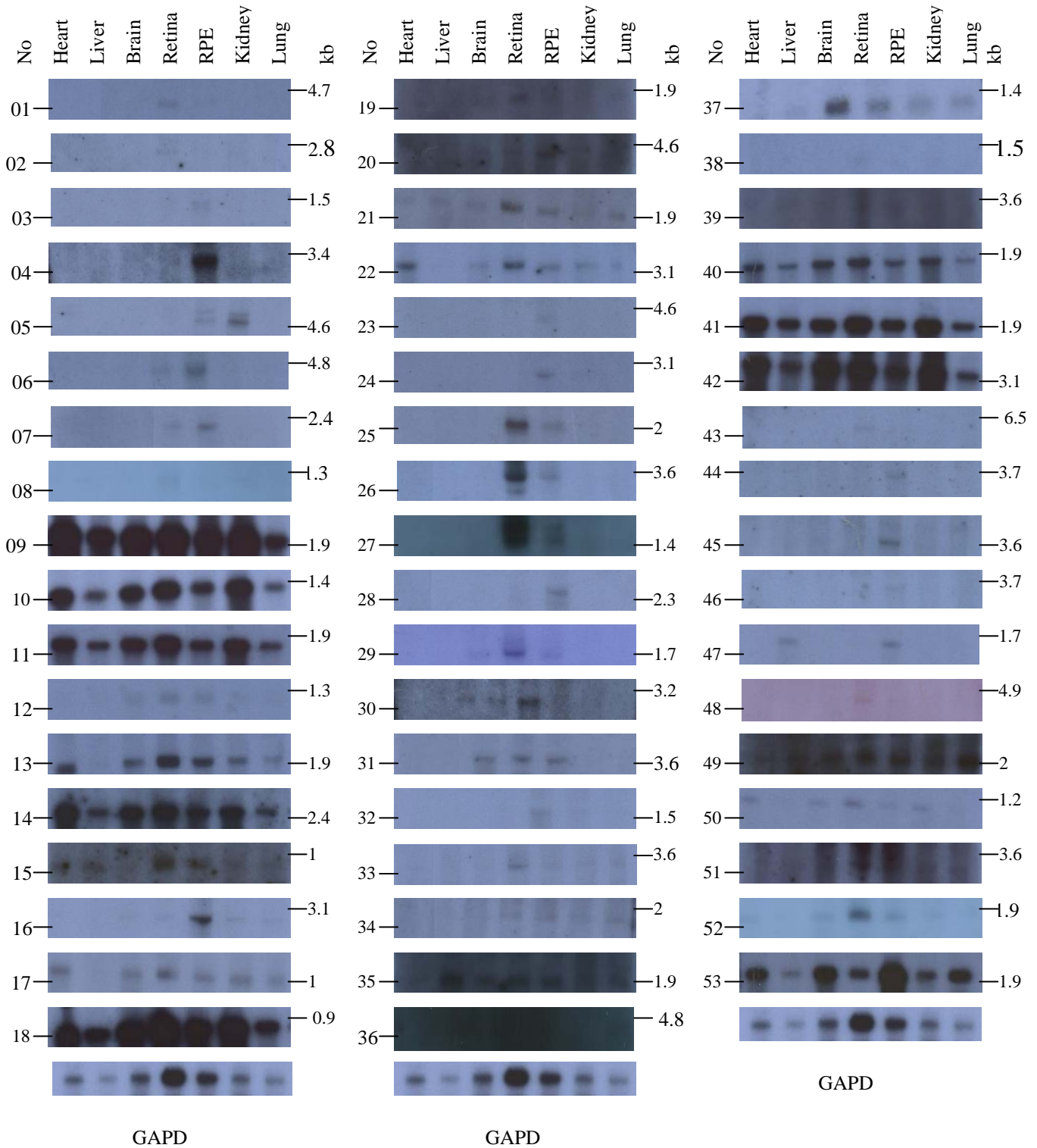


Figure 11: Northern blot hybridizations; unique 107 bovine cDNAs was hybridized to bovine mRNA from 7 tissues including heart, liver, brain, retina, RPE, kidney, and lung. Hybridization signal was detected for 53 transcripts, whereas evaluation was not possible for another 54 clones. Of these 53 transcripts with positive signals, 7 were RPE specific (03, 04, 23, 24, 44, 45, and 46), 3 retina specific (01, 02, and 43), and 14 tissue restricted distributed as follows; 7 were RPE/Ret (06, 07, 25, 26, 27, 28, and 48), 3 RPE/Ret/brain (29, 30, and 31), and one clone for each of RPE/Ret/kidney (32), RPE/Ret/brain/kidney (08), RPE/kidney (05), and RPE/liver (47). The remaining 29 clones were ubiquitously expressed including, 09- 22, 33-42, and 49-53. Taking the expressional pattern as selection criteria, 16 transcripts were chosen as AMD candidate genes: RPE1-D2 (25), RPE2-B7 (47), RPE3-E5 (27), RPE6-C10 (07), RPE7-B9 (02), (06), RPE10-B10 (26), RPE12-B10 (54), RPE12-A9 (48), RPE16-G8 (23), RPE23-F1 (03), RPE24-D11 (24), RPE25-A6 (04), RPE25-G9 (05), RPE26-F8 (28), and RPE26-A3 (46). GAPD = glyceraldehyde-3-phosphate dehydrogenase
No = correspond to the No in table 13 indicating the plate ID and clone ID

4.4 AMD candidate clones

Following the Northern blot analysis, 24 clones showed exclusive or preferential expression in the RPE or retina (Table 13, Figure 11). Of these, 16 transcripts were chosen as priority AMD candidate clones on the bases of the expression pattern and for some genes the function was considered. According to our classification, the result of the blast search against the human genome draft sequence for these clones identified 7 predicted genes, 5 human unknown transcripts, and 4 clones with no significant similarity in the database (Table 14). The results of Northern blot hybridization and RT-PCR analysis showed that 15 (93.8%) of the AMD candidates were expressed in the RPE, either exclusively (6 clones) or preferentially in a tissue restricted pattern (9 clones). Only one clone was exclusively expressed in the retina (Table 13 & 14, Figure 11).

Table 14: AMD candidate genes

Blot ID	Plate ID	Clone ID	Subcategory	Northern Blot	RT-PCR	Comment
093	RPE01	D02	Predicted gene	RPE/Retina		kg (RDH12)
107	RPE02	B07	No significant sim	RPE/LIVER		
086	RPE03	E05	Predicted gene	Retina/RPE	A/ Ret	
115	RPE06	C10	Human unknown	RPE/Retina		
186	RPE07	B09	Human unknown	Retina		
032	RPE08	A09	Human unknown	RPE/Retina		
066	RPE10	B10	Predicted gene	RPE/Retina		kg (MT-Protocadherin)
171	RPE12	B10	No significant sim	RPE		
125	RPE12	A09	No significant sim	Retina/RPE		Retina abundant
126	RPE16	G08	Predicted gene	RPE		kg (SLC4A5)
097	RPE23	F01	Human unknown	RPE		
138	RPE24	D11	Predicted gene	RPE		
024	RPE25	A06	Human unknown	RPE		
141	RPE25	G09	Predicted gene	RPE/Kidney		Kidney abundant
194	RPE10	D08	Predicted gene		RPE/Ret	kg with 2 novel isoforms
050	RPE26	A03	No significant sim	RPE		

Blot ID = represent the unique number given to each blot, plate ID and clone ID = indicate the unique bovine cDNA EST, subcategory = represent the orthologous human sequence, kg = known gene, A = abundant, Ret = retina, sim = similarity, during the course of the project some of the predicted genes were isolated and characterized by other groups such as the RPE1-D2 became known as RDH12 gene, RPE10-B10 became known as the MT-Protocadherin gene, and the human orthologous gene of the bovine RPE10-D8 EST was recently fully characterized as the TRPM3 gene. RPE 16-G08 showed similarity to the SLC4A5 gene.

4.4.1 Analysis of 2 novel isoforms of the transient receptor potential cation channel, subfamily M, member 3 (TRPM3)

4.4.1.1 Cloning of the 2 novel isoforms of the TRPM3 gene

3 EST clones; RPE10-D8, E10-RPE19, and H7-RPE19, from the subtracted RPE cDNA library showed restricted expression in the retinal pigment epithelium. Alignment of the 3 ESTs showed ~95% homology to the 5' region of the genomic sequence of the TRPM3 gene (NM_020952 and NM_024971) (previously melastatin 2, and FLJ11726). Other 3 cDNAs from the public databases, AU119249, BM706003, and BU731076 were found to have identity to the same region. Alignment of all 6 cDNAs, (RPE10-D8, E10-RPE19, H7-RPE19, AU119249, BM706003 and BU731076) with the genomic sequence revealed 7 exons spanning 90 kb of genomic sequences. In order to connect the exons, primers were designed on the bases of the available cDNA (Figure 12). Primer combinations TR-F1/R1, TR-F2/R1 and TR-F4/R3 were used to PCR amplify RPE cDNA. The PCRs revealed 3 overlapping fragments of 757 bp, 660 bp, and 665 bp respectively (Figure 12). The consensus sequence of the 3 fragments was assembled into 1114-bp cDNA transcript designated isoform 1, encompassing an open reading frame (ORF) of 690 bp which code for a 230 amino acid protein with a calculated molecular mass of 25.2 kDa. PCR amplification of RPE cDNA using TR-F4/R4 primers yielded a 980 bp (Figure 12). Assembly of TR-F4/R4 with the overlapping TR-F1/R1 fragment identified a 1391 cDNA transcript designated isoform 2. The cluster sequence contains an open reading frame of 936 bp, coding for a polypeptide of 264 amino acids with molecular weight of 29.2 kDa. The putative open reading frame of isoform 2 is encoded in 8 exons.

4.4.1.2 Genomic structure

The chromosomal localization of the recently identified full length TRPM3 is 9q21.12 and is located between the genomic markers D9S1874 and D9S1807 (Lee et al., 2003, Grimm et al., 2003). The gene is comprised of 24 exons spanning 311 kb (Figure 12). Alignment of the 2 novel isoforms to the genomic sequence of the 7 isoforms (a, b, c, d, e, f, and g, Figure 12) showed that isoform 1 shares exon 1, 2, 3, and 5 skipping exon 4 of isoform f. The ORF ends in exon 6 with the stop codon (TAG) starting with the T nucleotide of the splice donor site of the other isoforms (a-g) which continue up

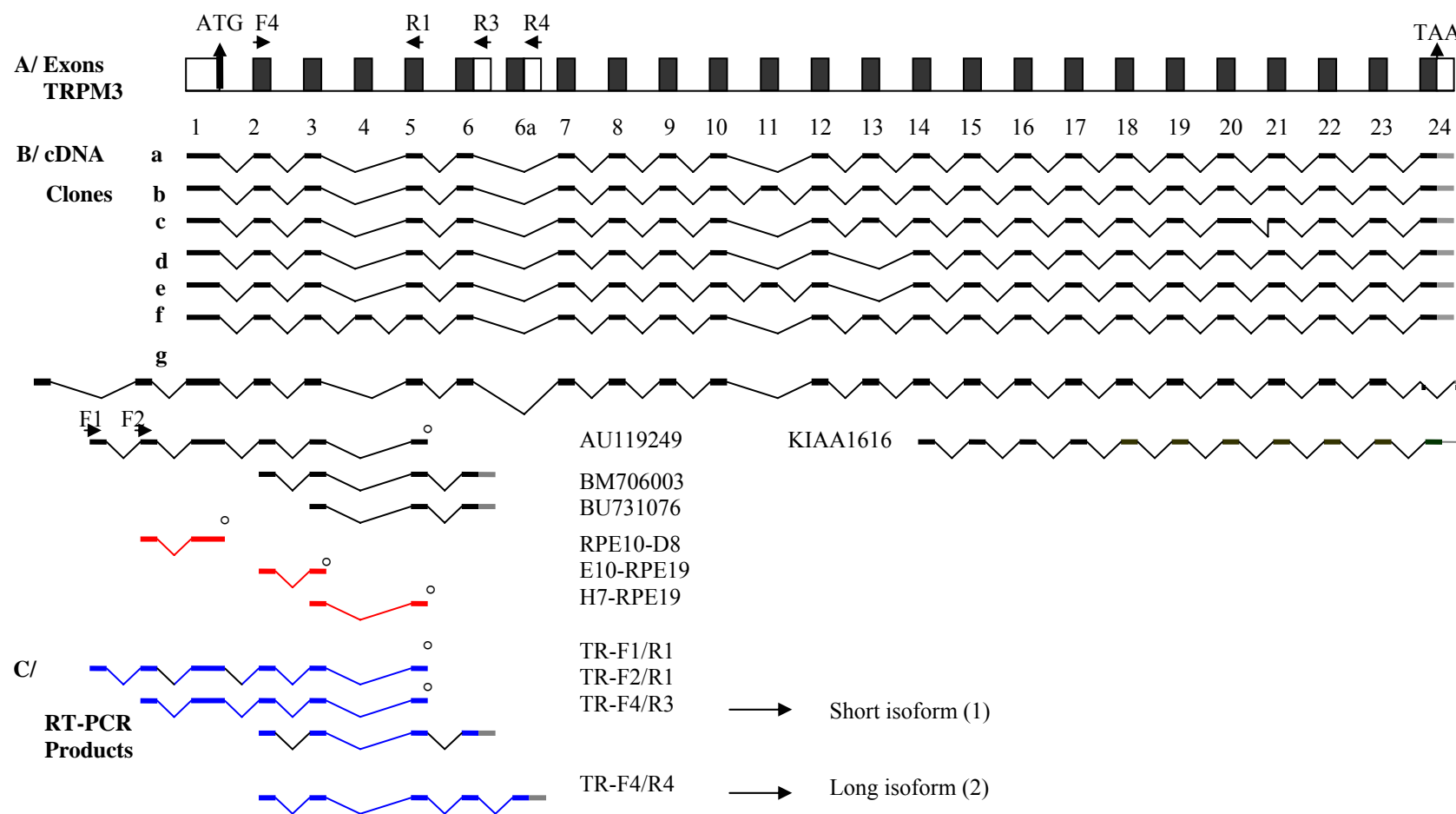


Figure 12: Schematic representation of the exon–intron structure and the splicing pattern of the human TRPM3 gene. A/ Black filled boxes indicate coding exons and white boxes are the untranslated regions. B/ cDNA clones including a, b, c, d, e, f, and g isoforms of full length TRPM3 gene as well as the partial cDNA AU119249, BM706003, BU731076, RPE10-D8, E10-RPE19, H7-RPE19, and KIAA1616. C/ RT-PCR showing primer pairs and PCR products amplified from RPE cDNA to assemble the two novel isoforms of the TRPM3 gene. ° = sequence ends before splice donor site.

until exon 24 (Figure 12). Isoform 2 comprises exon 1, 2, 3, 5 and 6, skipping exon 4 of isoform f and the ORF ends with a stop codon in the novel exon 6a. Both isoforms show additional 2 non-coding exons in the 5' region of the transcript, with the second exon corresponding to the second exon of isoform g of the TRPM3 (Figure 12). The first in-frame translation starting codon, ATG is in exon 1, located 346 bp downstream of the 5' end of the transcript, and an inframe stop codon (TGA) is located in the first non coding exon of the 5' region at 339 bp upstream of the putative start codon. The exon-intron splice junctions of both isoforms follow the consensus splice junction of the GT/AG rule (Burset et al., 2000) (Table 15).

Table 15
Exon–intron boundaries of alternatively spliced TRPM3-isoforms

Exon	size bp	3' splice acceptor	5' splice donor	intron size (kb)
Exon 1	63		TGCTCAGgtaaaat	
Exon 2	80	tttcagGCTCAGA	CCCATAGgtaatct	1.3
Exon 3	205	gttatagGTGTTGC	AGCCATGgtaatca	16.3
Exon 4	214	cttcagTATGTGC	AACACAGgtaattg	3.2
Exon 5	125	tttttagGTGTTAT	AAGAGATgtaagtc	14.9
Exon 6	172	cctgcagGTTGTCC	AACACAAgtaagta	43.5
Exon 7	176	aatgcagGAATCGG		
Exon 7	175	aatgcagGAATCGG	AAGGCGGgtaggta	7.4
Exon 8	247	cccacagCTGTACTION		

Isoform 1 terminates at exon 7. Isoform 2 terminates at exon 8.

4.4.1.3 Protein analysis

Isoform 1 is 230 amino acids (aa) long and shows 100 % identity to TRPM3 in Psi-Blast search and protein alignment. Isoform 2 is 264 aa and also shows 100% identity to TRPM3 over the first 230 aa. The last 34 aa encoded by the novel exon, reveal no significant similarity to any protein in public databases. Also the search in protein motifs and domain databases (Blocks, Pfam, ProDom) fails to identify similarity to known domains or motifs. However, a search against Prosite identified a protein kinase C phosphorylation site (PKC). The two isoforms are devoid of the transmembrane domains normally found in most members of the TRPM subfamily and lack the TRP signature motif (XWKFXR) (Figure 13).

TRPM3a	1	MYVRSVFDTKPDLLLHLMTKEWQLELPKLLISVHGGLQNFELQPKLKQVFGKGLIKAAMT	60
Isofrm 2		MYVRSVFDTKPDLLLHLMTKEWQLELPKLLISVHGGLQNFELQPKLKQVFGKGLIKAAMT *****	
Prim.cons.		MYVRSVFDTKPDLLLHLMTKEWQLELPKLLISVHGGLQNFELQPKLKQVFGKGLIKAAMT	
TRPM3a	61	TGAWIFTGGVNTGVIRHVGDALKDHASKSRGKICTIGIAPWGIVENQEDLIGRDVVRPYQ	120
Isofrm 2		TGAWIFTGGVNTGVIRHVGDALKDHASKSRGKICTIGIAPWGIVENQEDLIGRDVVRPYQ *****	
Prim.cons.		TGAWIFTGGVNTGVIRHVGDALKDHASKSRGKICTIGIAPWGIVENQEDLIGRDVVRPYQ	
TRPM3a	121	TMSNPMSKLTVLNSMHSFILADNGTTGKYGAEVKLRRLQLEKHISLQKINTRIGQGVV	180
Isofrm 2		TMSNPMSKLTVLNSMHSFILADNGTTGKYGAEVKLRRLQLEKHISLQKINTRIGQGVV *****	
Prim.cons.		TMSNPMSKLTVLNSMHSFILADNGTTGKYGAEVKLRRLQLEKHISLQKINTRIGQGVV 230	
TRPM3a	181	ALIVEGGPNVISIVLEYLRDTPPVVCDGSGRASDILAFGHKYSEEGGLINESLRDQL	240
Isofrm 2		ALIVEGGPNVISIVLEYLRDTPPVVCDGSGRASDILAFGHKYSEEGG----- *****	
Prim.cons.		ALIVEGGPNVISIVLEYLRDTPPVVCDGSGRASDILAFGHKYSEEGGLINESLRDQL	
TRPM3a	241	LVTIQKTFYTRTQAQHLFIILMECMKKKELITVFRMGSEGHQDIDLAILTALLKGANAS	300
Isofrm 2		-----CTLFQTS-----IRLEHSS--LKSK---	
Prim.cons.		LVTIQKTFYTRTQAQHLFIILMECMKKKEL2T2F222SEGHQDI2L2222ALLK22NAS	
TRPM3a	301	APDQLSLALAWNVRDIARSQIFIYQQWPVGSLEQAMLDALVLDVRDVFVKLLIENGVSMSH	360
Isofrm 2		-----LCHKNTHFDRTRDRIA-----	
	361	RFLTISRLEELYNTRHGPSNTLYHLVRDVKGNLPPDYRISLIDIGLVIEYLMGGAYRCN	420
	421	YTRKRFRFTLYHNLFGPKRPKALKLLGMEDDIPLRRGRKTTKKREEVDIDLDDPEINHFP	480
	481	FPFHELMVWAVLMKRQKMAFFWQHGEAMAKALVACKLCKAMAHEASENDMVDISQEL	540
	541	NHNSRDFGQLAVELLDQSYKQDEQLAMKLLTYELKNWSNATCLQLAVAAKHRDFIAHTCS	600
	601	QMLLTDMMWGRLRMRKNSGLKVLGILLPPSILSLEFKNKDDMPYMSQAQEIHLQEKEAE	660
	661	EPEKPTKEKEEEDMELTAMLRNNGESSRKKDEEEVQSKHRLIPLGRKIYEFYNAPIVKF	720
	721	WFYTLAYIGYLMLFNYIVLVKMERWPSTQEWIVISYIFTLGIEKMREILMSEPGKLLQKV	780
	781	KVWLQEYWNVTDLIAILLFSVGMILRLQDQPPFRSDGRVIYCVNIYWYIRLLDIFGVNKY	840
	841	LGPYVMMIGKMMIDMMYFVIIMLVVLSFGVARQAIFPNEEPSWKLAKNIFYMPYWMIY	900
	901	GEVFADQIDPPCGQNETREDGKIQLPCKTGAWIVP AIMACYLLVANILLVNLIAVFN	960
	961	NTFFEVKSISNQVWVQRYQLIMTFHERPVLPPPLIFSHMTMIFQHLCCRWRKHESDPD	1020
	1021	ERDYGLKLFITDELKKVHDFEEQCIIEYFREKDDRFNNSNDERIRVTSERVENMSMRLE	1080
	1081	EVNEREHSKASLQTVDIRLAQLEDLIGRMATALERLTGLERAESNKIRSRTSSDCTDAA	1140
	1141	YIVRQSSFNSEQNTFKLQESIDPAGEETMSPTSPTLMPRMRSHSFYSVNMDKGGIEKL	1200
	1201	ESIFKERSLSLHRATSSHSVAKEPKAPAAPANTLAIVPDSRRPSSCIDIYVSAMDELHCD	1260
	1261	IDPLDNSVNILGLGEPFSFSTPVSTAPSSAYATLAPTDRPPSRSIDFEDITSMDTRSF	1320
	1321	SDYTHLPECQNPWDSEPPMYHTIERSKSSRYLATTPFLLEEAPIVKSHSFMFSPRSYYA	1380
	1381	NFGVPVKTAEYTSITDCIDTRCVNAPQAIADRAAFPGLGDKVEDLTCCHPEREAELSHP	1440
	1441	SSDSEENEAKGRRATIAISSQEGDNSERTLSNNITVPKIERANSYSAEEPSAPYAHTRKS	1500
	1501	FSISDKLDRQRNTASLQNPFRQSRKSSKPEGRGDSLMSRRL	1540

Figure 13:

Alignment of the amino acid sequences of the human TRPM3 and isoform 2, the alignment shows 100% similarity up until amino acid 230, the last 34 aa did not show significant similarity. Grey background representing transmembrane domains, green background = TRP signature motif (XWKFXR), blue background = coiled-coil domain.

4.4.1.4 Expression analysis (RT-PCR)

To determine the expression of isoform 1 and 2, RT-PCR was employed. Total RNA from 6 human tissues including brain, heart, lung, retina, RPE and placenta was isolated and used to generate first strand cDNAs. Primers used for PCR include TR-F4 in exon 2 and isoform 1 specific primer TR-R3 located downstream of exon 6 (665

bp). For isoform 2, the specific primer TR-R4 downstream of exon 6a was coupled with TR-F4 (980 bp) (Figure 12).

RT-PCR analysis revealed that isoform 2 (TR-F4/R4) is exclusively expressed in the RPE, whereas isoform 1 (TR-F4/R3) is transcribed at a higher level in the RPE and at a lower level in the retina (Figure 14).

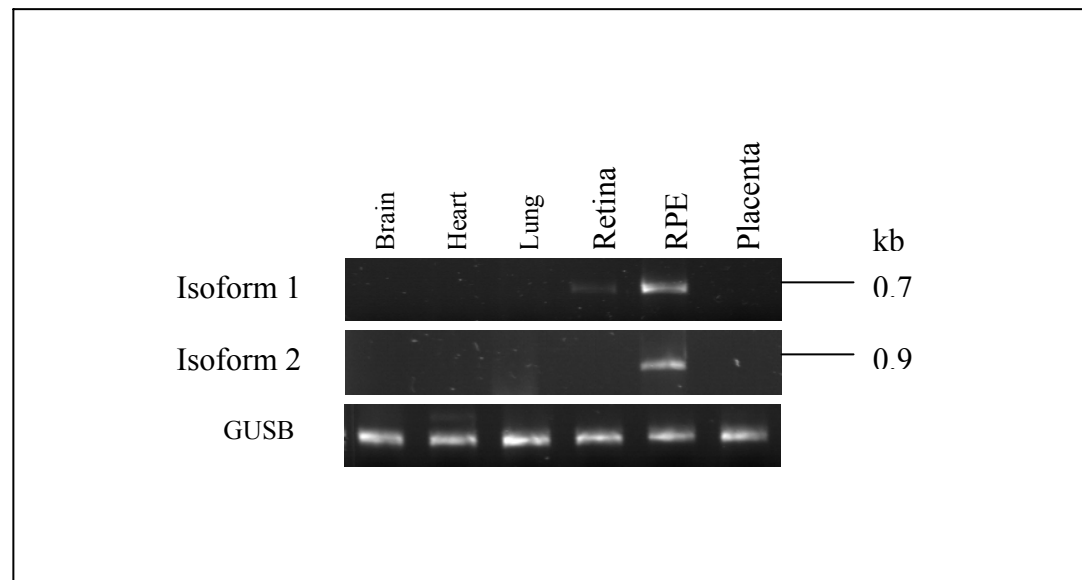


Figure 14: RT-PCR expression analysis of the 2 novel isoforms of TRPM3. Top: Isoform 2 with primer pair TR-F4/R4. Middle: isoform 1 with primer pair TR-F4/R3 (Figure 12). GUSB served as a control for cDNA integrity.

4.4.2 Analysis of MGC2477 gene

4.4.2.1 Isolation and characterization of the MGC2477 gene

RPE3-E5, the EST from our subtracted bovine cDNA was found to show a restricted expression in the retina and RPE. RPE3-E5 showed homology to the predicted gene MGC2477 which is localized on chromosome 11q12.3 (NM_024099). Other cDNAs from the public databases, AW603671, and BF028466 showed homology to the same predicted gene. Alignment of the 3 ESTs to genomic sequences showed overlapping fragments with high homology to the coding region of the predicted gene spanning exon 2-6, interrupted by genomic sequences indicating a partial cDNA from a single gene. (Figure 15 A,B). 9 retina libraries including, DKFZ1, DKFZ2, DKFZ3, DKFZ4, CIF1, CIF2, CIF3, HRλGT10V, HRλTE_x2V and one foetal brain library (HFBλGT10) (Appendix, Table 6) were PCR screened using primer pair 3-E5F2/R.

Positive signals were detected in DKFZ3 and HR λ GT10V libraries (Figure 16). DKFZ3 library was screened using 4 gene specific primers 3-E5F2, F3, R, R2 and 2 library specific primers including the Lambda triple 5' (LT, 5') and the Lambda triple 3' (LT, 3') (Figure 15). (For LT, 5' and LT, 3' sequence see Appendix Table 7).

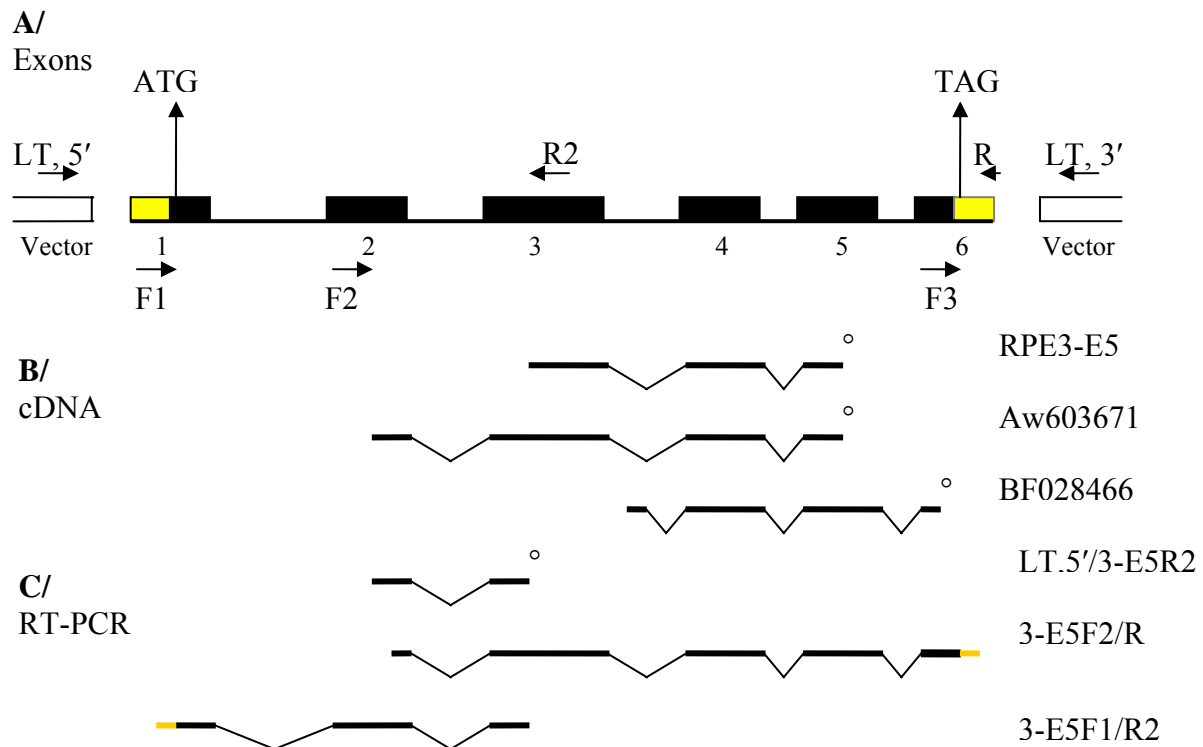


Figure 15: Genomic organization of the MGC2477 gene. (A) Exons are shown as black filled boxes. Black arrows indicate primers and their relative positions. (B) cDNA from our library and public database. (C) cDNA fragments isolated by RT-PCR. ° = sequence ends before splice donor site.

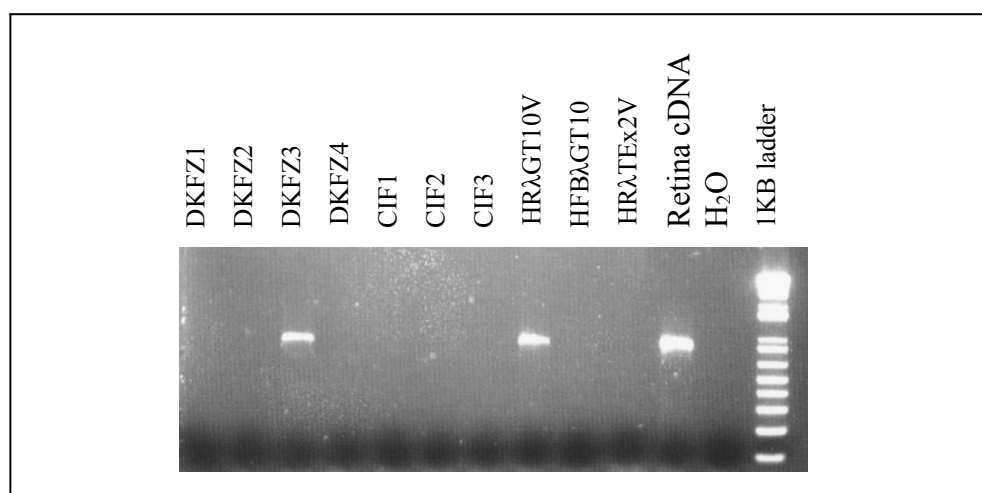


Figure 16: 9 retina libraries including DKFZ1, DKFZ2, DKFZ3, DKFZ4, C1F1, C1F2, C1F3, HR λ GT10V, HR λ Tex2V and one foetal brain library (HFB λ GT10) (Appendix, Table 6) were PCR screened using primer pair 3-E5F2/R (Figure 15). Retina cDNA served as positive control and H₂O as negative control. PCR products were obtained from DKFZ3 and from the HR λ GT10V retina libraries.

Nested primers 3-E5F2/R were used to PCR amplify the PCR product of library screening (3-E5R/LT, 5' and 3-E5F2/LT, 3') (Figure 17). The resulting fragment of 876 bp was directly sequenced (Figure 15, C).

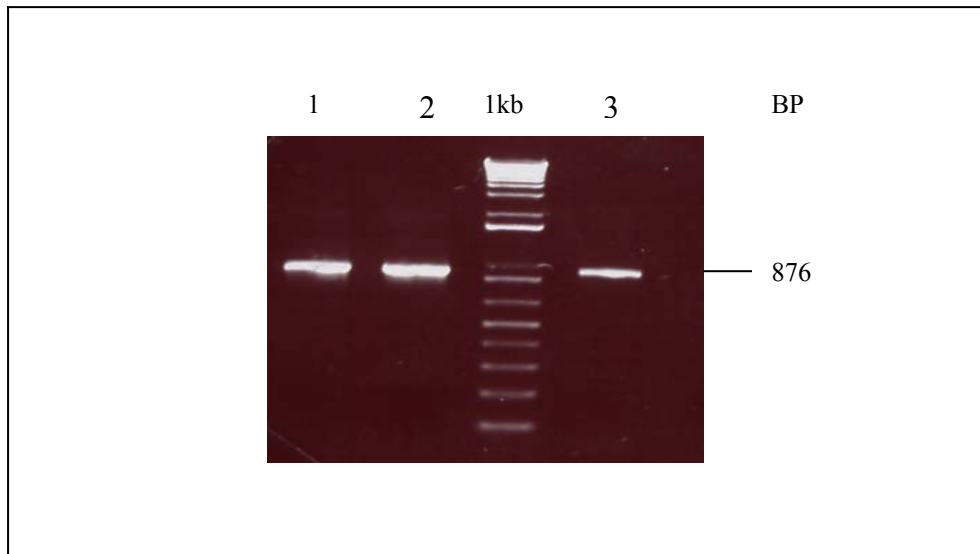


Figure 17: PCR amplification using 3-E5F2/R primers (Figure 15). Lane 1: template 3-E5R/LT, 5' (dilution 1:30). Lane 2: template 3-E5 F2/LT, 3' (dilution 1:30). Lane 3: template retina cDNA as control. 1 Kb = 1 kilo base ladder.

To extend the transcript in the 5' and 3' direction 2 pairs of nested primers LT, 5'/3-E5R2 and 3-E5F3-LT, 3' were used to PCR amplify the DKFZ3 retina library. The PCRs added 23 bp in the 5' UTR and 57 bp in the 3'UTR respectively. To further extend the cDNA fragment, 3-E5F1 primer was designed in exon 1 and the fragment 3-E5F1/R2 was PCR amplified from retina cDNA yielding an overlapping fragment of 920 bp. The assembly of all fragments resulted in a cDNA fragment of 1619 bp with 2 ORFs.

4.4.2.2 Genomic structure

Alignment of the 1619 bp transcript to genomic DNA identified 6 exons, with exon-intron splice boundaries following the consensus GT/AG rule (Table 16). Two ORFs were identified by the ExPASy translation tool. ORF 1 with a putative translation start codon ATG located in exon 1, at 516 bp downstream of the 5' end of the transcript and lies in a sequence context in accordance with the Kozak rule (Kozak, 1996). An in-frame stop codon TGA is located 36 bp upstream from the transcription initiation start codon ATG and a termination stop codon TAG is located in exon 6 followed by 312 bp of 3' UTR. A putative polyadenylation signal (AAUAAA) is located at 291 bp

from the stop codon (TAG). The second ORF has a transcription initiation start codon ATG in exon 3 at 907 bp downstream from the 5' end of the transcript. An in-frame stop codon TAA is located 42 bp from the start codon and a termination stop codon TAA lies in exon 6 followed by 233 bp of 3' UTR. The putative polyadenylation signal (AAUAAA) lies at 212 bp from the stop codon (TAA).

Table 16: Exon –intron structure of MGC2477

Exon	size bp	3' splice acceptor	5' splice donor	intron size (kb)
Exon 1	721 ^a		CATTCAGgttagta	78
Exon 2	163	tattcagGATTTCT	GAGCCAGgtgaggg	1893
Exon 3	225	atcccagGCTGGGC	TTTGAGGgtaagta	2549
Exon 4	125	ccggcagGAGCTGA	AGCGGGCgtaagta	1513
Exon 5	98	ccatcagGTCCAGT	ATGGAAGgtgaggc	76
Exon 6	328 ^b	tactcagTGGAAGC		

^a size of the exon with reference to 3-E5F1/R2 PCR analysis and includes a 5'UTR of 571 bp.
^b size of the last exon with reference to the polyadenylation signal AATAAA, and includes a 3'UTR OF 297 bp.

4.4.2.3 Protein analysis

ORF 1 is translated into 263 amino-acids with a molecular weight of 28.8 kDa and ORF 2 is translated into a 159 amino-acid peptide with a molecular weight of 18.4 kDa. Searches in protein and motif databases revealed no significant homology or similarity with known proteins or motifs, for both ORFs.

4.4.2.4 Expression analysis

Northern blot analysis for the bovine RPE3-E5 EST was performed. The results show expression of the transcript in retina and RPE (Figure 18) but not in heart, liver, brain, kidney and lung.

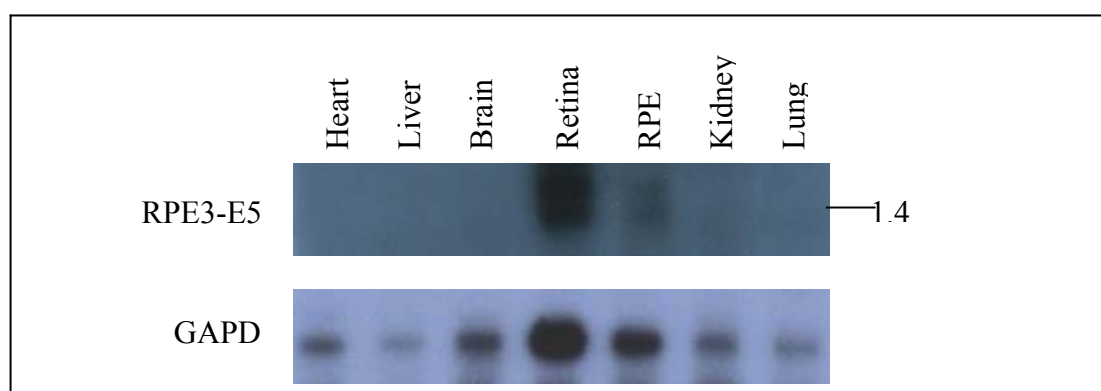


Figure 18: Northern blot for the MGC2477 gene. RPE3-E5 bovine EST (Figure 15, spanning exon 3, 4, and 5) was hybridized with a membrane containing mRNA from bovine heart, liver, brain, retina, RPE, kidney and lung. RNA integrity was checked with GAPD.

RT-PCR was performed using total RNA from 6 human tissues including brain, heart, lung, retina, RPE and placenta to generate first strand cDNAs. 3-E5F2/R primers were used for PCR across the cDNA panel. Abundant expression was found in retina as well as low signal intensity in brain and the other tissues tested (Figure 19).

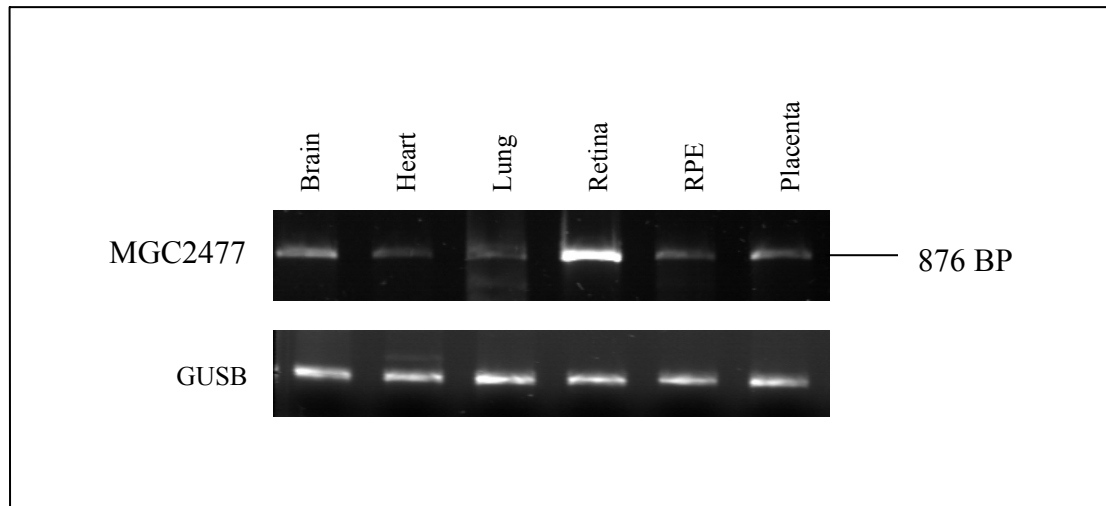


Figure 19: RT-PCR analysis of the MGC2477: RT-PCR analysis was performed using 3-E5F2/R human primers (Figure 15) to amplify PCR product across a panel of human cDNA derived from brain, heart, lung, retina, RPE and placenta. The result showed abundant expression in retina and low signal in brain and the other tissues tested. cDNA integrity was checked with GUSB human primers.

4.4.3 SNPs identification in the MT-protocadherin gene

RPE10-B10, the bovine EST from our RPE subtracted cDNA library had a restricted expression in RPE and retina (Figure 11, Table 13). The EST showed homology to the MT-Protocadherin gene which was assigned to chromosome 10-q22.1-q22.3 (NT_030059, NM_033100). The gene is comprised of 17 exons spanning 24.9 kb of genomic sequence and encoding an mRNA transcript of 5337 bp. SNPs were identified by screening all of the exons and exon–intron boundaries of the gene, plus 5 kb upstream and downstream of the start and stop codon of the gene (for primers and conditions see appendix table 1). In total 35 SNPs were identified (Table 17), 3 SNPs in the 5' UTR, 13 in the intervening sequences, 2 synonymous SNPs in exon 6 (A477G, Ala159Ala), and exon 17 (T2439C, Thr813Thr), and 17 SNPs in the 3'UTR. Of the 35 SNPs, 28 SNPs are highly frequent, with frequencies of the minor allele ranging from 0.17-0.5%. 5 SNPs were in linkage disequilibrium (blue background Table 17).

SNPs from the public databases were compared to SNPs identified in this study (Table 18). 28 SNPs were found in the public databases, of these 28 SNPs, one was validated by frequency, one validated by submitter and 26 have no information. The SNP validated by frequency was confirmed in this study. The SNP validated by submitter was not validated in this study and of the 26 SNPs with no information, 11 were validated by frequency in this study and 15 were found not to be polymorphic.

Table 17: SNP card of the MT-protocadherin gene

Location	Name of PCR fragment	Position and nucleotide change	Frequency (alleles)	Frequency of minor allele	SNP ID
5UTR	5UTR1	-4111T>C	33/90	0.37	
5UTR	5UTR5	-2195T>C	1/8	0.13	
5UTR	5UTR8	-297T>C	6/16	0.38	
Intron	Exon2	IVS2+95C>T	2/16	0.13	
Intron	Exon4	IVS3-86A>G	3/16	0.19	
Intron	Exon4	IVS4+89C>A	26/94	0.28	
Intron	Exon6	IVS5-61T>C	44/96	0.46	
Intron	Exon6	IVS5-83T>C	42/96	0.44	
Exon	Exon6	A477G(A159A)	44/96	0.46	rs4933975
Intron	Exon6	IVS6+129A>G	2/16	0.13	
Intron	Exon6	IVS6+225A>G	44/96	0.46	rs4933976
Intron	Exon7	IVS7+82A>G	6/16	0.38	
Intron	Exon8	IVS7-86T>G	44/96	0.46	
Intron	Exon8	IVS7-97A>G	1/86	0.01	
Intron	Exon9	IVS8-153C>T	2/12	0.17	
Intron	Exon14	IVS14+6T>C	1/14	0.07	
Intron	Exon14	IVS13+426G>A	28/96	0.29	rs4933978
Exon17	Exon17	T2439C(T813T)	43/94	0.46	rs3814213
3UTR	3UTR1	+173A>C	5/16	0.31	
3UTR	3UTR2	+869G>T	30/66	0.45	
3UTR	3UTR3	+907A>G	25/96	0.26	
3UTR	3UTR3	+1270G>A	2/76	0.026	
3UTR	3UTR7	+2588C>A	41/92	0.45	rs1059341
3UTR	3UTR7	+2589G>A	11/90	0.12	
3UTR	3UTR7	+2643A>T	23/84	0.27	rs1059342
3UTR	3UTR7	+2798A>G	44/96	0.46	
3UTR	3UTR7	+3020G>A	14/80	0.18	
3UTR	3UTR9	+3768G>C	7/14	0.50	rs2279229
3UTR	3UTR10	+4199G>C	44/96	0.46	rs4424615
3UTR	3UTR10	+4346T>A	15/84	0.18	rs4562751
3UTR	3UTR10	+4432	38/78	0.49	rs4562752
3UTR	3UTR10	+4562G>A	37/78	0.47	rs4244947
3UTR	3UTR10	+4614C>T	21/78	0.27	
3UTR	3UTR11	+4614C>T	20/96	0.21	
3UTR	3UTR11	+4855T>A	36/82	0.44	rs4933980

Blue background = SNPs in linkage disequilibrium.

Table 18: Validation comparison of SNPs in public databases versus SNPs in the present study in the MT-Protocadherin gene

SNP ID	lab name	5' flanking sequence	3' flanking sequence	Validation (P.D.B)*	DNA change	Validation in lab	Frequency of minor allele
rs730442	2256	GCACCATCCG	ATTGAGTGGC	No-info	C/G	-	
rs1059341	+2588	GCTGTCTGCT	GGTCCCAGTA	No-info	C/A	By-freq	(0.45%)
rs1059342	+2643	GCCTCCAGGG	AAGAGCTGGG	No-info	A/T	By-freq	(0.27%)
rs960731	IVS10+475	CTAGAGCCGG	CATGTGACCT	No-info	T/G	-	
rs3814213	2439	CCGTGCCTAC	GTCTCTGGCT	No-info	T>C	By-freq	(0.46%)
rs3814212	+4	CTTCTAGTGT	TGCCCTATGA	By-sub	A/C	-	
rs2279229	+3768G>C	CCTGAATGAG	TTCGGTTATT	By-freq.	C/G	By-freq	(0.5%)
rs4933975	A477G	AGGTCCATGC	GTGGACAGGG	No-info	A/G	By-freq	(0.46%)
s4399278	+760	AGAGGTAGCC	TAAAGGCAAC	No-info	C/T	-	
rs4933979	+1467	TACAAATAGG	TGTGCCCTGC	No-info	A/T	-	
rs4933313	IVS13+188	CTCACAGGAC	GTAATGAGGA	No-info	A/T	-	
rs4606427	IVS9+136	AAGGGCTGTG	CCAAGACAAG	No-info	A/G	-	
rs4606431	IVS6-324	AGATTACTCC	CAGACATTGC	No-info	A/G	-	
rs4933972	IVS2-278	CTACAGTTAG	CACGGCAGAC	No-info	A/G	-	
rs4933973	IVS5+376	ACATATGCTT	CTATATCCTA	No-info	C/T	-	
rs4933974	IVS5+488	GGTAACTATC	TTTTAATAGC	No-info	A/G	-	
rs4933976	IVS6+225	TCCCTCTTCC	ACGTCCCCAG	No-info	A/G	By-freq	(0.46%)
rs4933977	IVS9-9	GGTGCATCTC	CTTGACAGGG	No-info	C/T	-	
rs4933978	IVS13+426	GGGCATGGGA	CTGCCAACAT	No-info	A/G	By-freq	(0.29%)
rs4528260	IVS3-294	TCGACATCTC	CCTCAGTGTG	No-info	A/G	-	
rs4244946	IVS16+161	CTTTGGAAGC	GGTTGAGTTT	No-info	A/G	-	
rs4562751	+4346	ACTTTGTATG	TAAAAAATAA	No-info	A/T	By-freq	(0.18%)
rs4562752	+4432	AGAACACTAA	GTACTATTAT	No-info	G/T	By-freq	(0.49%)
rs4593957	+5303	CATATCAATC	CCCTTGATGC	No-info	C/T	-	
rs4424615	+4199	TTAATAAGAT	TGATATTCCA	No-info	C/G	By-freq	(0.46%)
rs4933980	+4855	TTTGCTTGGC	TGAAGGTCTG	No-info	A/T	By-freq	(0.44%)
rs4933981	+5142	AAAACCATCA	ATCTTTTGAG	No-info	A/G	-	
rs4244947	+4562	GCCAGGGTCT	TTCTTGCATC	No-info	A/G	By-freq	(0.47%)

* = public databases, - = found not to be polymorphic.

4.4.4 SNPs identification in the TRPM3 gene

The chromosomal localization of TRPM3 is 9q21.12 and comprised 24 exons spanning 311 kb. The long isoform isolated in this study contains 8 exons spanning 92.6 kb. All of the 8 exons, exon–intron junctions, plus 5 kb upstream of exon 1 and 5 kb downstream of the stop codon in exon 8 were screened for SNPs. In total, 35 SNPs were identified. Of these, 30 were highly frequent (0.17-0.5%), and 14 were novel. The localization of the SNPs is as follows; 3 in the 5' UTR, 3 in the exons, 27 in the intervening sequences, and 2 in the 3' UTR (Table 19).

In the public databases 114 SNPs were found in TRPM3 gene, only 40 SNPs were included in this study. Of these 40, 5 SNPs were validated by frequency and 35 SNPs have no information in public databases. In the current study, the 5 validated by

frequency were confirmed by frequency. Of the 35 SNPs with no information, 16 were validated by frequency, and 19 were shown not to be polymorphic (Table 20).

Table19: SNP card of the TRPM3 gene

Location	Name of PCR fragment	Position and nucleotide change	Frequency (alleles)	Frequency of minor allele	SNP ID
5UTR	TR-5UTR2	-6987A>T	3/16	0.19	
5UTR	TR-Exon1	-6095C>T	6/16	0.38	rs2993010
5UTR	TR-Exon1	-5768C>A	5/16	0.31	rs3812532
Intron2	TR-IVS2.1	IVS2+515C>T	4/16	0.25	
Intron2	TR-IVS2.1	IVS2+532C>T	4/16	0.25	
Intron2	TR-IVS2.1	IVS2+793G>A	2/16	0.13	rs2152757
Exon4	TR-Exon4	A171T	6/16	0.38	
Intron4	TR-IVS4.1	IVS4+775G>A	6/16	0.38	
Intron4	TR-IVS4.1	IVS4+1127C>T	6/16	0.38	rs1337027
Intron4	TR-IVS4.2	IVS4+1333T>C	2/16	0.13	rs1337029
Intron4	TR-IVS4.2	IVS4+1596G>A	6/16	0.38	
Intron4	TR-IVS4.2	IVS4+1659T>A	6/16	0.38	
Intron5	TR-Exon5	TR-IVS5+58T>C	6/16	0.38	rs1337030
Intron5	TR-Exon5	TR-IVS5+87C>T	6/16	0.38	rs1337031
Intron5	TR-IVS5.2	IVS5+3623G>T	6/16	0.38	rs1415228
Intron5	TR-IVS5.2	IVS5+3636A>G	4/12	0.33	rs1415229
Intron5	TR-IVS5.2	IVS5+3689T>C	7/16	0.44	rs1415230
Intron5	TR-IVS5.2	IVS5+3955T>A	2/16	0.13	
Intron5	TR-IVS5.3	IVS5+9784A>G	2/16	0.13	
Intron5	TR-IVS5.3	IVS5+9864G>A	6/16	0.38	rs2275242
Intron6	TR-Exon6	IVS6+39A>G	4/10	0.4	rs1034533
Intron6	TR-Exon6	IVS6+128C>T	3/10	0.3	rs1034539
Intron6	TR-IVS6.2	IVS6+865A>G	5/16	0.31	rs1034543
Intron6	TR-IVS6.3	IVS6+4752G>A	8/16	0.5	rs579587
Intron6	TR-IVS6.3	IVS6+4939C>T	3/16	0.19	
Intron6	TR-IVS6.4	IVS6+6300A>G	4/16	0.25	rs505107
Intron6	TR-IVS6.4	IVS6+6407A>T	4/16	0.25	rs506067
Intron6	TR-IVS6.5	IVS6+7842C>T	3/14	0.21	rs561022
Intron6	TR-IVS6.5	IVS6+8178G>A	4/16	0.25	rs564929
Intron7	TR-IVS7.2	IVS7+756C>T	5/16	0.31	
Intron7	TR-IVS7.4	IVS7+6038A>G	7/16	0.44	rs1328148
Exon8	TR-Exon8	A910G	2/12	0.17	
Exon8	TR-Exon8	T698G	1/16	0.06	
3UTR	TR-3UTR1	+356A>G	4/16	0.25	
3UTR	TR-3UTR3	+1406C>T	6/16	0.38	rs879857

Table 20: Validation comparison of SNPs in public databases versus SNPs in the present study in the TRPM3 gene

SNP ID	lab name	5' flanking sequence	3' flanking sequence	Validation (P.D.B)*	DNA change	Validation in lab	Frequency of minor allele
rs1034543	IVS6+865	GAAAGGTAGC	TCATCAAAAC	By-freq.	A/G	By-freq.	(0.31%)
rs1337031	IVS5+87	AAAATGTGCA	ATTATAGTAT	By-freq.	C/T	By-freq.	(0.38%)
rs2152757	IVS2+793	TCATTGTTTC	TCAAGAACAC	By-freq.	G/A	By-freq.	(0.13%)
rs2275242	IVS5+9864	ACTATTCTGC	TTAACTTGAA	By-freq.	G/A	By-freq.	(0.38%)
rs505107	IVS6+6300	ATATAAGTTC	ACCAACTTAA	By-freq.	A/G	By-freq.	(0.25%)
rs2011851	IVS6+350	CTTTTTGGTG	CTAAACAGAA	No-info.	A/G	-	
rs2011853	Ivs6+311	CATGGTACTC	AGGAGAAAA	No-info	C/T	-	
rs1034533	Ivs6+39	GCTCGTAGGA	GTATGCTGAA	No-info	A/G	By-freq	(0.4%)
rs1034539	IVS6+128	TTATTTCTAC	GGGCCAGAGC	No-info	C/T	By-freq	(0.3%)
rs1034542	IVS6+406	CTGGCTGTGC	AAGGCATTTC	No-info	A/G	-	
rs1410372	IVS6+804	TCTTAAGCGC	TAGGAATCTC	No-info	A/G	-	
rs1415227	IVS5+3133	AAAAAATAAA	CTTTTAGCAT	No-info	A/C	-	
rs1415228	IVS5+3623	ACTTGTCCCT	AGTGTGCTTC	No-info	G/T	By-freq	(0.38%)
rs1415229	IVS5+3636	TGTGCTTCTA	ATCTTCTGAA	No-info	A/G	By-freq	(0.33%)
rs1415230	IVS5+3689	CTGGGCTTCA	GTTACTTAAG	No-info	C/T	By-freq	(0.44%)
rs1337027	IVS4+1128	TCTCAAAAAA	AAAAATAACA	No-info	C/T	By-freq	(0.38%)
rs1337028	IVS4+1202	AGACCTACAC	GAGAATTCTC	No-info	C/T	-	
rs1337029	IVS4+1342	GCCCATACAC	GACATGATCT	No-info	C/T	By-freq	(0.13%)
rs1337030	IVS5+58	ATCAGAAAAG	ATAATAAAAT	No-info	C/T	By-freq	(0.38%)
rs1337032	IVS5+3097	CATTTTATAT	ATAAAAATCA	No-info	A/G	-	
rs3750404	IVS5-101	GTACCACAGA	CTGATGTTCT	No-info	A/T	-	
rs561022	IVS6+7842	GAGACTATAT	TTGAAATATT	No-info	C/T	By-freq	(0.21%)
rs879857	+1406	ATGTTGGTCA	GGACCACAGG	No-info	C/T	By-freq	(0.38%)
rs2993009	IVS1+252	CCTTTTTCCCT	AGTTAGTGGA	No-info	G/A	-	
rs1983943	IVS7+6591	AGTAGCTCCA	GTATTTAAGA	No-info	C/T	-	
rs2993010	-6095	ACCCAGAATC	CTTTTGCCAG	No-info	A/G	By-freq	(0.38%)
rs3812530	-7222	CAGAGGATTA	GGAAAAATGA	No-info	T/C	-	
rs3812532	-5768	TGTTAAGCTG	CCTGCTGAAG	No-info	A/C	By-freq	(0.31%)
rs564929	IVS6+8178	GACCTTACAG	TATACCTATT	No-info	A/G	By-freq	(0.25%)
rs560819	IVS6+7769	ATAAATGGCA	TAGGATTTTT	No-info	T/C	-	
rs505221	IVS6+6338	AGTAGCTGCT	AATAAACATG	No-info	C/T	-	
rs1831144	+1299	GCTAGGGATA	AGTGGATTAA	No-info	C/T	-	
rs506067	IVS6+6407	CTATGTATCC	GATAAGAATT	No-info	A/T	By-freq	(0.25%)
rs579587	IVS6+4752	GAGGCTCATG	GCAGCAGCCT	No-info	A/G	By-freq	(0.5%)
rs1328142	IVS7+607	ACAGCCCAA	CCCCCAACCC	No-info	G/T	-	
rs1328146	IVS7+5703	GAATAAGGCA	GGCCCTAGCT	No-info	C/G	-	
rs1328147	IVS7+5720	AGCTATCAAG	ACTTTATAAT	No-info	A/T	-	
rs1328148	IVS7+6038	TCTAAATAAG	TTGAAGAAAA	No-info	A/G	By-freq	(0.44%)
rs1328149	IVS7+6113	GTGTGTGTGT	TGTGTCTGTT	No-info	C/G	-	
rs1328150	IVS7+6223	TGTGTGTATA	ATATGCTTAA	No-info	A/T	-	

* = public databases.

4.4.5 SNP identification in the MGC2477 gene

The predicted gene is comprised of 6 exons spanning 13.7kb of genomic sequence. All exons, exon-intron junctions, intronic sequences and 5 kb of up and downstream of the gene were screened for SNPs. 15 SNPs were identified, 8 in the 5'UTR region,

3 in the intervening sequences, and 4 in the 3' UTR. Of the 15 identified SNPs, 13 were highly frequent (0.25-0.44%) and 10 were novel (Table 21).

Comparison of 18 SNPs from the public databases with SNPs identified in this study (Table 22) revealed that 2 SNPs validated by frequency in the public database (rs7386, s13941) were confirmed by frequency in this study. Of the remaining 16 SNPs with no information, 4 were validated by frequency (rs489778, rs693698, rs597259, rs3809079) and 12 were found not to be polymorphic.

Table 21: SNP card of the MGC 2477 gene

Location	Name of PCR fragment	Position and nucleotide change	Frequency (alleles)	Frequency of minor allele	SNP ID
5UTR	MGC-5utr1	-2066C>T	7/16	0.44	s13941
5UTR	MGC-5utr2	'-1392C>T	1/96	0.01	
5UTR	MGC-5utr2	-1343C>T	27/96	0.28	
5UTR	MGC-5utr2	-1316A>C	27/96	0.28	rs693698
5UTR	MGC-5utr2	-1247 A>G	26/96	0.27	
5UTR	MGC-5utr3	-995C>A	7/16	0.44	
5UTR	MGC-EXON1	-144C>G	7/16	0.44	rs489778
5UTR	MGC-EXON1	-84G>C	1/16	0.06	
Intron2	MGC-EXON2	IVS2+113G>A	7/16	0.44	
Intron3	MGC-IVS3.1	IVS3+822C>T	5/16	0.31	
Intron5	MGC-EXON5-6	IVS5+49T>A	7/16	0.44	rs597259
3UTR	MGC-EXON5-6	+266C>T	6/16	0.38	rs7386
3UTR	MGC-3UTR1	+676C>T	4/16	0.25	
3UTR	MGC-3UTR2	+1020A>T	7/16	0.44	
3UTR	MGC-3UTR2	+1038A>T	7/16	0.44	

Table 22: Validation comparison of SNPs in public databases versus SNPs in the present study in the MGC2477 gene

SNP ID	lab name	5' flanking sequence	3' flanking sequence	Validation (P.D.B)*	DNA change	Validation in lab	Frequency of minor allele
rs7386	+266	TGGAGAAGGG	CTCTCTAGCA	by-freq.	C/T	By- freq.	(0.385)
s13941	-2066	GACCTCCCGC	GGCGCCGCCT	by-freq.	G/A	By- freq.	(0.44%)
rs494164	194	GTGGAATCCA	TGAGGTGAAT	No-info	G/C	-	
rs489778	-144	ATTTCCCCT	CCCTGAAAGC	No-info	G/C	By- freq.	(0.44%)
rs693698	-1316	GTCACCCGCG	GTTTTCAACA	No-info	G/T	By- freq.	(0.28%)
rs694082	IVS3+1159	GTCACTTGGT	TATGTCGCCA	No-info	A/G	-	
rs597259	IVS5+49	TTTATTTGGG	TAATACTTCC	No-info	A/T	By- freq.	(0.44%)
rs567069	+483	GCTCACGCCT	TAATGCCAGC	No-info	A/C	-	
rs483343	+1109	GGCATAATCT	GGCTCACTGC	No-info	G/T	-	
rs3809078	-1327	GTCACCCGCG	GTTTCCTGC	No-info	G/T	-	
rs3809079	-1343	CCGAGCTGTG	TCTGTGGTTT	No-info	A/G	By- freq.	(0.28%)
rs669760	-908	TATTGCTTTT	GTTTTGCTTC	No-info	G/T	-	
rs2956136	IVS4+481	AGCCTGGGCC	CAGAGTGAGA	No-info	G/T	-	
rs4489748	IVS3-370	TACAGCTAAA	CCACACTTAC	No-info	C/T	-	
rs2467644	+1902	TGATCTGCCC	CCTCAGCCTC	No-info	C/T	-	
rs4963305	+4405	AAAAAACAAA	AAAAAAAACG	No-info	G/T	-	
rs588121	+2835	AGTGGTTTTT	TTTGTTTTCT	No-info	G/T	-	
rs2730029	+4774	CAGGAGAATG	CGTGAATCCG	No-info	A/C	-	

* = public databases.

5. DISCUSSION

Age related macular degeneration is the leading cause of visual impairment and legal blindness in elderly people over 65 years of age in the Western Europe, Australia, Japan, and the United States of America (Ambati et al., 2003). The aetiology of the disease is still poorly understood (Souied et al., 1999).

The current AMD treatment modalities do not cure the manifestations nor do they alter the progress and prognosis of the disease. Drusen regression and resorption has been observed following argon laser photocoagulation (Figueroa et al., 1994). However, the incidence of choroidal neovascularization development is increasing in those who receive laser treatment (Choroidal Neovascularization Prevention Trial Group 1998). To date, the value of prophylactic laser therapy is not conclusive and further studies are in progress in many centres (Algvere and Seregard, 2002).

Other treatment modalities are directed towards choroidal neovascularization in an attempt to alter the formation of the new blood vessels which are responsible for 80% of AMD blindness. Radiation therapy is based on the fact that ionising radiation affects new blood vessels more than mature vessels (Archer et al., 1991). Consequently, the highly sensitive new capillaries are regressing without damaging the surrounding tissues (Chong and Bird, 1998). However, many of the radiation therapy studies conducted thus far are small, non-randomized, and have no control cohorts (Ciulla et al., 1998). Also some of those who received radiation therapy suffered more decrease in visual acuity than patients receiving other treatment modalities (Spaide et al., 1998). Photodynamic therapy (PDT) is based on the interaction between the systemically administered photosensitizing dye, oxygen molecules and the laser radiations. The reaction lead to the release of the free radical singlet oxygen which in turn activate a succession of physiological and chemical processes leading ultimately to permanent or temporary neovascular occlusion (Lange et al., 2001). Photodynamic therapy is only beneficial for a small percentage of patients with choroidal neovascularization, particularly those with small lesions. Furthermore, patients treated with photodynamic therapy complain of increased sensitivity for bright light, and they have to wear special clothing and protective sunglasses (Algvere and Seregard, 2002). Several surgical interventions have been developed. The retinal relocation procedure involve a complete retinal detachment by applying subretinal infusion, followed by moving and relocating the fovea to a place

with less degenerate retinal pigment epithelium. However, there are no clear improvements, and the outcome is unpredictable. Furthermore, some patients even have developed vitreoretinopathy (Ambati et al., 2003). Several drug therapy modalities have been proposed. Interferon α is known to have inhibitory effects on the proliferation and migration of vascular endothelial cells, which are essential for neovascularization. Upon administration to non-human primates with induced angiogenesis, a reduction of iris neovascularization was observed (Miller et al., 1993). Double-blind multicenter trials, were conducted to analyse the effects of interferon α on human AMD patients with CNV, but without benefit or improvement (Pharmacological therapy for macular degeneration study group, 1997). Similarly, in vitro experiments have shown that thalidomide inhibits RPE cell proliferation induced by platelet-derived growth factor (PDGF), basic fibroblast growth factor (bFGF), and vascular endothelial growth factor (VEGF) (Kaven et al., 2001), but no reduction or decrease in angiogenesis was reported in AMD patients (Maguire et al., 2001). There is very limited success for the treatment of the exudative form. Patients with the wet form are the minority group, and within this minority half of those who are eligible for treatment suffered persistent or recurrent CNV during 3 years of follow up (Macular Photocoagulation Study Group, 1994). Those who present with subretinal haemorrhage or retinal pigment epithelium detachment are not eligible for such treatments (Freund et al., 1993).

The dry form of the disease is more prevalent than the wet form. Unfortunately, there is no satisfactory treatment for all of its presentation modalities including hard drusen, soft drusen and geographic atrophy. There are clear limitations in all forms of the current treatment modalities.

As life span is increasing, it is expected that AMD will represent a major health problem. In addition, AMD patients with vision loss in one or both eyes are emotionally distressed as their quality of life is reduced and they need help for their daily life activities (Williams et al., 1998). Thus, it is extremely important to identify factors that influence the development and progression of AMD. Once such factors are identified, they could be modified such as changing the life style or rectified through medical interventions to reduce the risk or alter the course of AMD development and progression (Hawkins et al., 1999). There is strong need to understand the pathogenesis and mechanisms which are underlying the various AMD

manifestations such as geographic, CNV, disciform scarring, and photoreceptor apoptosis.

Unravelling the secrets of these processes would pave the way for novel therapeutic modalities (Ambati et al., 2003). As a first step, understanding the genetic component of AMD would be of paramount importance in elucidating the pathogenesis and the mechanism of the disease. In this regard the accumulating knowledge about monogenic retinal dystrophies and the approaches undertaken to unravel these diseases, could be used to complement and highlight the areas and directions where the efforts should concentrate. In recent years, more than 50 monogenic non-syndromic retinal dystrophy genes have been mapped and cloned (Table 1). Several genes were identified using the positional cloning/positional candidate gene approach such as the VMD2 gene responsible for Best disease (Marquardt et al., 1998, Petrukhin et al., 1998), the tissue inhibitor of metalloproteinases-3 (TIMP3) gene associated with Sorsby fundus dystrophy (Weber et al., 1994), the RS1 gene leading to X-linked juvenile retinoschisis (Sauer et al., 1997) and the rhodopsin gene causing autosomal dominant retinitis pigmentosa, autosomal recessive retinitis pigmentosa and autosomal dominant congenital stationary night blindness. (Dryja et al., 1990, and 1993, Rosenfeld et al. 1992.). Application of classical molecular genetic approaches to AMD is hampered by several factors. Firstly, AMD is a late onset disease, the fact which makes linkage analysis difficult due to limitations in availability of enough family members (Zhang et al., 1996). Secondly, there appear to be strong environmental influences (Zack et al., 1999). Finally, the complex genetics of the disease and the possibility of genetic heterogeneity in which any given gene might be responsible for less than 5-10 % to AMD susceptibility. Genome-wide scans did not find significant evidence for linkage at a single locus (Gorin et al., 1999).

There is a need for a more systematic approach. One such approach is a thorough and meticulous examination of ocular tissues known to harbour pathological features of age related macular degeneration. Typically, this could be achieved by looking at genes which are exclusively or preferentially expressed in those tissues. The assumption is that those genes play a vital and indispensable role in normal cell function in these tissues, and therefore any alteration in those genes may lead to malfunction and the appearance of pathological features. This fact is strengthened by the observation that most of the mapped and cloned monogenic nonsyndromic retinal

dystrophy genes are either specific or restricted in the retina or RPE (den Hollander et al., 1999) (Table 1). Part of the single-gene retinopathies is caused by ubiquitously expressed genes. This does not answer the question why the phenotype is localised exclusively to the retina and does not include other tissues. A reasonable answer could include the existence of as yet unidentified retina-specific modifier genes. The retina has been extensively studied, while thus far little attention has been given to the retinal pigment epithelium. Nevertheless mutations in genes which are exclusively or preferentially expressed in the RPE are thought to contribute to retinal disorders. Indeed, RPE 65 is expressed specifically in the RPE (Gu et al., 1997) and was shown to cause autosomal recessive Leber congenital amaurosis, and autosomal recessive retinitis pigmentosa. Other RPE disease genes include the retinaldehyde binding protein 1 (RLBP1) associated with autosomal recessive retinitis pigmentosa (Maw et al., 1997), as well as other rare retinal dystrophies (Burstedt et al., 1999, Eichers et al., 2002) and the rhodopsin homolog gene (RGR) leading to autosomal recessive retinitis pigmentosa (Morimura et al., 1999).

Functional genomic approaches are powerful tools to study and evaluate for example variations in transcript expression. ESTs derived from a specific cell or tissue can provide useful information about differential expression of genes and the transcriptome of that cell or tissue (Bortoluzzi et al., 1998). There are several methods used to identify and isolate differentially expressed genes, among these enzymatic degradation subtraction (Zeng et al., 1994), representational difference analysis (RDA) (Lisitsyn, 1995) and differential display (Liang and Pardee, 1992). However, they all reveal limitations. As an example, analysis in the differential display method is mainly focused in differences at the 3' region, leaving differences at the 5' region undetected. Also, throughout the subtraction process the concentration of the differentially expressed genes remain disproportional, the fact which increases the difficulty in isolating rare transcripts. Similarly, RDA is also limited in resolving the problem of differences in the abundance of transcripts, so multiple rounds of subtractions are needed (Von Stein et al., 1997).

The suppression subtractive hybridization is a promising new tool. With this method redundant sequences are normalised through the hybridization step. Also, the technique enriches for the rare transcripts (Diatchenko et al., 1996). Transcripts which may exist in single copy in the cell are enriched and can be identified. Thus, there is

potential for novel gene or splice variant discovery. Interest has increased in alternative transcripts and alternative splicing as a major source of diversity (Wistow et al., 2002). Splice variants could have an important biological function. It has been speculated that in postmitotic cells such as the RPE, mis-splicing or splicing errors could result in accumulation of aberrant transcripts or proteins in the cell, leading ultimately to detrimental effects on cell function. Besides the novel genes and novel splice variants, analysis of the RPE cDNA subtracted library could help in cataloguing the normal collection of genes which are functionally active in the retinal pigment epithelium (Wistow, 2002). This could help understand the mechanisms and pathways involved in the physiology of RPE and retina. Furthermore, some of these genes could qualify as AMD candidate genes.

In order to construct an RPE cDNA library of high quality, large quantities of RPE cells are needed, with excellent quality and not contaminated with the adjacent tissues such as the choriocapillaris and the retina. As these conditions can not be achieved with RPE from human eyes, bovine eyes were used for the present project. RPE cells from bovine eyes were recovered by gently brushing the tissue without disturbing the underlying choroid. Using bovine RPE-specific poly (A)⁺ RNA and bovine heart and liver poly (A)⁺ RNA, a normalised and enriched bovine RPE-specific cDNA library was constructed as described. From this library, a total number of 2379 differentially expressed bovine ESTs were generated. Pathway analysis of 341 known genes including 168 from the first phase and 173 from the second phase showed that they fall into different functional categories including cell structure/growth/maintenance, apoptosis, cell adhesion, cell signalling, energy/metabolism, lysosomal enzyme, phagocytosis, phototransduction, signal transduction, transcription/translation factors, ubiquitin pathway, RNA/DNA binding, chaperones, vitamin A cycle, oxidative stress, transport, unknown/unclassified group and a miscellaneous group containing several functional groups represented by a single or few clones each. The distribution of the functional pattern reflect the role of the RPE in remodelling of extracellular membrane (ECM), syntheses of various growth factors, pigments and enzymes, and its involvement in transport of nutrients, ions and retinoids. Pathway analysis of the mapped and cloned monogenic nonsyndromic retinal dystrophy genes (Table 1) showed that they fall into different functional categories such as phototransduction, cell to cell interaction, metabolism, RNA processing, phagocytosis, structure,

transport, vision, vitamin A cycle, and transcription factors. The functional profile of the known genes in this study is similar to the functional distribution of the monogenic nonsyndromic retinal dystrophy genes. The close similarity between the functional profiles gives a strong support that disease causing genes might exist within the collection of genes identified in this study.

In order to conduct the differential screening, expression analysis was performed using reverse Northern blot hybridizations, as it's a high throughput method where many genes can be analysed simultaneously. To insure high sensitivity for the experiment, the 186 known genes were included as controls, the 2 sets of membranes were duplicated, and genes such as Actin, GAPD and RPE-1 were sampled on the filter membranes more than once as controls. The finding of relatively low number of known genes (21) and unknown clones (10) in group I of the reverse Northern blot analysis is not surprising, because the library was normalised to limit the appearance of housekeeping genes. The appearance in this group of RLBP1 gene which is known to be expressed preferentially in the RPE (Kennedy et al., 1998) was unexpected. One explanation could be the signal intensity threshold applied by the software to separate the groups is so close, that the slightest decrease or increase may lead to a change in the group. Group II contains 260 clones (Appendix Table 4). Of these, 151 clones exhibited identity to known genes, while 109 were unknown transcripts. Among the known genes in this group is clone RPE23-C10 with identity to the tissue inhibitor of metalloproteinase 3 (TIMP3) associated with Sorsby fundus dystrophy, and clone RPE20A-E09 with identity to the optic atrophy 3 gene (autosomal recessive, with chorea and spastic paraplegia, OPA3) responsible for optic atrophy syndrome. The inclusion of these 2 genes in this group is expected as they are expressed in several tissues. The presence of 260 genes in this group may indicate that a sizable fraction of genes in the RPE are expressed at low levels, and this is consistent with the fact that the library was enriched for rare transcripts. Group III contains 27 clones with 14 transcripts showing identity to known genes (Table 10), and some of these genes are known to be preferentially expressed in the RPE such as the retinal G protein coupled receptor (RGR), lecithin retinol acyltransferase (LRAT), and retinal pigment epithelium-specific protein-65 (RPE65) (Table 1). Furthermore, the above mentioned genes are associated with different retinal dystrophies (Table 1). Also, the membrane frizzled-related protein (MFRP) resides in this group. The MFRP is abundantly

expressed in the RPE and mutations in the MFRP mouse homolog gene cause autosomal recessive retinal degeneration-6 (rd6) (Kameya et al., 2002). The presence of known retinal dystrophy genes confirms the validity of the library construction. Moreover, the existence of these genes in this particular group, is in accordance with the goals of the library construction as it was subtracted to allow for those genes which are abundantly expressed in the RPE. A few retina specific genes were included in the 3 groups. The unc-119 homolog gene (unc119) appeared in group I and is known to be associated with dominant cone-rod dystrophy. In group II, three retina specific genes, associated with monogenic retinal dystrophies (Table 1) were present; clone RPE1-B06 with identity to ATP-binding cassette, sub-family A (ABCA4), clone RPE12-G07 with identity to guanine nucleotide binding protein, alpha transducing activity polypeptide-1 (GNAT1), and RPE10-D03 representing arrestin (SAG). In group III, the retinal degeneration slow (RDS) and rhodopsin (RHO) which both are monogenic retinal dystrophy genes (Table 1) were included (Table 10). The presence of retina-specific genes in an RPE subtracted library is not uncommon, as it is difficult to separate the retina from the RPE due to the tight adherence between them. (Den Hollander et al., 1999, Sharma et al., 2002).

The results of the reverse Northern blot analyses facilitated the prioritization of the subsequent functional analyses of the RPE genes. Northern blot hybridizations were performed as a second step in expression analyses as it is more sensitive than the reverse Northern blot analyses, and at the same time deliver less false positives in comparison with the RT-PCR. After the final normalisation, 107 unique unknown transcripts were chosen for Northern blot analysis. Total RNA used included RPE and retina to differentiate precisely between these two tissues, heart and liver, as they were used in the subtraction process, and brain, kidney and lung as non-ocular tissues. Signals were detected for a total number of 53 (49.5%) clones (Figure 11). For 54 (50.5%) transcripts, evaluation was not possible due to absence or reduced quality of signals (Table 12). Out of the 53 transcripts, for which signals were detected on Northern blot hybridizations, 50 (94.3%) transcripts showed expression in RPE. Of these, 7 were identified as having specific RPE expression, 7 transcripts showed RPE and retina expression, 7 transcripts were considered to have a tissue restricted expression in RPE and one or more other tissues, and 29 clones with

ubiquitous expression. Only three transcripts have no RPE expression and these are the retina specific clones (Table 13).

This result confirms the findings of the reverse Northern blot analyses that sizable number of genes in the RPE are found at low level, and at the same time it proved the usefulness of the subtractive hybridization approach as a powerful tool for gene enrichment. Three clones (RPE1-D02, RPE10-B10, RPE10-D08) which showed restricted expression in RPE and retina (Table 14) have been cloned and characterised by other groups during the course of this project. The cloning and characterisation of these three genes is a strong confirmation of the success of this project and a strong indication that other important genes could be identified. Furthermore, the RPE 10-B10 which is known as the MT-Protocadherin has been identified as a retinal disease candidate gene (Sharon et al., 2002). Predicted genes and unknown human transcripts which showed exclusive or preferential expression in RPE (Table 13) may have specialised physiological role in the RPE. Some clones with detectable signals in Northern blot hybridizations showed no significant similarity in public databases (Table 13). The reason could be that these transcripts may have originated from the 3'-untranslated region of the bovine gene, which is more likely to be less conserved in the orthologous human gene. The ubiquitously expressed genes are important similar to those which are specific or restricted to RPE, These genes could be splice variants of ubiquitously expressed genes and the probe taken for the Northern blot analyses happened to be from the conserved region between the isoforms. It is of interest that 3 clones showed restricted expression in RPE/kidney and one clone is expressed only in RPE and liver. It is intriguing to know the physiological correlation between RPE/kidney and RPE/liver. It could be speculated that a gene specifically expressed in RPE and kidney would play a role in epithelial cell physiology as both tissues contain these cell types. On the other hand a gene restricted to RPE and liver might be important for metabolism such as lysosomal enzymes. The wide expressional picture in this bovine subtracted library reflects the diversity of genes which are present in the RPE and at the same time it shows the complexity of the mechanisms governing the physiological function of the tissue and the retina in general. Understanding the role and regulatory mechanisms of each of these genes will help us understand the physiology and pathology of the retina and retinal diseases.

Using functional genomic methods, like the one used in this study is a direct approach to identify candidate genes for complex genetic diseases. The hypothesis in this study is based on the suggestion that genes which are expressed in the RPE might play a role in the pathogenesis of AMD. The suggestion built on the fact that part of the AMD pathological features are manifested in RPE. To narrow down the number of candidate genes, a first step would be to eliminate genes which are not expressed in this mono-cellular layer. Implementing this step still leaves a considerable number of candidate genes. Functional information such as the expressional pattern could be used to prioritise genes for further screening. Typically, in this study genes which are exclusively or preferentially expressed in the RPE were selected as priority AMD candidate genes (Table 14). This does not preclude the widely expressed genes from being considered as potential candidate genes, as many of these genes are important in RPE or retinal physiology and function. Furthermore, some of the ubiquitously expressed genes were shown to cause retinal dystrophies (Table 1) such as the c-met proto-oncogene tyrosine kinase gene (MERTK) associated with autosomal recessive retinitis pigmentosa (Gal et al., 2000), and prominin-1 gene (PROM1) responsible for autosomal recessive retinal degeneration (Maw et al., 2000). Further prioritization of candidate genes could be achieved by looking at the function of genes, as many retinal dystrophies are caused by mutations in genes falling into certain functional categories, such as phototransduction, transport, cell maintenance and structure, vitamin A cycle, transcription factors, and metabolism (Table 1). Other functional categories not previously shown to be associated with retinal disease have been suggested to play a role in retinal pathogenesis. These include oxidative stress, lysosomal enzymes, heat shock proteins (molecular chaperones), apoptotic and anti-apoptotic molecules, and ubiquitin pathways (Appendix, Table 5). The RPE has several antioxidants defence mechanisms through which it can counteract the effects of the oxidative stress. Among these, the DNA repair mechanism through the DNA polymerase and ligase, antioxidant enzymes such as catalase, glutathione peroxidase, and superoxide dismutase, and antioxidant vitamins such as vitamin A, C and carotenoids (Winkler et al., 1999, Beatty et al., 2000). Kimura et al., (2000) reported a possible association between the exudative age-related macular degeneration and mutation in the manganese superoxide dismutase. However, the authors concluded that a larger and well controlled association study is needed to confirm their results. In this study several known genes with a possible role in the oxidative stress pathways

were identified, among these peroxiredoxin 1 (PRDX1) (RPE8-C5), microsomal glutathione S-transferase 1 (MGST1) (RPE24-B6), monoamine oxidase B (MAOB) (RPE3-D9), glutathione S-transferase M5 (GSTM5) (RPE23-E4), glutathione peroxidase 4 (GPX4) (RPE26-E8), ATX1 antioxidant protein 1 (ATOX1) (RPE12-A6), and glutathione S-transferase M1 (GSTM1) (RPE8-H5). Molecular chaperones like the heat shock 90 KD (HSPCB) (RPE16-F3) identified in this study as well as others such as heat shock protein 70 KD (HSP70), heat shock protein 60 KD and (HSP60), and heat shock protein 27 KD (HSP27), are also known to participating in cell survival under stress conditions. Heat shock proteins help protein production through folding of the protein, then through transport and translocation to the final end stage of degradation for those proteins which are disrupted (Bukau and Horwich, 1998). Many neurodegenerative diseases are caused by deposition of abnormal proteins in the brain (Sherman and Goldberg, 2001). Thus, heat shock proteins play an important role in cell survival (Parcellier et al., 2003). Bernstein et al., (2000) reported a decrease in mRNA level of HSP70 in the primate retina with aging. The authors stated that a decline in HSP70 levels renders the retina more susceptible to age-acquired retinal disease. Similarly, Strunnikova et al. (2001) showed that HSP27 was expressed at high levels in ARPE-19 cells which were subjected to oxidant-mediated injury by hydrogen peroxide and myeloperoxidase. The study highlighted the importance of HSP27 in RPE protection from death and the authors suggested that HSP27 levels may play role in retinal diseases such as AMD. Recently it has been shown that the small heat shock protein α B-crystallin protects the RPE against oxidative stress by preventing the apoptotic cell death (Alge et al., 2002). Ubiquitin molecules are essential in various cellular processes such as transcriptional regulation, signal transduction and apoptosis (Hershko et al., 1998). In this study ubiquitin-activating enzyme E1 (UBE1) (RPE-25-C3) has been identified. As Ubiquitin-mediated proteolysis pathway has been implicated in down regulation of rhodopsin, it has been suggested that selective inhibitors of the system may be helpful in improving visual sensitivity in patients with retinitis pigmentosa and macular degeneration, particularly in their early stages. Furthermore, enrichment of molecules of the ubiquitin system has also been identified in retina libraries (Blackshaw et al., 2001). Likewise, apoptosis has also been associated with retinal diseases. Apoptosis seems to be a common pathway of photoreceptor death for different retinal disease phenotypes. Chang et al., (1993) have shown that DNA fragmentation was present in eyes of mice

with mutations in retinal degeneration, retinal degeneration slow/peripherin and rhodopsin. As DNA fragmentation is a major feature of the programmed cell death, the authors concluded that apoptosis was the common end stage of all three mutant genes. It has been suggested that the use of anti-apoptotic agonists might be effective in preventing photoreceptor degeneration (Blackshaw et al., 2001). In this study, several members from the programmed cell death genes were identified including testis enhanced gene transcript (BAX inhibitor-1) (TEGT) (RPE2-D12), BCL2-like 1 (BCL2L1) (RPE3-F3), and the defender against cell death-1 gene (DAD1) (RPE23-C9). A decrease in lysosomal enzymes is thought to result in accumulation of cell debris and undigested materials in the RPE leading to drusen formation. Thus, enzymes such as the cathepsin K (CTSK) (RPE24-E2) identified in this study should be evaluated and its role in RPE physiology and function analysed. Taking into account the expressional pattern as well as the functional analysis, the number of genes for assessment could be increased to include other unknown genes as well as known genes with potential role in RPE and retina physiology.

RPE10-D08 (TRPM3) is an AMD candidate clone (Table 14). Two novel isoforms of the TRPM3 gene have been isolated and characterized in this study. Recently, in May 2003, the full length cDNA of the transient receptor potential cation channel subfamily M, member 3 (TRPM3) has been published (Lee et al., 2003, Grimm et al. 2003). The TRPM3 gene is localized in chromosome 9q21.12 spanning 311 kb between the genomic markers D9S1874 and D9S1807 ((Lee et al., 2003). TRPM3 is a member of the transient receptor potential subfamily M (TRPM). TRPM is one of 6 subfamilies and belong to the transient receptor potential (TRP) superfamily of Ca^{2+} -permeable cation channels (Montell, 2001). TRP members share structural similarities and are characterized by a core of six transmembrane domains at the N-terminus of the protein. The existence of the transmembrane domains indicates that the TRP may play a role as a channel (Philips et al., 1992). Additional structural features include the ankyrin repeats, a stretch of 33 amino acid residue at the NH_2 terminal which is involved in protein-protein interactions and linking membrane proteins to the cytoskeleton (Michaely and Bennett, 1993). The group is also characterized by the TRP domain, situated at the COOH terminal and encompasses 25 amino acids (Montell, 2001). The domain function is still not known. The TRPM subfamily exhibits ~20% amino acid identity to *Drosophila* TRP, over an area which covers the

TRP domain and the transmembrane regions S2-S6 (Minke and Cook, 2002). The TRPM members do not have ankyrin repeats (Montell, 2001). The founding member of this subfamily is melastatin-1 a putative tumour suppressor gene. Although other TRP family members have been extensively studied such as TRP-classic (TRPC), and TRP-vanilloid (TRPV), little is known about the expression and function of the TRPM subfamily (Xu, et al 2001). In *Drosophila* the TRP has been shown to play an important role in phototransduction, (Hardie and Minke, 1992), and mutation in this gene leading to a single amino acid change (phe550Ile) in the fifth transmembrane segment, was identified as the cause of photoreceptor degenerations (Hong et al., 2002). The two isoforms isolated and characterized in this study are relatively short and are devoid of the transmembrane domains normally found in most members of the TRPM subfamily. Thus, the two isoforms cannot function as channels. Interestingly, melastatin 1 (MLSN1) is also alternatively spliced into a short transcript (MLSN-S) (Fang and Setaluri 2000) that lacks the transmembrane segments and a longer transcript (MLSN-L) (Hunter et al., 1998). It has been shown that expression of MLSN-L induces Ca^{2+} influx, in contrast to MLSN-S when introduced in HEK293 cells. Subsequently, coexpression of both isoforms in HEK293 cells, lead to a significant suppression of MLSN-L dependent Ca^{2+} activity indicating that MLSN-S has an inhibitory effect on MLSN-L (Xu et al., 2001). Similarly, MTR1 gene (MLSN1- and TRP-related gene-1) is alternatively spliced (Prawitt et al., 2000). The short variant of MTR1 gene may be a regulatory element (Xu et al., 2001). Comparisons of MLSN1, MLSN2, and other related transcripts in Unigene and GenBank suggest that alternative splicing is very common among TRPM family members (Wistow et al., 2002). This allows us to speculate that the two novel isoforms isolated in the current study may interact and regulate the TRPM3 transcript in the retinal pigment epithelium.

The second candidate clone is the RPE3-E5. This bovine RPE3-E5 EST showed homology to the human MGC2477 predicted gene. Northern blot analysis of bovine EST indicated an abundant expression in the retina and low level of expression in the RPE (Figure 18). This result was confirmed by RT-PCR expression analysis, which was performed using human mRNA and showed abundant expression in the retina and low expression in all other tissues tested (Figure 19). Two putative open reading frames were identified, but the translated proteins did not show any homology in

protein and motif public databases. The pattern of expression seems to indicate an important role for this gene in the physiology and function of the RPE and retina. Furthermore, the gene was identified to be expressed in several cDNA libraries of the National Eye Institute (NEI) including retina cDNA unnormalized library, lens cDNA normalized library, EST data base (dbEST) human retina, dbEST human eye anterior segment, dbEST human optic nerve cDNA library, and dbEST human RPE and choroid cDNA library. The gene has not been identified in the unnormalized cDNA libraries of the cornea, fovea, iris and the trabecular meshwork, as well as dbEST of human ciliary body cDNA, and dbEST of the trabecular meshwork cDNA.

The third candidate clone is RPE10-B10 (MT-Protocadherin). Nakajima et al., (2001) identified a non-classical cadherin designated KIAA1775 which later became known as MT-Protocadherin. The cadherin superfamily is classified into classical cadherins and non-classical cadherins (Uemura, 1998). Classical cadherins shares conserved domains among all members including a single transmembrane domain, large extracellular domain, and a conserved cytoplasmic domain (Faulkner-Jones et al., 1999). The extracellular domain contains the DXNDNAPXF, DRE, and the DXD motifs which play an active role in Ca^{2+} binding (Takeichi, 1990). The extracellular domain of the protocadherins contains five or six tandem repeats like the classical cadherins, but the cytoplasmic domain does not resemble those of the classical cadherins (Yagi, 2000). Based on experimental expressional data using NF-protocadherin (NFPC) gene in *Xenopus* embryos, Bradley et al., (1998) indicated that NFPC might function as adhesion molecule during early stages of development. They added that the mechanism of action might be different from that of the classical cadherins. In a similar study, using paraxial protocadherin (PAPC) in *Xenopus*, Kim et al., (1998) demonstrated that PAPC is functioning as an adhesion molecule. Adhesion molecules are thought to be involved in the pathogenesis of AMD (Penfold et al., 2001).

Collectively, from the functional analysis of the MT-protocadherin, and the expressional data of RPE10-B10 bovine orthologous EST which exhibited abundant expression in retina and relatively low expression in RPE, the gene was included in the priority list for SNP identification and assessment in the AMD case control association study.

After the completion of the human genome sequence project, much attention was given to the single nucleotide polymorphism (SNP), the most prevalent among many types of polymorphic variations. It has been estimated that the human genome may contain over ten million SNPs scattered at about one SNP every thousand base pairs or less. Due to the fact that SNPs are common and distributed throughout the human genome, they are considered to be more superior to other genetic markers such as the restriction fragment length polymorphisms (RFLP), minisatellites and microsatellites. There are many ways in which they could be used such as identification of disease related loci or the very exciting possibility of establishing individualised medicine in which the acceptability and usefulness of a pharmacological component is dependent upon the individual polymorphic variation, and last but not least SNPs could be used as a diagnostic tool (Weiner and Hudson, 2002). Current assays commonly used to identify SNPs include denaturing high-performance liquid chromatography (dHPLC) (Wolford et al., 2000), single strand conformation polymorphisms (SSCPs) (Orita et al., 1989), variant detector arrays (VDAs) (Wang et al., 1998), and direct DNA sequencing. Denaturing high-performance liquid chromatography is used to detect heteroduplexes formed during reannealing of the denatured strands of a DNA fragment from a heterozygous person. For SSCP, the amplified PCR product containing the SNP is denatured and run on non-denaturing polyacrylamide gels. The band containing the SNP will be detected by its abnormal migration pattern (Gray et al., 2000). For the VDA, the PCR product expected to contain the SNP is hybridized to a glass chip containing array of oligonucleotides. The difference in hybridization signals indicates the presence of an SNP (Wang et al., 1998). The SSCP requires intensive work. The HPLC technology is cost effective. Despite the fact that the VDA is a high throughput method which could be compared to sequencing, still DNA sequencing is the favourite approach. On the other hand, SNP could be identified *in silico* as several computer programmes are available. However, there are several disadvantages associated with this approach. The sample size is small when using *in silico* searches, as there would be few mRNA sequences and ESTs per gene, compared to the number of chromosomes which could be included in a laboratory based test. Most ESTs are clustered around the 3' end of genes and this would leave out the more important SNPs which could affect the protein. The approach taken in this study is mainly a laboratory based assays, but the SNPs from public databases

which are relevant to candidate genes were included in the study and verified. HPLC and direct sequencing were used for SNP identification in this project.

The number of novel SNPs identified in this study clearly shows the importance of laboratory based assays in discovering SNPs. The study also shows that SNPs deposited in public databases need to be revised and validated via laboratory based assays.

SNPs can be used to construct the common haplotypes. Redundant SNPs will be excluded and only essential SNPs which capture the common haplotypes are considered. The use of common haplotypes can reduce the efforts of genotyping in association studies (Johnson et al., 2001).

Croucher et al., (2003), reported positive association of three haplotypes to Crohn's disease. Haplotypes were constructed from 23 SNPs spanning 290 kb of genomic sequences. The area included all exons and exon-intron junctions of the caspase recruitment domain family, member-15 gene (CARD15) gene plus 1 kb at 3' and 5' ends of the gene at 50, 100, 150, and 200 kb. The study was conducted in two ethnically divergent population Koreans and Europeans including 47 patients from each. Two sets of haplotypes were identified. Set 1 includes SNPs found in both population and set 2 representing SNPs only found in Europeans. Three haplotypes from set 2 were reported to have statistically significant association to Crohn's disease. No association was found in SNPs from set 1.

In a similar study, Stern et al., (2003) reported a statistically significant association of erosive hand osteoarthritis with an SNP (IL5810AA) in the interleukin-1 beta gene. Their study included seven SNPs in interleukin 1, alpha (IL1A), interleukin 1, beta (IL1B), and interleukin 1 receptor antagonist (ILRN) genes. The study also included an IL1RN variable number of tandem repeat and six microsatellite markers from other chromosomes. Sample size included 68 Caucasian Americans cases and 51 Caucasian Americans controls.

Crohn's disease and the heritable osteoarthritis are genetically complex diseases as AMD. The application of exactly the same approach in our study can result in identification of AMD association with an SNP or a haplotype. Such association can help identify the AMD disease susceptibility gene.

6. CONCLUSION AND FUTURE PERSPECTIVES

ESTs analyses are powerful tools for identification and cataloguing of genes expressed in a specific tissue or cell type. The suppression subtraction hybridization (SSH) approach was used to generate a bovine cDNA library highly enriched for rare RPE transcripts. The data obtained from the expression analyses demonstrates the efficacy of the SSH approach and facilitated selection of candidate clones for further analysis. Computer homology searches were used in this study to identify human orthologous genes.

The present study added valuable data on the generation of a catalogue of known human genes that are actively expressed in the RPE. In addition, the analyses identified unknown human transcripts as well as novel human splice variants. In the near future, the work will continue in construction of the common haplotypes for the selected AMD susceptibility candidate genes, followed by association studies in large cohorts of AMD patients and ethnically and age matched controls.

Unravelling the RPE expression profile will give a better understanding of the biological processes and pathways which could be involved in the physiology and pathogenesis of retina. Identification of RPE and retinal disease susceptibility genes can be useful in many ways. First, diagnostic and prognostic information will be available for patients. Second, DNA microarrays can be generated and used to identify differential expression in disease and during development. Third, animal models can be created to help understand the pathogenesis of retinal diseases. Fourth, drug discovery targets can be identified and screened. Finally, understanding the genetic basis of AMD can herald the way for gene therapy approaches such as the replacement of a defective gene or the introduction of a new gene through viral or nonviral vectors.

These novel preventive and treatment modalities will help improve the health and quality of life for those who suffer from AMD.

7. REFERENCES

- Alge, C., Priglinger, S., Neubauer, A., Kampik, A., Zillig, M., Bloemendal, H., and Welge-Lussen, U. (2002). Retinal pigment epithelium is protected against apoptosis by alphaB-crystallin. *Invest Ophthalmol. Vis Sci.* 43(11):3575-82.
- Algvere, P., and Seregard, S. (2002). Age- related maculopathy: Pathogenetic features and new treatment modalities. *Acta Ophthalmologica Scandinavica.* 80:136-143.
- Ambati, J, Ambati, B., Yoo, S., Ianchulev, S., and Adamis, A. (2003). Age-related macular degeneration: etiology, pathogenesis, and therapeutic strategies. *Surv Ophthalmol.* 48(3):257-93.
- Anderson, D., Hageman, G., Neitz, M., Neitz, J., Wu, W., Nealon, M., De los Rios, M., and Johnson, L. (1998). Local cellular sources of drusen-associated molecules. *Invest Ophthalmol Vis Sci.* 39, p. S369.
- Anderson, D., Mullins, R., Hageman, G., and Johnson, L. (2002). A role for local inflammation in the formation of drusen in the aging eye. *Am. J. Ophthalmol.* 134(3):411-31.
- Archer, D., Amoaku, W., and Gardiner, T. (1991). Radiation retinopathy-clinical, histopathological, ultrastructural and experimental correlations. *Eye.*;5 (Pt 2):239-51.
- Bakall, B., Marknell, T., Ingvast, S., Koisti, M., Sandgren, O., Li, W., Bergen, A., Andreasson, S., Rosenberg, T., Petrukhin, K., and Wadelius, C. (1999). The mutation spectrum of the bestrophin protein--functional implications. *Hum Genet.* 104(5):383-9.
- Beatty, S., Boulton, M., Henson, D., Koh, H., and Murray, I. (1999). Macular pigment and age related macular degeneration. *Br J Ophthalmol.* 83(7):867-77.
- Beatty, S., Koh, H., Phil, M., Henson, D., and Boulton, M. (2000). The role of oxidative stress in the pathogenesis of age-related macular degeneration. *Surv Ophthalmol.* 45(2):115-34.
- Bermann, M., Schutt, F., Holz, F., and Kopitz, J. (2001). Does A2E, a retinoid component of lipofuscin and inhibitor of lysosomal degradative functions, directly affect the activity of lysosomal hydrolases? *Exp Eye Res.* 72(2):191-5.
- Bernstein, S., Liu, A., Hansen, B., and Somiari, R., (2000). Heat shock cognate-70 gene expression declines during normal aging of the primate retina. *Invest Ophthalmol Vis Sci.* 41(10):2857-62.
- Bessant, D., Ali, R., and Bhattacharya, S. (2001). Molecular genetics and prospects for therapy of the inherited retinal dystrophies. *Curr Opin Genet Dev.* 11(3):307-16.
- Bird, A., Bressler, N., Bressler, S., Chisholm, I., Coscas, G., Davis, M., de Jong, P., Klaver, C., Klein, B., Klein, R, et al., (1995). An international classification and grading system for age-related maculopathy and age-related macular degeneration.

- The International ARM Epidemiological Study Group. *Surv Ophthalmol.* 39(5):367-74.
- Blackshaw, S., Fraioli, R., Furukawa, T., and Cepko, C., (2001). Comprehensive analysis of photoreceptor gene expression and the identification of candidate retinal disease genes. *Cell.* 30;107(5):579-89.
- Blodi, C., and Stone, E. (1990). Best's vitelliform dystrophy. *Ophthalmic Paediatr Genet.* 11(1):49-59.
- Bok, D. (1985). Retinal photoreceptor-pigment epithelium interactions. *IVOVIS:* 26, 1659-1694.
- Bok, D. (1993). The retinal pigment epithelium: a versatile partner in vision. *Journal of cell Science. Supplement.* 17, 189-195.
- Bortoluzzi, S., Rampoldi, L., Simionati, B., Zimbello, R., Barbon, A., et al. (1998). Comprehensive, High-Resolution Genomic Transcript Map of Human Skeletal Muscle. *Genome Res.* 8(8):817-25.
- Boulton, M., Moriarty, P., Jarvis-Evans, J., and Marcyniuk, B. (1994). Regional variation and age-related changes of lysosomal enzymes in the human retinal pigment epithelium. *Br J Ophthalmol.* 78, 125-9.
- Bradley, R., Espeseth, A., and Kintner, C. (1998). NF-protocadherin, a novel member of the cadherin superfamily, is required for *Xenopus* ectodermal differentiation. *Curr Biol.* 12;8(6):325-34.
- Bressler, N., Munoz, B., Maguire, M., Vitale, S., Schein, O., Taylor, H., and West, S. (1995). Five-year incidence and disappearance of drusen and retinal pigment epithelial abnormalities. Waterman study. *Arch Ophthalmol.* 113(3):301-8.
- Brunk, U., and Terman, A. (2002). Lipofuscin: mechanisms of age-related accumulation and influence on cell function. *Free Radic Biol Med.* 1; 33(5):611-9.
- Bukau, B., and Horwich, A. (1998). The Hsp70 and Hsp60 chaperone machines. *Cell.* 6;92(3):351-66.
- Burset, M., Seledtsov, I., and Solovyev, V. (2000). Analysis of canonical and non-canonical splice sites in mammalian genomes. *Nucleic Acids Res.* 1;28(21):4364-75.
- Burstedt, M., Sandgren, O., Holmgren, G., and Forsman-Semb, K. (1999). Bothnia dystrophy caused by mutations in the cellular retinaldehyde-binding protein gene (RLBP1) on chromosome 15q26. *Invest Ophthalmol Vis Sci.* 40(5):995-1000.
- Cai, J, Nelson, K., Wu M., Sternberg, P., and Jones D. (2000). Oxidative damage and protection of the RPE. *Prog Retin Eye Res.* 19(2):205-21.
- Campochiaro, P. (1999). The pathogenesis of age-related macular degeneration. *Molecular vision.* 5, 24.

- Campochiaro, P. (2000). Retinal and choroidal neovascularization. *Journal of cellular physiology*. 184, 301-310.
- Chang, G., Hao Y., and Wong, F. (1993). Apoptosis: final common pathway of photoreceptor death in rd, rds, and rhodopsin mutant mice. *Neuron*. 11(4):595-605.
- Chong, N., and Bird, A. (1998). Alternative therapies in exudative age related macular degeneration. *British Journal of Ophthalmology*. 82: 1441-1443.
- Choroidal Neovascularization Prevention Trial Research Group (1998). Laser treatment in eyes with large drusen. *Ophthalmology*. 105: 11-23.
- Christen, W., Glynn, R., Manson, J., Ajani, U., and Buring, J. (1996). A prospective study of cigarette smoking and risk of age-related macular degeneration in men. *JAMA*. 9;276(14):1147-51.
- Cingle, K., Kalski, R., Bruner, W., O'Brien, C., Erhard P., and Wyszynski R. (1996). Age-related changes of glycosidases in human retinal pigment epithelium. *Curr. Eye Res*. 15, 433-8.
- Ciulla, T., Danis, R., and Harris, A. (1998). Age-Related Macular Degeneration; A review of experimental treatments. *Survey of Ophthalmology*. Volume 43, Issue 2 , Pages 134-146.
- Collins, F. (1992). Positional cloning: Let's not call it reverse anymore. *Nature genetics*. volume 1.
- Crabb, J., Miyagi, M., Gu, X., Shadrach, K., West, K., Sakaguchi, H. et al., (2002). Drusen proteome analysis: An approach to the etiology of age-related macular degeneration. *Proc Natl Acad Sci U S A*. 12;99(23):14682-7.
- Croucher, P., Mascheretti, S., Hampe, J., Huse, K., Frenzel, et al., (2003). Haplotype structure and association to Crohn's disease of CARD15 mutations in two ethnically divergent populations. *Eur J Hum Genet*. 11(1):6-16.
- Davis, K. (1991). In: Oxidative damage and repair: Chemical, biological and medical aspects. 99. 91. *Pergamon Press*, Oxford/New York, pp. 99–109.
- Delcourt, C., Diaz, J., Ponton-Sanchez, A., and Papoz, L. (1998). Smoking and age-related macular degeneration. The POLA Study. *Arch Ophthalmol*. 116(8):1031-5.
- Den Hollander, A., van Driel, M., de Kok, Y., van de Pol, D., Hoyng, C., Brunner, H., Deutman, A., and Cremers, F. (1999). Isolation and mapping of novel candidate genes for retinal disorders using suppression subtractive hybridization. *Genomics*. 15;58(3):240-9.
- Dice, J. (2000). Lysosomal pathways of protein degradation, Georgetown. Tx: Eureka.com/Landes Bioscience.108.

- Diatchenko, L., Lau, Y., Campbell, A., Chenchik, A., Moqadam, F., Huang, B., Lukyanov, S., Lukyanov, K., Gurskaya, N., Sverdlov, E., and Siebert, P. (1996). Suppression subtractive hybridization: a method for generating differentially regulated or tissue-specific cDNA probes and libraries. *Proc Natl Acad Sci U S A*. Jun 11; 93(12):6025-30.
- Dowling, J., and Boycott, B., (1966). Organization of the primate retina: electron microscopy. *Proc. R. Soc., B (Lond)* 166, 80-111.
- Dryja, T. (1997). Gene-based approach to human gene-phenotype correlations. *Proc Natl Acad Sci U S A*. 28;94(22):12117-21.
- Dryja, T., Berson, E., Rao, V., and Oprian, D. (1993). Heterozygous missense mutation in the rhodopsin gene as a cause of congenital stationary night blindness. *Nat Genet*. 4(3):280-3.
- Dryja, T., McGee, T., Reichel, E., Hahn, L., Cowley, G., Yandell, D., Sandberg, M., and Berson, E. (1990). A point mutation of the rhodopsin gene in one form of retinitis pigmentosa. *Nature*. 25;343(6256):364-6.
- Dryja, T., McGee, T., Hahn, L., Cowley, G., Olsson, J., Reichel, E., Sandberg, M., and Berson, E. (1990). Mutations within the rhodopsin gene in patients with autosomal dominant retinitis pigmentosa. *N Engl J Med*. 8;323(19):1302-7.
- Eichers, E., Green, J., Stockton, D., Jackman, C., Whelan, J., McNamara, J., Johnson, G., Lupski, J., and Katsanis, N. (2002). Newfoundland rod-cone dystrophy, an early-onset retinal dystrophy, is caused by splice-junction mutations in RLBP1. *Am J Hum Genet*. 70(4):955-64.
- Evans, J. (2001). Risk factors for age-related macular degeneration. *Prog Retin Eye Res*. 20(2):227-53.
- Fang, D., and Setaluri, V. (2000). Expression and Up-regulation of alternatively spliced transcripts of melastatin, a melanoma metastasis-related gene, in human melanoma cells. *Biochem Biophys Res. Commun*. 9: 279(1):53-61.
- Faulkner-Jones, B., Godinho, L., and Tan, S. (1999). Multiple cadherin mRNA expression and developmental regulation of a novel cadherin in the developing mouse eye. *Exp Neurol*. 156(2):316-25.
- Feinberg, A., and Vogelstein, B. (1983). A technique for radiolabeling DNA restriction endonuclease fragments to high specific activity. *Anal Biochem*. 1;132(1):6-13.
- Ferris, F., 3rd; Fine, S., and Hyman, L. (1984). Age-related macular degeneration and blindness due to neovascular maculopathy. *Archives Of Ophthalmology*. Volume 102, Issue 11, Pages 1640-1642.
- Figuroa, M., Regueras, A., and Bertrand, J. (1994). Laser photocoagulation to treat macular soft drusen in age-related macular degeneration. *Retina*. 14: 391-394.

- Freund, K., Yannuzzi, L., and Sorenson, J. (1993). Age-related macular degeneration and choroidal neovascularization. *Am J Ophthalmol.* 15;115(6):786-91.
- Gal, A., Li, Y., Thompson, D., Weir, J., Orth, U., Jacobson, S., Apfelstedt-Sylla, E., and Vollrath, D. (2000). Mutations in MERTK, the human orthologue of the RCS rat retinal dystrophy gene, cause retinitis pigmentosa. *Nature Genet.*, 26: 270-271.
- Gass, J. (1972). Drusen and disciform macular detachment and degeneration. *Trans Am Ophthalmol Soc.*70:409-36.
- Gibson, J., Shaw, D., and Rosenthal, A. (1986). Senile cataract and senile macular degeneration: an investigation into possible risk factors. *Trans Ophthalmol Soc U K.*;105 (Pt 4):463-8.
- Gorin, M., Breitner, J., De Jong, P., Hageman, G., Klaver, C., Kuehn, M., and Seddon, J. (1999). The genetics of age-related macular degeneration. *Mol Vis.* 3;5:29.
- Gottfredsdottir, M., Sverrisson, T., Musch, D., and Stefansson, E. (1999). Age related macular degeneration in monozygotic twins and their spouses in Iceland. *Acta Ophthalmol Scand.* 77(4):422-5.
- Gray, I., Campbell, D., and Spurr, N. (2000). Single nucleotide polymorphisms as tools in human genetics. *Hum Mol Genet.* 9(16):2403-8.
- Green, W. (1999). Histopathology of age-related macular degeneration. *Mol Vis.* 3; 5:27.
- Green, W., and Enger, C. (1993). Age-related macular degeneration histopathologic studies. The 1992 Lorenz E. Zimmerman Lecture. *Ophthalmology.* 100(10):1519-35
- Grimm, C., Kraft, R., Sauerbruch, S., Schultz, G., and Harteneck, C. (2003). Molecular and Functional Characterization of the Melastatin-related Cation Channel TRPM3. *J Biol Chem.* 13;278(24):21493-501.
- Gu, S., Thompson, D., Srikumari, C., Lorenz, B., Finckh, U., Nicoletti, A., Murthy, K., Rathmann, M., Kumaramanickavel, G., Denton, M., and Gal, A. (1997). Mutations in RPE65 cause autosomal recessive childhood-onset severe retinal dystrophy. *Nat Genet.* 17(2):194-7.
- Hageman, G., Luthert, P., Victor, Chong, N., Johnson, L., Anderson, D., and Mullins, R. (2001). An integrated hypothesis that considers drusen as biomarkers of immune-mediated processes at the RPE-Bruch's membrane interface in aging and age-related macular degeneration. *Prog Retin Eye Res.* 20(6):705-32.
- Hageman, G., and Mullins, R. (1999). Molecular composition of drusen as related to substructural phenotype. *Mol Vis.* 3; 5:28.
- Hageman, G., Mullins, R., Russell, S., Johnson, L., and Anderson, D. (1999). Vitronectin is a constituent of ocular drusen and the vitronectin gene is expressed in human retinal pigmented epithelial cells. *FASEB J.* 13(3):477-84.

- Halliwell, B. (1991). Reactive oxygen species in living systems: source, biochemistry, and role in human disease. *Am J Med* 91 Suppl, pp. 14–22
- Hammond, B.Jr., Wooten, B., and Snodderly, D. (1996). Cigarette smoking and retinal carotenoids: implications for age-related macular degeneration. *Vision Res.* 36(18):3003-9.
- Hardie, R., and Minke, B. (1992). The trp gene is essential for a light-activated Ca²⁺ channel in *Drosophila* photoreceptors. *Neuron.* 8, 643–651.
- Hawkins, B., Bird, A., Klein, R., and West, S. (1999). Epidemiology of age-related macular degeneration. *Mol Vis.* 3;5:26.
- Hershko, A., and Ciechanover, A. (1998). The ubiquitin system. *Annu Rev Biochem.* 67:425-79.
- Hjelmeland, L., Cristofolo, V., Funk, W., Rakoczy, E., and Katz, M. (1999). Senescence of the retinal pigment epithelium. *Mol Vis.* 3; 5:33.
- Holz, F., Schutt, F., Kopitz, J., Eldred, G., Kruse, F., Volcker, H., and Cantz, M. (1999). Inhibition of lysosomal degradative functions in RPE cells by a retinoid component of lipofuscin. *Invest Ophthalmol Vis Sci.* 40,737-743.
- Hong, Y., Park, S., Geng, C., Baek, K., Bowman, J., Yoon, J., and Pak, W. (2002). Single amino acid change in the fifth transmembrane segment of the TRP Ca²⁺ channel causes massive degeneration of photoreceptors. *J Biol Chem.* 13; 277(37):33884-9.
- Hunter, J., Shao, J., Smutko, J., Dussault, B., Nagle, D., Woolf, E., Holmgren, L., Moore, K., and Shyjan, A. (1998). Chromosomal localization and genomic characterization of the mouse melastatin gene (*Mlns1*). *Genomics.* 15;54(1):116-23.
- Hyman, L., Lilienfeld, A., Ferris, F., 3rd, and Fine, S. (1983). Senile macular degeneration: a case-control study. *Am J Epidemiol.* 118(2):213-27.
- Inglehearn, C. (1998). Molecular genetics of human retinal dystrophies. *Eye* 12, 571-579.
- Ivy, G., Kanai, S., Ohta, M., Smith, G., Sato, Y., Kobayshi, M., and Kitani, K. (1989). Lipofuscin-like substances accumulate rapidly in brain, retina and internal organs with cyseine protease inhibition. *Adv. Exp. Med. Biol.*, 266:31-47.
- Jablonski, M., Tink, -Joyce, T., Mrazek, D., and Iannaccone, A. (2000). Pigment epithelium-derived factor supports normal development of photoreceptor neurons and opsin Expression after Retinal Pigment Epithelium Removal. *The Journal of Neuroscience.* 1 20(19):7149-7157.
- Johnson, G., Esposito, L., Barratt, B., Smith, A., Heward, J., Di Genova, G., et al. (2001). Haplotype tagging for the identification of common disease genes. *Nat Genet.* 29(2):233-7.

- Johnson, L., Ozaki, S., Staples, M., Erickson, P., and Anderson, D. (2000). A potential role for immune complex pathogenesis in drusen formation. *Exp Eye Res.* 70(4):441-9.
- Jonasson, F., Arnarsson, A., Sasaki, H., Peto, T., Sasaki, K., and Bird, A. (2003). The Prevalence of Age-Related Maculopathy in Iceland. *Arch Ophthalmol.* 121:379-385.
- Kahn, H., Leibowitz, H., Ganley, J., Kini, M., Colton, T., Nickerson, R., and Dawber, T. (1977). The Framingham Eye Study. I. Outline and major prevalence findings. *Am J Epidemiol.* 106(1):17-32.
- Kajiwara, K., Hahn, L., Mukai, S., Travis, G., Berson, E., and Dryja, T. (1991). Mutations in the human retinal degeneration slow gene in autosomal dominant retinitis pigmentosa. *Nature.* 354(6353):480-3.
- Kameya, S., Hawes, N., Chang, B., Heckenlively, J., Naggert, K. and Nishina, P. (2002). Mfrp, a gene encoding a frizzled related protein, is mutated in the mouse retinal degeneration 6. *Hum. Molec. Genet.* 11:, 1879-1886.
- Kaven, C, Spraul, C., Zavazava, N., Lang, G., and Lang, G. (2001). Thalidomide and prednisolone inhibit growth factor-induced human retinal pigment epithelium cell proliferation in vitro. *Ophthalmologica.* 215(4):284-9.
- Kennedy, B., Goldflam, S., Chang, M., Campochiaro, P., Davis, A., Zack, D., and Crabb, J. (1998). Transcriptional regulation of cellular retinaldehyde-binding protein in the retinal pigment epithelium. A role for the photoreceptor consensus element. *J Biol Chem.* 273(10):5591-8.
- Kim, S., Yamamoto, A., Bouwmeester, T., Agius, E., and Robertis, E. (1998). The role of paraxial protocadherin in selective adhesion and cell movements of the mesoderm during Xenopus gastrulation. *Development.* 125(23):4681-90.
- Kimura, K., Isashiki, Y., Sonoda, S., Kakiuchi-Matsumoto, and Ohba, N. (2000). Genetic association of manganese superoxide dismutase with exudative age-related macular degeneration. *American Journal of Ophthalmology*, Volume 130, Issue 6, Pages 769-773.
- Klaver, C., Kliffen, M., van Duijn, C., Hofman, A., Cruts, M., Grobbee, D., van Broeckhoven, C., and de Jong, P. (1998). Genetic association of apolipoprotein E with age-related macular degeneration. *Am J Hum Genet.* 63(1):200-6.
- Klaver, C., Wolfs, R, Assink, J., van Duijn, C., Hofman, A, and de Jong, P. (1998). Genetic risk of age-related maculopathy. Population-based familial aggregation study, *Arch Ophthalmol.* 116(12):1646-51.
- Klein, M., Mauldin, W., and Stoumbos, V. (1994). Heredity and age-related macular degeneration. Observations in monozygotic twins, *Arch Ophthalmol.* 112(7):932-7.
- Klein, R., Klein, B., and Linton, K. (1992). Prevalence of age-related maculopathy, the Beaver Dam Eye Study. *Ophthalmology.* 99(6):933-43.

- Klein, R., Davis, M., Magli, Y., Segal, P., Klein, B., and Hubbard, L. (1991). The Wisconsin age-related maculopathy grading system. *Ophthalmology*. 98(7):1128-34.
- Klein, R, Klein, B., and Moss, S. (1998). Relation of smoking to the incidence of age-related maculopathy. The Beaver Dam Eye Study. *Am J Epidemiol*. 15;147(2):103-10.
- Klionsky, D., and Emr, S. (2000). Autophagy as a regulated pathway of cellular degradation. *Science*. 1;290(5497):1717-21.
- Kozak, M. (1996). Interpreting cDNA sequences: some insights from studies on translation. *Mamm Genome*. 7, 563-574.
- Krämer, F., White, K., Pauleikhoff, D., Gehrig, A., Passmore, L., Rivera, A., et al. (2000). Mutations in the VMD2 gene are associated with juvenile-onset vitelliform macular dystrophy (Best disease) and adult vitelliform macular dystrophy but not age-related macular degeneration. *Eur J Hum Genet*. 8(4):286-92.
- Lange, N., Ballini, J., Wagnieres, G., and van den Bergh, H. (2001). A new drug-screening procedure for photosensitizing agents used in photodynamic therapy for CNV. *Invest Ophthalmol Vis Sci*. 42(1):38-46.
- Lee, N., Chen, J., Sun, L., Wu, S., Gray, K., Rich, A., Huang, M., Lin, J., Feder, J., Janovitz, E., Levesque, P., and Blamar, M. (2003). Expression and characterization of human transient receptor potential melastatin 3 (hTRPM3). *J Biol Chem*. 6;278(23):20890-7.
- Leu, S., Batni, S., Radeke, M., Johnson, L., Anderson, D., and Clegg, D. (2002). Drusen are Cold Spots for Proteolysis: Expression of Matrix Metalloproteinases and Their Tissue Inhibitor Proteins in Age-related Macular Degeneration. *Exp Eye Res*. 74(1):141-54.
- Liang, F., and Godley, B. (2003). Oxidative stress-induced mitochondrial DNA damage in human retinal pigment epithelial cells: a possible mechanism for RPE aging and age-related macular degeneration. *Exp Eye Res*. 76 (4):397-403.
- Liang, P, and Pardee, A. (1992). Differential display of eukaryotic messenger RNA by means of the polymerase chain reaction. *Science*, 14;257(5072):967-71.
- Lisitsyn, N. (1995). Representational difference analysis: finding the differences between genomes. *Trends Genet*. 11(8):303-7.
- Lutty, G., Grunwald, J., Majji, A., Uyama, M., and Yoneya, S. (1999). Changes in choriocapillaris and retinal pigment epithelium in age-related macular degeneration. *Mol Vis*. 3; 5:35.
- Macular Photocoagulation Study Group (1994). Persistent and recurrent neovascularization after laser photocoagulation for subfoveal choroidal neovascularization of age-related macular degeneration. *Arch Ophthalmol*. 112:489-499.

- Maguire, M., Fine, S., Maguire, A et al. (2001). Results of the age-related macular degeneration and thalidomide study (AMDATS). *Invest Ophthalmol Vis Sci* 42, p. S233.
- Marmor, M. (1990). Control of subretinal fluid: experimental and clinical studies. *Eye*, 4: 340-344,
- Marquardt, A., Stohr, H., Passmore, L., Kramer, F., Rivera, A., and Weber, B. (1998). Mutations in a novel gene, VMD2, encoding a protein of unknown properties cause juvenile-onset vitelliform macular dystrophy (Best's disease). *Hum Mol Genet.* 7(9):1517-25.
- Marzella, L., Ahlberg, J., and Glaumann, H. (1981). Autophagy, heterophagy, microautophagy and crinophagy as the means for intracellular degradation. *Virchows Arch B Cell Pathol Incl Mol Pathol.* 36(2-3):219-34.
- Maw, M., Corbeil, D., Koch, J., Hellwig, A., Wilson-Wheeler, J., Bridges, R., Kumaramanickavel, G., John, S., Nancarrow, D., Roper, K., Weigmann, A., Huttner, W., and Denton, M. (2000). A frameshift mutation in prominin (mouse)-like 1 causes human retinal degeneration. *Hum Mol Genet.* 1;9(1):27-34.
- Maw, M., Kennedy, B., Knight, A., Bridges, R., Roth, K., Mani, E., Mukkadan, J., Nancarrow, D., Crabb, J., and Denton, M. (1997). Mutation of the gene encoding cellular retinaldehyde-binding protein in autosomal recessive retinitis pigmentosa. *Nat Genet.* 17(2):198-200.
- Merin, S. (1991). Inherited macular diseases, In: *Inherited eye diseases: diagnosis and clinical management*. New York: Dekker,:137-75.
- Meyers, S., Greene, T., and Gutman, F. (1995). A twin study of age-related macular degeneration. *Am J Ophthalmol.* 120(6):757-66.
- Michaely, P., and Bennet V. (1993). The membrane-binding domain of ankyrin contains four independently folded subdomains, each comprised of six ankyrin repeats. *J Biol Chem.* 268:22703-22709.
- Miller, J., Stinson, W., and Folkman, J. (1993). Regression of experimental iris neovascularization with systemic alpha-interferon. *Ophthalmology*, 100(1):9-14.
- Minke, B., and Cook, B. (2002). TRP channel proteins and signal transduction. *Physiol. Rev.*, 82(2):429-72.
- Montell, C. (2001). Physiology, phylogeny, and functions of the TRP superfamily of cation channels. *Sci STKE.* (90):re1
- Morimura, H., Saindelle-Ribeau, F., Berson, E., and Dryja, T. (1999). Mutations in RGR, encoding a light-sensitive opsin homologue, in patients with retinitis pigmentosa. *Nat Genet.* 23(4):393-4.

- Mullins, R., and Hageman, G. (1997). Histochemical comparison of ocular drusen in monkey and human. In: M. M. et al. LaVail, Editor, *Degenerative Retinal Diseases*, Plenum Press, pp. 1–10.
- Mullins, R., Russell, S., Anderson, D., and Hageman, G. (2000). Drusen associated with aging and age-related macular degeneration contain proteins common to extracellular deposits associated with atherosclerosis, elastosis, amyloidosis, and dense deposit disease. *FASEB J.* 14(7):835-46.
- Mylan, R., VanNewkirk, M., Mukesh, B., Nanjan, Wang, J., Paul, M., Hugh, R., Taylor, and McCarty, C. (2000). The prevalence of age-related maculopathy. *Ophthalmology*, , 107: 1593-1600.
- Nakajima, D., Nakayama, M., Kikuno, R., Hirosawa, M., Nagase, T., and Ohara, O. (2001). Identification of three novel non-classical cadherin genes through comprehensive analysis of large cDNAs. *Brain Res Mol Brain Res.* 19;94(1-2):85-95.
- Noble, K. (1986). Hereditary macular dystrophies. In:Renie W A, ed. *Goldberg's genetic and metabolic eye disease*. Boston: Little, Brown,:439-64.
- Noell, W., Walker V., Kang B., and Berman S. (1966). Retinal damage by light in rats. *Invest Ophthalmol.* 5(5):450-73.
- Orita, M., Iwahana, H., Kanazawa, H., Hayashi, K., and Sekiya, T. (1989). Detection of polymorphisms of human DNA by gel electrophoresis as single-strand conformation polymorphisms. *Proc. Natl Acad. Sci. USA*, 86, 2766–2770.
- O'Shea, J. (1998). Age-related macular degeneration. *Postgrad Med J*, 74, 203-207.
- Parcellier, A., Gurbuxani, S., Schmitt, E., Solary, E., and Garrido, C. (2003). Heat shock proteins, cellular chaperones that modulate mitochondrial cell death pathways. *Biochemical and Biophysical Research Communications*. Volume 304, Issue 3, 9 Pages 505-512.
- Penfold, P., Madigan, M., Gillies, M., and Provis, J. (2001). Immunological and aetiological aspects of macular degeneration. *Prog Retin Eye Res.* 20(3):385-414.
- Petrukhin, K., Koisti, M., Bakall, B., Li, W., Xie, G., et al. (1998). Identification of the gene responsible for Best macular dystrophy. *Nat Genet.* 19(3):241-7.
- Pharmacological Therapy for Macular Degeneration Study Group (1997). Interferon alfa-2a is ineffective for patients with choroidal neovascularization secondary to age-related macular degeneration. Results of a prospective randomized placebo-controlled clinical trial. *Arch Ophthalmol* 115, pp. 865–872.
- Phelan, J., and Bok, D. (2000). A brief review of retinitis pigmentosa and the identified retinitis pigmentosa genes. *Molecular vision.* 6 116-124

- Philips, A., Bull, A., and Kelly L. (1992). Identification of a *Drosophila* gene encoding a calmodulin-binding protein with homology to the *trp* phototransduction gene. *Neuron* 8:631-642
- Prawitt, D., Enklaar, T., Klemm, G., Gartner, B., Spangenberg, C., Winterpacht, A., Higgins, M., Pelletier, J., and Zabel, B. (2000). Identification and characterization of MTR1, a novel gene with homology to melastatin (MLSN1) and the *trp* gene family located in the BWS-WT2 critical region on chromosome 11p15.5 and showing allele-specific expression. *Hum Mol Genet.* 22;9(2):203-16.
- Rakoczy, P., Sarks, S., Daw, N., and Constable, I. (1999). Distribution of cathepsin D in human eyes with or without age related maculopathy. *Exp Eye Res.* 69:367-374
- Rattner, A., Sun, H., and Nathans, J. (1999). Molecular genetics of human retinal disease. *Annual review of genetics.* 33:89-131.
- Retinoschisis Consortium (1998). Functional implications of the spectrum of mutations found in 234 cases with X-linked juvenile retinoschisis (XLRS). *Hum Mol Genet.* 7(7):1185-92.
- Rosenfeld, P., Cowley, G., McGee, T., Sandberg, M., Berson, E., and Dryja, T. (1992). A null mutation in the rhodopsin gene causes rod photoreceptor dysfunction and autosomal recessive retinitis pigmentosa. *Nat Genet.* 1(3):209-13.
- Rychlik, W., and Roads, (1989). A computer program for choosing optimal oligonucleotides for filter hybridization, sequencing and in vitro amplification of DNA. *Nuc Acids Res* 17 (21):8543-51.
- Sarks, J., Sarks, S., and Killingsworth, M. (1988). Evolution of geographic atrophy of the retinal pigment epithelium. *Eye.* 2 (Pt 5):552-77.
- Schatz, H., and McDonald, H. (1989). Atrophic macular degeneration, Rate of spread of geographic atrophy and visual loss. *Ophthalmology.* 96(10):1541-51.
- Schutt, F., Bergmann, M., Holz, F. and Kopitz, J. (2002). Isolation of intact lysosomes from human RPE cells and effects of A2-E on the integrity of the lysosomal and other cellular membranes. *Graefes Arch Clin Exp Ophthalmol.* 240(12):983-8.
- Seddon, J., Willett, W., Speizer, F., and Hankinson, S. (1996). A prospective study of cigarette smoking and age-related macular degeneration in women. *JAMA.* 9;276(14):1141-6.
- Sharma, S., Chang, J., Della, N., Campochiaro, P., and Zack, D. (2002). Identification of novel bovine RPE and retinal genes by subtractive hybridization. *Mol Vis.* Jul 16;8:251-8.
- Sharon, D., Blackshaw, S., Cepko, C., and Dryja, T. (2002). Profile of the genes expressed in the human peripheral retina, macula, and retinal pigment epithelium determined through serial analysis of gene expression (SAGE). *Proc Natl Acad Sci U S A.* 8;99(1):315-20.

- Sherman, M., and Goldberg, A. (2001). Cellular defenses against unfolded proteins: a cell biologist thinks about neurodegenerative diseases. *Neuron*. 29(1):15-32.
- Silvestri, G., Johnston, P., and Hughes, A. (1994). Is genetic predisposition an important risk factor in age-related macular degeneration? *Eye*. 8 (Pt 5):564-8.
- Smith, W., Mitchell, P., and Leeder, S. (1996). Smoking and age-related maculopathy. The Blue Mountains Eye Study. *Arch Ophthalmol*. 114(12):1518-23.
- Souied, E., Ducroq, D., Gerber, S., Ghazi ,I., Rozet, J., Perrault, I., Munnich, A., Dufier, J., Coscas, G., Soubrane, G., and Kaplan, J. (1999). Age-related macular degeneration in grandparents of patients with Stargardt disease: genetic study. *Am J Ophthalmol*. 128(2):173-8.
- Spaide, R., Guyer, D., McCormick, B., Yannuzzi, L., Burke, K., Mendelsohn, M., Haas, A., Slakter, J., Sorenson, J., Fisher, Y., and Abramson, D. (1998). External beam radiation therapy for choroidal neovascularization. *Ophthalmology*. 105(1):24-30.
- Stern, A., de Carvalho, M., Buck, G., Adler, R., Rao, T., Disler, D., Moxley, G., et al. (2003). Association of erosive hand osteoarthritis with a single nucleotide polymorphism on the gene encoding interleukin-1 beta. *Osteoarthritis Cartilage*. 11(6):394-402.
- Stone, E., Sheffield, V., and Hageman, G. (2001). Molecular genetics of age-related macular degeneration. *Hum Mol Genet*. 1; 10(20):2285-92.
- Strachan, T., and Read, A. (1999). In: Human molecular genetics, *BIOS scientific publishers Ltd*, 2 nd edition, page 366-367.
- Strunnikova, N., Baffi, J., Gonzalez, A., Silk, W., Cousins, S., and Csaky, K. (2001). Regulated heat shock protein 27 expression in human retinal pigment epithelium. *Invest Ophthalmol Vis Sci*. 42(9):2130-8.
- Sunness, J. (1999). The natural history of geographic atrophy, the advanced atrophic form of age-related macular degeneration. *Mol Vis*. 3; 5:25.
- Sunness, J., Schuchard, R., Shen, N., Rubin, G., Dagnelie, G., and Haselwood, D. (1995). Landmark-driven fundus perimetry using the scanning laser ophthalmoscope. *Invest Ophthalmol Vis Sci*. 36(9):1863-74.
- Tamakoshi, A., Yuzawa, M., Matsui, M., Uyama, M., Fujiwara, N., and Ohno, Y. (1998). Smoking and neovascular form of age related macular degeneration in late middle aged males: findings from a case-control study in Japan. Research Committee on Chorioretinal Degenerations. *Br J Ophthalmol* 82(2):207. *Br J Ophthalmol*. 1997 81(10):901-4
- Van Leeuwen, R., Klaver, C., Vingerling, J., Hofman, .A, and de Jong, P. (2003). The risk and natural course of age-related maculopathy: follow-up at 6 1/2 years in the Rotterdam Study. *Arch Ophthalmol*. 121(4):519-26.

- Takeichi, M. (1990). Cadherins: a molecular family important in selective cell-cell adhesion. *Annu Rev Biochem.*;59:237-52.
- Uemura, T. (1998). The cadherin superfamily at the synapse: more members, more missions. *Cell.* 26;93(7):1095-8.
- Verdugo, M., and Ray, J. (1997). Age-related increase in activity of specific lysosomal enzymes in the human retinal pigment epithelium. *Exp Eye Res.* 65(2):231-40.
- Verdugo, M., Aguirre, G., and Ray, J. (1996). studies of lysosomal enzymes in cultured human retinal pigment epithelium. *Ivest. Ophthalmol. Vis. Sci.* 37, S 379.
- Vinding, T., Appleyard, M., Nyboe, J., and Jensen, G. (1992). Risk factor analysis for atrophic and exudative age-related macular degeneration. An epidemiological study of 1000 aged individuals. *Acta Ophthalmol (Copenh).* 70(1):66-72.
- Von Stein, O., Thies, W., and Hofmann, M. (1997). A high throughput screening for rarely transcribed differentially expressed genes. *Nucleic Acids Res.* 1;25(13):2598-602.
- Wang, D., Fan, J., Siao, C., Berno, A., Young, P., Sapolsky, R., Ghandour, G., Perkins, N., Winchester, E., Spencer, J., et al. (1998). Large-scale identification, mapping, and genotyping of single-nucleotide polymorphisms in the human genome. *Science*, 280, 1077–1082.
- Weber, B. (1998). Recent advances in the molecular genetics of hereditary retinal dystrophies with primary involvement of the macula. *Acta anatomica*; 162: 65-74.
- Weber, B., Vogt, G., Pruett, R., Stohr, H., and Felbor U. (1994). Mutations in the tissue inhibitor of metalloproteinases-3 (TIMP3) in patients with Sorsby's fundus dystrophy. *Nat Genet.* 8(4):352-6.
- Weiner, M., and Hudson, T. (2002). Introduction to SNPs: discovery of markers for disease. *Biotechniques.* Jun;Suppl:4-7, 10, 12-3.
- Weleber, R., Carr, R., Murphey, W., Sheffield, V., and Stone, E. (1993). Phenotypic variation including retinitis pigmentosa, pattern dystrophy, and fundus flavimaculatus in a single family with a deletion of codon 153 or 154 of the peripherin/RDS gene. *Arch. Ophthalmol.* 111 (11):1531-42.
- Williams, R., Brody, B., Thomas, R., Kaplan, R., and Brown, S. (1998). The psychosocial impact of macular degeneration. *Arch Ophthalmol.* 116(4):514-20.
- Winkler, B., Boulton, M., Gottsch, J., and Sternberg, P. (1999). Oxidative damage and age-related macular degeneration. *Mol Vis.* 3; 5:32.
- Wistow, G. (2002). A project for ocular bioinformatics: NEIBank. *Mol Vis.*; 8:161-3.

- Wistow, G., Bernstein, S., Wyatt, M., Ray, S., Behal, A., Touchman, J., Bouffard, G., Smith, D., and Peterson, K. (2002). Expressed sequence tag analysis of human retina for the NEIBank Project: retbindin, an abundant, novel retinal cDNA and alternative splicing of other retina-preferred gene transcripts. *Mol Vis.* 15; 8:196-204.
- Wistow, G., Bernstein, S., Ray, S., Wyatt, M., Behal, A., Touchman, J., Bouffard, G., Smith, D., and Peterson, K. (2002). Expressed sequence tag analysis of adult human iris for the NEIBank Project: steroid-response factors and similarities with retinal pigment epithelium. *Mol Vis.* 15;8:185-95.
- Wolford, J., Blunt, D., Ballecer, C., and Prochazka, M. (2000). High-throughput SNP detection by using DNA pooling and denaturing high performance liquid chromatography (DHPLC). *Hum Genet.* 107(5):483-7.
- Wooten, B., and Hammond, B. (2002) Macular pigment: influences on visual acuity and visibility. *Prog Retin Eye Res.* 21(2):225-40.
- Xu, X.,-Z., Moebius, F., Gill, D., L., and Montell, C. (2001). Regulation of melastatin, a TRP-related protein through interaction with a cytoplasmic isoform. *Proc. Natl. Acad. Sci. USA*, Vol. 98, Issue 19, 10692-10697.
- Yagi, T., and Takeichi, M. (2000). Cadherin superfamily genes: functions, genomic organization, and neurologic diversity. *Genes Dev.* 15;14(10):1169-80.
- Yates, J., and Moore, A. (2000). Genetic susceptibility to age related macular degeneration. *J Med Genet.* 37(2):83-7.
- Young, R. (1987). Pathophysiology of age-related macular degeneration. *Surv Ophthalmol.* 31(5):291-306.
- Young, R. (1988). Solar radiation and age-related macular degeneration. *Surv Ophthalmol.* 32:252-69.
- Young, R. (1976). Visual cells and the concept of renewal. *Invest. Ophthalmol. Vis. Sci.* 15, 700-25.
- Zack, D., Dean, M., Molday, R., Nathans, J., Redmond, T., Stone, E., Swaroop, A., Valle, D., and Weber, B. (1999). What can we learn about age-related macular degeneration from other retinal diseases? *Mol Vis.* 3;5:30.
- Zhang, K., Yeon, H., Han, M., and Donso, L. (1996). Molecular genetics of macular dystrophies. *British journal of ophthalmology.* 80: 1018-1022.
- Zeng, J, Gorski, R., and Hamer, D. (1994). Differential cDNA cloning by enzymatic degrading subtraction (EDS). *Nucleic Acids Research*, Vol 22, Issue 21 4381-4385.
- Zimmerman, W., Godchaux, W., and Belkin, M. (1983). The relative proportions of lysosomal enzyme activities in bovine retinal pigment epithelium. *Exp. Eye Res.* 36, 151-8.

Zinn, K., and Marmor, M. (1979). *The Retinal Pigment Epithelium*. *Harvard University Press*. Cambridge, MA.

Zito, I, Downes, S., Patel, R., Cheetham, M., Ebenezer, N., Jenkins, S., Bhattacharya, S., Webster, A., Holder, G., Bird, A., Bamiou, D., and Hardcastle, A. (2003). RPGR mutation associated with retinitis pigmentosa, impaired hearing, and sinorespiratory infections. *J Med Genet*. 40(8):609-615.

8. APPENDIX

Table 1: Oligonucleotides primers and conditions (MT-Protocadherin gene)

Primer name	primer sequence	Annealing temp.	MgCl ₂
10B10-5'UTR-F1	TCCTTTGATGTGTTCTCTAC	58	1.0-
10B10-5'UTR-R1	GAATAGGGTCAGGGGATCTG-	58	1.0-
10B10-5'UTR-F2	TGGACTGGGACAGTACCTGA	58	1.0-
10B10-5'UTR-R2	TCTACCTGAGTGTGCCAACC	58	1.0-
10B10-5'UTR-F3	TATGTTTGTGAGCAGCTGTGTG	58	1.0-
10B10-5'UTR-R3	CCTGTCTCAAATCACCTAAG	58	1.0-
10B10-5'UTR-F4	CCAGAAGAAGAGCTGTCAGAAG	54	1.0+
10B10-5'UTR-R4	CTGATGTAGAAGGGTCTGAGAA	54	1.0+
10B10-5'UTR-F5	CAGCAGGAGTTGGAGTGG	58	1.0-
10B10-5'UTR-R5	GATTCACATACAGTTTGGGTTG	58	1.0-
10B10-5'UTR-F6	GAGTTTGAACCTTCTTTGGAG	58	1.0-
10B10-5'UTR-R6	TGGTTTTAGAATGTGCAGCAG	58	1.0-
10B10-5'UTR-F7	GCAAAAGAGCCAAGCCTAAG	54	1.0+
10B10-5'UTR-R7	CAGTCTGGGACCATGAAGG	54	1.0+
10B10-5'UTR-F8	GGCCCTTCACTCTTCCTTG	58	1.0-
10B10-5'UTR-R8	CGCCTGACGAGACCAATTA	58	1.0-
10B10-EX1F	GGGGAGTCCTCTTGTCACG	54	1.0+
10B10-EX1R	TGCCACCAAGCCTACAGC	54	1.0+
10B10-EX2F	GAAGGAGGGGTTGGATTGC	55	1.0+
10B10-EX2R	CATGGCAGCAATGACCTTC	55	1.0+
10B10-EX3F-	AAACATACAAAGAGGGAAGCAG	58	1.0-
10B10-EX3R	GGAGGAGCATGAAAGTAAAGC	58	1.0-
10B10-EX4F	AAGAACCCCGACACAAAAG	58	1.0-
10B10-EX4R	GCTGTGGAATGTGGGTTAGAC	58	1.0-
10B10-EX5F	ACCACAGCCCAGGAACTC	58	1.0-
10B10-EX5R	TTGGAATAAAAGCGAATGTTG	58	1.0-
10B10-EX6F	TTCCCTTCCCTCTTTCCTG	58	1.0-
10B10-EX6R	TCTGCTTCTTTGAGTGTGTC	58	1.0-
10B10-EX7F	AGCTGAGCAGGAGGAAAAAC	58	1.0-
10B10-EX7R	CTTACCTGGGGGATCCTG	58	1.0-
10B10-EX8F	GAGAGAATAACCCCACTGTC	58	1.0-
10B10-EX8R	CTGAGGCTGGGTGAGTCC	58	1.0-
10B10-EX9F	AGGGCTGAGTGTGGTGTG	55	1.0-
10B10-EX9R	CCTCCGTGTTGCTCTCAG	55	1.0-
10B10-EX10F	GCATAAGAAAAGGGACACAG	56	1.0-
10B10-EX10R	ATCAGTTCTCTCCCCTCCAG	56	1.0-
10B10-EX11F	CTGCAGGGGAGGTAGGAG	55	1.0-
10B10-EX11R	GAGAGTGGAAACAAGGAAGATG	55	1.0-
10B10-EX12F	ATCAACCTGCTCTGCGTATG	-	-
10B10-EX12R	ATCCCACACCACCACCTG	-	-
10B10-EX13F	ACGGGGTAGGGGAAGATG	55	1.0-
10B10-EX13R	ATAAATGAGGAAGAGGGGATG	55	1.0-
10B10-EX14F	ACCCATCCCCTCTTCTC	58	1.0-
10B10-EX14R	CTCACCCATCTATCACTATCCAG	58	1.0-
10B10-EX15F	GGCCATAGGAAGAGAGAAAGAC	58	1.0-

-/+ = indicate with or without formamide

Primer name	primer sequence	Annealing temp	MgCl ₂
10B10-EX15R	TTCTTATGCCTCAGTATCTCTTGG	58	1.0-
0B10-EX16F	TCCTTTCCCAACTCAATCCTC	58	1.0-
10B10-EX16R	GGAAGCCTGGAGATGGTC	58	1.0-
10B10-EX17F	GGCTTAAGGAAGCACATACCTAC	58	1.0-
10B10-EX17R	TTGACTGGACGGGGCTTC	58	1.0-
10B10-3'UTR-F1	CCGTGCCTACTGTCTCTGG	58	1.0-
10B10-3'UTR-R1	CCTCCTTTTCCTGCTCCTG	58	1.0-
10B10-3'UTR-F2	CACGTGGAGCAACTGAC	58	1.0-
10B10-3'UTR-R2	GCCCTCATCACCCTATTTC	58	1.0-
10B10-3'UTR-F3	CAATTCAGGGCAGTTGATG	58	1.0-
10B10-3'UTR-R3	AACCCAGAGGCCTTGTA	58	1.0-
10B10-3'UTR-F4	TGTTCTTCCCTCACTCCATC	58	1.0-
10B10-3'UTR-R4	TGTGGAGGGCAAGCATGA	58	1.0-
10B10-3'UTR-F5	GTCCCAACGTGAACAGTAT	58	1.0-
10B10-3'UTR-R5	GCTCCAGCCTAGAGGTCTT	58	1.0-
10B10-3'UTR-F6	TCTTGAACAGCAGGACATTTG	58	1.0-
10B10-3'UTR-R6	CATTCGTAACACAGGGACTTG	58	1.0-
10B10-3'UTR-F7	ACCGCAAGTGTTGTCAG	58	1.0-
10B10-3'UTR-R7	CAGGTGGGTGGAAACATC	58	1.0-
10B10-3'UTR-F8	CACCATGTCCTGAAAGAGAG	-	-
10B10-3'UTR-R8	TTTCTAAGGGGTCCTCCAT	-	-
10B10-3'UTR-F9	TGAGGAATGAGGCAGGAGAC	58	1.0-
10B10-3'UTR-R9	GGGCTAATATCCTTCACATGTTT	58	1.0-
10B10-3'UTR-F10	CTTCTCAAGGGCATGACAACT	58	1.0-
10B10-3'UTR-R10	GCTGCCCTTGAAAACTCT	58	1.0-
10B10-3'UTR-F11	CCACTGCGAAATTGCCTTAT	58	1.0-
10B10-3'UTR-R11	GGGCTACCATGAAGGTGAGA	58	1.0-

Table 2: oligonucleotide primers and conditions (TRPM3 gene)

Primer name	primer sequence	Annealing emp	MgCl ₂
TR-5'U1F	TGTTTCCTACCTATCACCTCTG	58	1.0-
TR-5'U1R	GCTCTTTCCAGGGTCAATCT	58	1.0-
TR-5'U2F	AGATTGACCCTGGAAAGAGC	58	1.0-
TR-5'U2R	TCTTATCCTGCTGCCCCTCT	58	1.0-
TR-5'U3F	AGAGGGGCAGCAGGATAAGA	58	1.0-
TR-5'U3R	ATGAACTTGGGCAGATTAGC	58	1.0-
TR-EX1F	GCTAATCTGCCAAGTTCAT	58	1.0-
TR-EX1R	CAGGCAGGAAGATTTACAAG	58	1.0-
TR-EX2F	TAGCATTGTCTTTCTGTTCTGA	58	1.0-
TR-EX2R	GTTTTCTTTATCGGCTCTT	58	1.0-
TR-IVS2F1	AGCACCTACTTACCTTCTTA	58	1.0-
TR-IVS2R1	ATCAAAGCACGAAGGTCTCTG	58	1.0-
TR-EX3F	CAGAGACCTTCGTGCTTTGAT	58	1.0-
TR-EX3R	TGAGATAGCATTGGGAGCA	58	1.0-
TR-EX4F	AGTCCTGCCTTGTCTCCCTA	58	1.0-
TR-EX4R	GACAGAGGTAGGGCTTCCAAT	58	1.0-
TR-IVS4F1	ATGGAATGGATGCCTGTAAT	58	1.0-

Primer name	primer sequence	Annealing temp	MgCl ₂
TR-IVS4R1	CAAACAGCATCCAAACTACGA	58	1.0-
TR-IVS4F2	TCGTAGTTTGGATGCTGTTTG	58	1.0-
TR-IVS4R2	CACTTTGGGTATTGGATTGAAC	58	1.0-
TR-EX5F	CGGGAGAAACCATTACCACAG	58	1.0-
TR-EX5R	CAGAGAGGGGGTAGGTGGTAA	58	1.0-
TR-IVS5F1	CTGCCATCTGTCCTTTTTCTTC	58	1.0-
TR-IVS5R1	GCCAGCCCCACAAAATAAC	58	1.0-
TR-IVS5F2	TTTGTGGGGCTGGCTCTC	58	1.0-
TR-IVS5R2	TCCCTCACCTTCCACCTTC	58	1.0-
TR-IVS5F3	CCACTACCCTGCCTCTTGTCT	58	1.0-
TR-IVS5R3	CTGCTGGCTTGAAGAGACAT	58	1.0-
TR-EX6F	TTGCCATAAATCTTGCCTCT	58	1.0-
TR-EX6R	ATTACTTCTTACGCCTCCAA	58	1.0-
TR-IVS6F1	ATTGGAGGCGTAAGAAGTAA	-	-
TR-IVS6R1	GTTTCACATGATGCTTTAGCTTAG	-	-
TR-IVS6F2	CTAAGCTAAAGCATCATGTGAAAC	58	1.0-
TR-IVS6R2	AGAGAGTGTAGGAAGGAGAAGC	58	1.0-
TR-IVS6F3	CCAAGACTGGATCTGGGACA	58	1.0-
TR-IVS6R3	GTAAGTCCCCTGGTATTTGG	58	1.0-
TR-IVS6F4	CCATCAGTGTCTATGAATGAAAAA	58	1.0-
TR-IVS6R4	GCCATGATGCTGCTACTGAG	58	1.0-
TR-IVS6F5	TAGTTGTCCCTCCTGCCTCA	58	1.0-
TR-IVS6R5	AGCAAAAGCACTGGTTATGGAA	58	1.0-
TR-EX7F	TGAGAGTTGAGGGGAGAGG	58	1.0-
TR-EX7R	GATTTGAGGTCTTGGTTGAGC	58	1.0-
TR-IVS7F1	GCTCAACCAAGACCTCAAATC	-	-
TR-IVS7R1	AGTTGGATTGGAGGGGAGTG	-	-
TR-IVS7F2	CACTCCCCTCCAATCCAAT	58	1.0-
TR-IVS7R2	TGCCTCTTGTTATTCCTCATTT	58	1.0-
TR-IVS7F3.	TCTCTATAAGACCTGCCAAAAG	-	-
TR-IVS7R3	GATGGAAAAGGGGAAGAGGAA	-	-
TR-IVS7F4	TTCTCTTCCCCTTTTCCATC	58	1.0-
TR-IVS7R4	ACTGCCGTGGTATTTTCTCC	58	1.0-
TR-IVS7F5	GGAGAAAATACCACGGCAGT	58	1.0-
TR-IVS7R5	GCTAAGGAAATCTCAGAGGAA	58	1.0-
TR-EX8F	CCTCACCTGCATTCTCCTC	58	1.0-
TR-EX8R	GACAAGTGGGAGGTTAGGAC	58	1.0-
TR-3U1F	CAGACAAGGTGCGGGTTTAC	58	1.0-
TR-3U1R	CTTTGTAGGTGAGAGCCAGG	58	1.0-
TR-3U2F	CCTGGCTCTCACCTACAAAG	58	1.0-
TR-3U2R	AAAGGAAAGGAATGAAACACCAG	58	1.0-
TR-3U3F	CTGGTGTTCATTCCTTTCCTTT	58	1.0-
TR-3U3R	GGCAAAAACCAAGGAGATGA	58	1.0-

Table 3: Oligonucleotide primers and conditions (MGC2477 gene)

Primer name	primer sequence	Annealing temp	MgCl ₂
MG-5'UF1	AGGGCTCATTCTGGGTGGA	58	1.0+
MG-5'UR1	TGGTAGTCCCAGGAAGG	58	1.0+
MG-5'UF2	GAGGTGTCCAAGAAGTGCTG	58	1.0+
MG-5'UR2	CACGCCACACACTAACAAC	58	1.0+
MG-5'UF3	AACAACCTATTCCTTTTCTCGTC	58	1.0+
MG-5'UR3	GTTACACGAATCCAGCCTTTTAG	58	1.0+
MG-EX1F	AGGTTGGGAAAAATCAGTAAGC	58	1.0+
MG-EX1R	AGGGACAGCAGGGAGGTTG	58	1.0+
MG-EX2F	GGCTTACCCTCCAGTTTG	58	1.0+
MG-EX2R	GGCACCCATTCTGATACC	58	1.0+
MG-EX3F	TTTTGTCCCCTCTCTTCCTC	58	1.0+
MG-EX3R	GGAGTTACGGAGATTACATACAA	58	1.0+
MG-IVS3F1	GTATGTAATCTCCGTAACCTCAA	58	1.0+
MG-IVS3R1	CTGGGGGTGGACTTTTCTC	58	1.0+
MG-IVS3F2	GCAGCAATGGCAGTAGGAG	58	1.0+
MG-IVS3R2	GAGTGGGGAGGGTAAGGTG	58	1.0+
MG-IVS3F3	CACCTTACCCTCCCCTC	-	-
MG-IVS3R3	CGGAGGAAGAGGGAAAGG	-	-
MG-EX4F	GTTTCCTCAAGCGTTCCTG	58	1.0+
MG-EX4R	GAATCCAAAACCCAAAGAAAGG	58	1.0+
MG-EX5-6F	AGCCAGAACTATTTGTGTGACC	58	1.0+
MG-EX5-6R	ACCCATCCCATTCTACAT	58	1.0+
MG-3'UF1	ATGAAAAGATTGGGGAGTATGG	58	1.0+
MG-3'UR1	CCTTTACCTCTGCTATCCCTAC	58	1.0+
MG-3'UF2	TGTAGGGATAGCAGAGGTAAAG	58	1.0+
MG-3'UR2	CCAGGGCTCATTTTACTAATC	58	1.0+

Table 4: Group II of reverse Northern blot analyses

Equally weak signals on filters hybridized with RPE and heart/liver cDNA probes

No	Plate ID	Clone ID	Subcategory
1	RPE01	D02	Known human gene
2	RPE01	A11	No significant similarity
3	RPE01	D04	Known human gene
4	RPE01	F11	human Unknown
5	RPE01	G02	Known human gene
6	RPE01	C09	Predicted gene
7	RPE01	A05	No significant similarity
8	RPE01	D06	Predicted gene
9	RPE01	C07	human Unknown
10	RPE01	G08	Known human gene
11	RPE01	G04	Known human gene
12	RPE01	B06	Known human gene
13	RPE01	E11	Known human gene
14	RPE01	F12	Known human gene
15	RPE02	B05	Ribosomal RNA
16	RPE02	D09	Predicted gene
17	RPE02	D07	human Unknown
18	RPE02	B01	Known human gene
19	RPE02	B07	No significant similarity
20	RPE02	A10	Predicted gene

No	Plate ID	Clone ID	Subcategory
21	RPE02	D11	Known human gene
22	RPE02	E01	Known human gene
23	RPE02	F02	Known human gene
24	RPE02	A03	Known human gene
25	RPE02	A01	Predicted gene
26	RPE03	G05	Known human gene
27	RPE03	E05	Predicted gene
28	RPE03	B03	Known human gene
29	RPE03	F12	Known human gene
30	RPE03	H09	Known human gene
31	RPE03	F03	Known human gene
32	RPE03	H11	Known human gene
33	RPE03	B12	Predicted gene
34	RPE03	D12	Predicted gene
35	RPE03	B06	human Unknown
36	RPE03	B01	No significant similarity
37	RPE03	D03	human Unknown
38	RPE03	D09	Known human gene
39	RPE06	H11	Known human gene
40	RPE06	C07F	Predicted gene
41	RPE06	A03	Known human gene
42	RPE06	F04	Known human gene
43	RPE06	F09	Known human gene
44	RPE06	D11F	Known human gene
45	RPE06	A08	Known human gene
46	RPE06	F08	Known human gene
47	RPE06	H01	Known human gene
48	RPE06	D10F	Known human gene
49	RPE06	A01	No significant similarity
50	RPE06	F05	No significant similarity
51	RPE06	E05F	Known human gene
52	RPE06	C02F	Known human gene
53	RPE06	F02F	No significant similarity
54	RPE06	C10F	Predicted gene
55	RPE06	B01	Known human gene
56	RPE06	F11	Predicted gene
57	RPE06	C09F	Predicted gene
58	RPE06	C08F	No significant similarity
59	RPE07	F11	Predicted gene
60	RPE07	E12	Known human gene
61	RPE07	G08	No significant similarity
62	RPE07	H10	Known human gene
63	RPE07	D02	No significant similarity
64	RPE07	H11	Known human gene
65	RPE07	A12	Known human gene
66	RPE07	B09	human Unknown
67	RPE08	H10	Known human gene
68	RPE08	F02	No significant similarity
69	RPE08	B01	Known human gene
70	RPE08	G01	Predicted gene
71	RPE08	H05	Known human gene
72	RPE08	H11	No significant similarity
73	RPE08	E05	No significant similarity
74	RPE08	D10	Known human gene
75	RPE08	B03	Known human gene
76	RPE08	H09	Known human gene
77	RPE08	F01	No significant similarity

No	Plate ID	Clone ID	Subcategory
78	RPE08	F06	Known human gene
79	RPE08	E11	Known human gene
80	RPE08	E04	Known human gene
81	RPE08	F10	No significant similarity
82	RPE08	B05	Predicted gene
83	RPE08	B12	Known human gene
84	RPE08	C05	Known human gene
85	RPE08	D12	Known human gene
86	RPE08	D03	Known human gene
87	RPE10	E10	Predicted gene
88	RPE10	D08	Predicted gene
89	RPE10	F08	Known human gene
90	RPE10	D01	Known human gene
91	RPE10	D03	Known human gene
92	RPE10	F01	Predicted gene
93	RPE10	C09	Human Unknown
94	RPE10	D06	Human Unknown
95	RPE10	G10	Known human gene
96	RPE10	B11	No significant similarity
97	RPE10	H08	Known human gene
98	RPE10	E01	Known human gene
99	RPE10	A10	No significant similarity
100	RPE10	B10	Predicted gene
101	RPE10	C06	Known human gene
102	RPE10	D10	Known human gene
103	RPE10	C04	Known human gene
104	RPE10	E08	Known human gene
105	RPE10	H06	Known human gene
106	RPE10	H01	No significant similarity
107	RPE10	A01	Known human gene
108	RPE10	E07	Predicted gene
109	RPE10	B04	Known human gene
110	RPE10	F07	No significant similarity
111	RPE10	B09	No significant similarity
112	RPE12	B10	No significant similarity
113	RPE12	G03	Human Unknown
114	RPE12	A09	No significant similarity
115	RPE12	H06	Predicted gene
116	RPE12	G07	Known human gene
117	RPE12	C03	Known human gene
118	RPE12	G05	Known human gene
119	RPE12	H03	Known human gene
120	RPE12	E06	No significant similarity
121	RPE12	D09	Known human gene
122	RPE12	B11	Known human gene
123	RPE12	E04	No significant similarity
124	RPE12	A10	Known human gene
125	RPE16	E11	Known human gene
126	RPE16	E05	Known human gene
127	RPE16	H09	Known human gene
128	RPE16	F09	No significant similarity
129	RPE16	E10	Known human gene
130	RPE16	C07	No significant similarity
131	RPE16	D01	human Unknown
132	RPE16	B02	No significant similarity
133	RPE16	H08	No significant similarity
134	RPE16	C02	Known human gene

No	Plate ID	Clone ID	Subcategory
135	RPE16	D10	Known human gene
136	RPE16	H01	Known human gene
137	RPE16	H05	Known human gene
138	RPE16	F08	Known human gene
139	RPE16	D09	Known human gene
140	RPE16	G08	Known human gene
141	RPE16	B11	Known human gene
142	RPE16	B06	Known human gene
143	RPE16	G12	Predicted gene
144	RPE16	F03	Known human gene
145	RPE20A	H11	No significant similarity
146	RPE20A	E09	Known human gene
147	RPE20A	H04	Predicted gene
148	RPE20A	G04	Known human gene
149	RPE20A	D04	Known human gene
150	RPE20A	F02	Human Unknown
151	RPE20A	E04	Predicted gene
152	RPE20A	E03	No significant similarity
153	RPE20A	A07	Predicted gene
154	RPE20A	F12	Known human gene
155	RPE20A	D12	No significant similarity
156	RPE20A	F08	mc
157	RPE20A	G03	Known human gene
158	RPE20A	D02	Known human gene
159	RPE20A	E05F	Human Unknown
160	RPE21	B08	Known human gene
161	RPE21	A09	No significant similarity
162	RPE21	C03	Known human gene
163	RPE21	A03	Known human gene
164	RPE21	C07	Predicted gene
165	RPE21	G11	Known human gene
166	RPE21	B05	Known human gene
167	RPE21	F07	Known human gene
168	RPE21	B04	Known human gene
169	RPE21	E06	Known human gene
170	RPE22	E06	Known human gene
171	RPE22	C07	Hypothetical protein
172	RPE22	D08	Known human gene
173	RPE22	A02	Known human gene
174	RPE22	A11	Known human gene
175	RPE22	D03	No significant similarity
176	RPE22	F04	Known human gene
177	RPE22	H05	Known human gene
178	RPE22	A03	No significant similarity
179	RPE22	F03	Known human gene
180	RPE22	D07	Known human gene
181	RPE22	C09	Known human gene
182	RPE22	D06	Predicted gene
183	RPE23	G11	No significant similarity
184	RPE23	B02	Known human gene
185	RPE23	D05	Known human gene
186	RPE23	A09	Known human gene
187	RPE23	A03	Known human gene
188	RPE23	H10	Predicted gene
189	RPE23	A02	Predicted gene
190	RPE23	D11	Predicted gene
191	RPE23	D12	Known human gene

No	Plate ID	Clone ID	Subcategory
192	RPE23	H08	Known human gene
193	RPE23	C07	Predicted gene
194	RPE23	C10	Known human gene
195	RPE23	C12	Predicted gene
196	RPE23	A10	No significant similarity
197	RPE23	G06	Known human gene
198	RPE23	H07	Predicted gene
199	RPE23	D08	Known human gene
200	RPE23	E09	Known human gene
201	RPE23	H11	Known human gene
202	RPE23	H12	Known human gene
203	RPE23	C05	Known human gene
204	RPE23	F09	Predicted gene
205	RPE23	B05	Human Unknown
206	RPE23	F08	No significant similarity
207	RPE23	G04	Predicted gene
208	RPE23	E08	No significant similarity
209	RPE23	F01	human Unknown
210	RPE23	C04	Known human gene
211	RPE24	C08	Known human gene
212	RPE24	D02	Known human gene
213	RPE24	B10	Known human gene
214	RPE24	B06	Known human gene
215	RPE24	C09	Known human gene
216	RPE24	H09	Known human gene
217	RPE24	B04	mc
218	RPE24	C11	Known human gene
219	RPE24	A10	Predicted gene
220	RPE24	H07	Predicted gene
221	RPE24	F02	Predicted gene
222	RPE24	A09	Known human gene
223	RPE24	A11	Known human gene
224	RPE24	D11	No significant similarity
225	RPE24	E05	Human Unknown
226	RPE24	G06	Known human gene
227	RPE24	E02	Known human gene
228	RPE25	D01	Known human gene
229	RPE25	G12	Predicted gene
230	RPE25	F12	Known human gene
231	RPE25	D12	Known human gene
232	RPE25	C07	Known human gene
233	RPE25	E12	Predicted gene
234	RPE25	G04	Known human gene
235	RPE25	C06	Known human gene
236	RPE25	C03	Known human gene
237	RPE25	H06	Known human gene
238	RPE25	D03	No significant similarity
239	RPE25	A02	Known human gene
240	RPE25	C11	Known human gene
241	RPE25	F08	No significant similarity
242	RPE25	H05	Known human gene
243	RPE25	G06	Known human gene
244	RPE25	E01	Predicted gene
245	RPE25	A06	Human Unknown
246	RPE25	H12	Known human gene
247	RPE26	G10	Known human gene
248	RPE26	E11	Known human gene

No	Plate ID	Clone ID	Subcategory
249	RPE26	B10	Known human gene
250	RPE26	C06	Predicted gene
251	RPE26	C11	Human Unknown
252	RPE26	A03	No significant similarity
253	RPE26	C08	No significant similarity
254	RPE26	C01	Known human gene
255	RPE26	A06	Known human gene
256	RPE26	B03	Known human gene
257	RPE26	D03	mc
258	RPE26	H11	Known human gene
259	RPE26	F08	Predicted gene
260	RPE26	A11	No significant similarity

mc = multiple chromosomal location

Table 5: Genes from pathways suspected to be involved in AMD pathogenesis

Apoptosis related genes	
TEGT	testis enhanced gene transcript (BAX inhibitor 1)
BCL2	B-cell CLL/lymphoma 2
DAD1	defender against cell death 1
Oxidative stress related genes	
PRDX1	peroxiredoxin 1
MGST1	microsomal glutathione S-transferase 1
MAOB	monoamine oxidase B
GSTM5	glutathione S-transferase M5
GPX4	glutathione peroxidase 4 (phospholipid hydroperoxidase)
ATOX1	ATX1 antioxidant protein 1 homolog (yeast)
GSTM1	glutathione S-transferase M1
Heat shock protein	
HSPCB	heat shock 90kDa protein 1, beta
Ubiquitin pathway	
UBE1	ubiquitin-activating enzyme E1
Lysosomal enzymes	
CTSK	cathepsin K (pseudodeficiency)

Table 6: cDNA libraries used in isolation of MGC2477 gene

DKFZ1	human retina cDNA in lambda Triple Ex vector
DKFZ2	human retina cDNA in lambda Triple Ex vector
DKFZ3	human retina cDNA in lambda Triple Ex vector
DKFZ4	human retina cDNA in lambda Triple Ex vector
CIF1	human retina cDNA in lambda Triple Ex vector
CIF2	human retina cDNA in lambda Triple Ex vector
CIF3	human retina cDNA in lambda Triple Ex vector
HRλGT10V	human retina cDNA in lambda GT10 vector
HRλTE ₂ V	human retina cDNA in lambda Triple Ex 2 vector
HFBλGT10	human foetal brain cDNA in lambda GT10 vector

Table 7: Sequence of the Lambda Triple Ex vector specific primers

LT, 5 prime	AAGCAGTGGTATCAACGCAGAGT
LT, 3 prime	ATTCTAGAGGCCGAGGCCGCGCCGACATG-D (T)30 N-1N

N-1 = A, G or C

PUBLICATION AND PRESENTATIONS

Theses-related publication is in preparation

Presentations:

Oral presentations:

International Symposium of the German Priority Research Program "Age-Related Macular Degeneration", Kloster Seeon, Germany, Nov 1-4, 2001.

Identification and characterization of novel retinal pigment epithelium-specific genes involved in pathways possibly related to age related macular degeneration.

<http://www.med.uni-heidelberg.de/augen/sppamd/timetable.html>

German Human Genome Meeting 2002 –Medical Genetics, 29.9 -02.10.2002, Leipzig, Germany.

Identification and characterization of genes from the retinal pigment epithelium (RPE) as candidates for age related macular degeneration (AMD).

<http://www.dhgp.de/info/archiv/meeting02/lectures/lecture28.html>

CURRICULUM VITAE

Personal Details:

Date of birth: 6th July 1958
Place of birth: Omdurman, Sudan
Nationality: British
Marital status: married

Education:

2000 – 2003 PhD in molecular and bio-computational biology, University of Wuerzburg, Germany.
 1998 - 2000 MSc Medical Molecular Biology (with merit), Westminster University, UK.
 1980 – 1986 Diploma in General Medicine, Institute of medicine and pharmacy, Iasy, Romania.
 1979 High secondary school certificate, Omdurman, Sudan.

Work experience:

1996 – 1997 clinical attachment, John Radcliffe Hospital, Nuffield department of clinical medicine, Oxford, UK.
 1988 – 1996 General practitioner, ministry of health, Yemen Republic.
 1986 - 1988 Internship, Khartoum Teaching Hospital, Sudan.